

Abelian lattice gauge theories in three dimensions

Inaugural dissertation
at the Faculty of Science,
University of Bern

presented by

Alessandro MARIANI

from Italy

Supervisor of the doctoral thesis:

Prof. Dr. Uwe-Jens WIESE

Institute for Theoretical Physics
Albert Einstein Center for Fundamental Physics
University of Bern

Abelian lattice gauge theories in three dimensions

Inaugural dissertation
at the Faculty of Science,
University of Bern

presented by
Alessandro MARIANI
from Italy

Supervisor of the doctoral thesis:
Prof. Dr. Uwe-Jens WIESE
Institute for Theoretical Physics
Albert Einstein Center for Fundamental Physics
University of Bern

Accepted by the Faculty of Science.

Bern, 03.07.2024

The Dean

Prof. Dr. Marco Herwegh

Abstract

Lattice gauge theories in three spacetime dimensions are relevant for condensed matter physics, but also as a testbed for ideas in particle physics. Here we focus on pure gauge theories without matter, which, especially in the Abelian case, are often thought to be less interesting; in this work we hope to demonstrate that they display a very rich physics.

The first theory that we consider is the non-compact integer-valued gauge theory whose gauge group is \mathbb{Z} . This is relevant for the study of vortices, topological excitations which are found in superfluids. We consider the problem of their construction in a fully quantum theory. Our novel result is the numerical calculation of a set of critical exponents associated to the vortices as well as the demonstration that they obey a simple scaling relation.

We then consider the compact gauge theory whose gauge group is $U(1)$. We review the well-known literature on this topic, as well as the celebrated proof of confinement in this theory. Our novel contribution is the numerical calculation of its equation of state at finite temperature. It allows us to probe the spectrum of the theory and discuss some of the peculiar features of confinement in this theory, such as the existence of inequivalent length scales as well as its effective description as a scalar theory.

Finally, we consider a novel modification of the $U(1)$ gauge theory which can be constructed by introducing a topological angle α . This is most natural in the Hamiltonian formalism. We compute several quantities in the case $\alpha = \pi$, and show that this theory displays quite unusual properties for a gauge theory, such as a broken \mathbb{Z}_2 symmetry in the continuum limit as well as fractionalized flux strings.



This work is licensed under a Creative Commons Attribution 4.0 International License
<https://creativecommons.org/licenses/by/4.0/>

Contents

Introduction	8
1 Vortices in the O(2) model	9
1.1 Classical vortices in the O(2) model	10
1.2 Quantum theory	12
1.3 Duality transformation	16
1.4 The phase diagram and the vortex operator	19
1.5 Boundary conditions and symmetries	23
1.6 Numerical calculations and results	26
1.7 Infraparticles	32
1.8 Conclusions	34
2 Confinement in U(1) gauge theory	35
2.1 The confining string	37
2.2 Effective string theory	42
2.3 Known results on the 3D U(1) gauge theory	44
2.4 U(1) gauge theory at finite temperature	53
2.5 The equation of state	57
2.6 Conclusions	63
3 A new type of gauge theory	64
3.1 The new gauge theory action	64
3.2 Motivation for the new gauge theory	67
3.3 Analytical treatment	71
3.4 Numerical simulation	75
3.4.1 Order parameters	75
3.4.2 Mass and string tension	77
3.5 Conclusions	82
Bibliography	84
Acknowledgements	94
Selbstständigkeitserklärung	95

Introduction

This doctoral thesis comes as the completion of almost four years of research work. Over the years I've taken part in several research projects, all at the more theoretical side of lattice field theory, at the interface between particle and condensed matter physics. There are many philosophies as to how to write a thesis – here I have chosen a subset made of three research works which share a common thread. Each forms one of the three chapters in this thesis. What is their common denominator? First of all, they are all Abelian gauge theories, as is obvious from the title of this thesis. They are also *pure* gauge theories, i.e. without matter fields. This choice may seem strange – does anything interesting happen in this case? We hope to convince the reader that indeed, even such apparently simple theories display very rich physics.

Another aspect of the common thread that is clear from the title is that all three theories are in three spacetime dimension. A remarkable feature of quantum field theories is that they have some notion of their own range of validity. Via their renormalization group flow, certain theories tell us that they shouldn't be taken too seriously as interacting theories, that is they are only valid at low energy. This happens generically in high dimensions. But how high is high? For gauge theories, the critical dimension is four: gauge theories above four dimensions are free. Thus it is quite natural to study quantum field theories in low dimensions. However, two spacetime dimensions is a case where very special techniques can be applied. While four dimensions is most interesting for particle physics, three dimensions is an interesting “in between” where no special techniques can be applied, while still being relevant both for particle physics (as toy models) as well as for condensed matter physics.

We can also follow the common thread down its more subtler aspects. In all three chapters, we will see that a crucial role will be played by topology and topological excitations. Even though they are subtle non-perturbative effects, they can dramatically alter the properties of the theories.

Even among Abelian gauge theories, I have chosen to only discuss “standard” quantum field theories with an infinite-dimensional Hilbert space. This leaves out for example \mathbb{Z}_N gauge theories, as well as quantum link models. We also do not discuss topological quantum field theories such as Chern-Simons theory. This does not leave many options. In Chapter 1 I discuss the gauge theory with gauge group \mathbb{Z} , which is relevant for the study of vortices in superfluids. In Chapter 2 I discuss the gauge theory with gauge group $U(1)$, which is exceptionally well-understood at the analytical level. In the first two chapters, it should become apparent why there's no chapter devoted to the gauge theory with gauge group \mathbb{R} . Finally, in the third chapter I discuss another gauge theory with gauge group $U(1)$, which has been modified to accommodate a novel type of topological angle.

1

Vortices in the O(2) model

This chapter is based on:

[1] A. Mariani, “Vortex condensate and critical exponents in the (2+1)-dimensional O(2) model”, [Phys. Rev. B](#) **108**, 134520 (2023), [arXiv:2305.13156](#).

When a gas of Helium 4 is lowered below the critical temperature of $2.17K$, it exhibits a phase transition to a state where it flows with no viscosity. Such a fluid state is known as a *superfluid*, and it displays all sorts of funny properties, such as creeping along walls. When rotation is imparted to a superfluid, rather than rotating as a whole, it prefers to form a lattice of quantized vortices which absorb the angular momentum. Both the phenomenology and theory of superfluidity are very rich and here we can only refer the reader to more specialized texts [2].

Superfluidity is a quantum phenomenon which can be intuitively understood as a sort of Bose-Einstein condensation [2]. Roughly speaking, below a certain temperature, the Helium 4 atoms (which are bosons) undergo Bose-Einstein condensation to a macroscopic state. Here they all share the same quantum state, whose wavefunction serves as an order parameter of the transition. In the spirit of Landau-Ginzburg effective theory [3], one then writes down a theory for a complex-valued field Φ , with Lagrangian

$$\mathcal{L} = \frac{1}{2} \partial_\mu \Phi \partial_\mu \Phi^* + \frac{\lambda}{4!} \left(|\Phi|^2 - v^2 \right)^2. \quad (1.1)$$

This theory includes both a quadratic and a quartic term, which may be thought to effectively encapsulate the interparticle interactions. This Lagrangian has a global O(2) symmetry, which is related to particle number conservation.

In this chapter, as we will see in more detail in later sections, we are interested in the construction of fully quantum topological excitations. In order to study the quantum theory, one then considers the path integral or partition function,

$$Z = \int D\Phi \exp \left(- \int d^3x \mathcal{L} \right). \quad (1.2)$$

The quantum theory defined by eqs.(1.1) and (1.2) may be interpreted in two different ways:

1. In one interpretation, one studies the statistical mechanics of a three-dimensional system at thermal equilibrium. In this case \mathcal{L} plays the role of a classical Hamilton function, and the inverse temperature “ β ” has been absorbed into the couplings. We then study the system as the equilibrium temperature is varied. In this case, the object of study is therefore a three-dimensional superfluid and its vortex lines. In this interpretation, the model is invariant under space rotations and translations.

2. In a different interpretation, the partition function (1.2) describes the Euclidean (Wick-rotated) action of a $(2 + 1)$ -dimensional quantum field theory. In this case \mathcal{L} is the Lagrangian of a quantum field theory at zero temperature. By varying the couplings, we then study the quantum phase transition of a two-dimensional system. Here the vortices are point-like objects living in two space dimensions. In this interpretation, the rotational symmetry of the model is interpreted as the Euclidean version of Lorentz invariance.

In particular, both systems admit experimental realizations consistent with a description given by the Lagrangian (1.1). In the statistical mechanics interpretation, this corresponds to Helium 4 near the λ -transition, and its associated vortex lines [3–6], while for the quantum field theory interpretation the relevant system is a Bose gas in an optical lattice near the superfluid-insulator transition [7–9], where relativity can be emergent. In what follows, we will reference both the quantum field theory and the statistical mechanics interpretations.

At this point, the reader may have many questions. For one, this thesis is ostensibly about gauge theories, but the theory we discussed, eq. (1.1), is a scalar theory. As we will see in Section 1.2, in three spacetime dimensions scalar theories are exactly dual to gauge theories. The relevant theory has gauge group \mathbb{Z} . In fact, working in the dual representation turns out to be advantageous to discuss topological excitations such as vortices. Moreover, to discuss the *quantum* properties of vortices, it is also important to clearly establish their *classical* (as well as *semiclassical*) properties, so that they can be contrasted properly. This we do in Section 1.1. Then, in Section 1.4, we discuss the construction of the vortex operator in the lattice theory and finally in Section 1.6 we discuss the numerical simulations and our results.

Let us mention that the work presented in this chapter is closely related to [10] (on which the thesis [11] is based) where the vortex mass is computed with the same techniques. The numerical study of topological excitations using this construction was initiated in four dimensions in [12] and further studied in [13].

1.1 Classical vortices in the O(2) model

Topological excitations are a phenomenon which exists both at the classical as well as at the quantum level. In fact, it is a phenomenon first observed classically. The propagation of waves in a medium can be modelled via appropriate partial differential equations. If the equation is linear, it is not hard to superimpose various solutions to create localized stable wavepackets which travel independently from each other. Remarkably, also some *nonlinear* differential equations admit so-called “soliton” solutions, which are stable and localized [14]. Their existence and stability can often be linked to “topological properties”, as we will see in more detail in this chapter. The study of classical topological excitations has led to a very elegant mathematical theory, which for example allows exact analytical solutions for many scalar field theories in $1 + 1$ dimensions [14].

In our case, we look for classical vortex solutions of the equations of motion given by the Lagrangian eq. (1.1). In particular we can look for a static solution of the form

$$\Phi(\vec{x}) = f(r)e^{i\theta} , \tag{1.3}$$

in polar coordinates. The resulting differential equation for $f(r)$ can be solved numerically [11], and the resulting $\Phi(\vec{x})$ is pictured in Fig. 1.1. Since a numerical solution can only be performed in finite volume, appropriate boundary conditions need to be applied. Here C -periodic boundaries were chosen, where a charge conjugation transformation is performed when crossing a boundary. We will discuss this choice in more depth in Section 1.5. For more details on the numerical solution as well pictures of solutions with different vortex number, the reader is encouraged to consult [11].

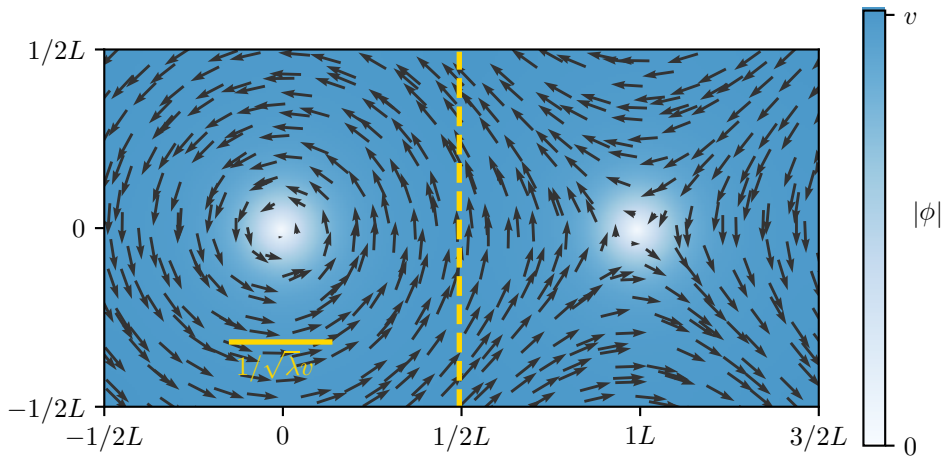


Figure 1.1: Classical static vortex solution of the (2+1)-d U(1) scalar field theory with C -periodic boundary conditions. The arrows represent the complex field $\Phi(\vec{x})$. The right side of the figure is the C -periodic copy of the left side. Reprinted from [10].

The word “topological” is used in physics in many different senses. Here the function $\Phi(\vec{x})$ is “topologically non-trivial” in the sense that it has non-zero *winding number*. What does this mean? Suppose that we fix a radius r . With this choice, Φ is then a map $\Phi : S^1 \rightarrow S^1$, where the first S^1 refers to the spatial circle defined by fixing r , and the second S^1 refers to the phase of the complex field. Generally speaking the maps $S^n \rightarrow X$ are classified by the homotopy group $\pi_n(X)$ [15]. All maps which share the same element of the homotopy group can be continuously deformed into each other, but maps in different homotopy classes cannot be continuously deformed into each other. In this case, the relevant homotopy group is $\pi_1(S^1) \cong \mathbb{Z}$. Therefore to each map $S^1 \rightarrow S^1$ we can assign an integer $w \in \pi_1(S^1) \cong \mathbb{Z}$, called the *winding number*. In the case of our classical solution, eq. (1.3), the winding number is $w = 1$. Therefore this solution is topologically non-trivial, because it cannot be deformed into a map in the trivial homotopy class with winding number $w = 0$. More generally, an example of a map with arbitrary winding number w is $\theta \rightarrow e^{iw\theta}$. We will also refer to the winding number as the “vortex number”.

Note that eq. (1.3) describes a *single* vortex. In fact since in principle a solution of the equations of motion is a map $\Phi : \mathbb{R}^2 \rightarrow \mathbb{C}$, its winding number depends on which subset $S^1 \subset \mathbb{R}^2$ we pick. In the above discussion, we picked an arbitrary circle $\cong S^1$ which encircles the origin; but for any other point of the plane, there is a sufficiently small circle S^1 such that Φ restricted to this circle has zero winding number. Therefore, the above configuration describes a single vortex with vortex number 1 located at the origin. By examining the winding number of a configuration Φ for various choices of circles $S^1 \subset \mathbb{R}^2$ around any point \vec{x}_0 , we can detect whether there is a vortex at \vec{x}_0 .

More generally, we can detect various other kinds of topological excitations by restricting a solution to a subset, much like we did in this case. Sometimes, it is also appropriate to compactify space or spacetime (i.e. $\mathbb{R}^2 \rightarrow S^2$), for example when the boundary conditions require that the field takes the same value at all points at infinity. Alternatively, if one insists that the solution of the equations of motion has finite energy, then it should have zero potential at infinity. The set of zeros of the potential forms the vacuum manifold \mathcal{V} . Then depending on whether the field is required to be constant at infinity or not, one can consider either the sphere at infinity S^{d-1} or compactify space(time) to S^d . The appropriate homotopy groups to consider are then $\pi_d(\mathcal{V})$

or $\pi_{d-1}(\mathcal{V})$. This should make it clear that even in the simple case of scalar theories, there are many ways of detecting topologically non-trivial configurations. In fact since homotopy theory is well-developed mathematically, we have chosen subsets homeomorphic to spheres; but in general one can have more complicated topology. The terminology for topological excitations can vary depending on the context. Generally, they are named according to their codimension (a set of dimension k embedded in a d -dimensional space has codimension $d - k$). For example, vortices are point-like in two dimensions but string-like in three dimensions (i.e. “vortex lines”). One calls excitations of codimension one *domain walls* (or *kinks*), those of codimension two *vortices* (or *cosmic strings*), those of codimension three *monopoles*, and those of codimension four *textures*. For scalar theories, the simplest classification of topological defects follows from homotopy: in particular, defects of codimension k are associated with non-trivial homotopy group π_{k-1} [14, 16].

Given the Lagrangian eq. (1.1), we can obtain its Hamiltonian via a standard Legendre transformation, and therefore compute the energy of a configuration. On a spatial box of size $L \times L$, this turns out to be [11]

$$E \sim \pi v^2 \log \frac{L}{L_0} . \quad (1.4)$$

The energy of this configuration is therefore logarithmically divergent with the spatial volume and, in particular, it is infinite in the infinite volume limit. The fact that the vortex in this theory has infinite mass is actually not at all surprising: a large class of actions in dimension higher than $1 + 1$ only admits topological excitations with infinite energy. This is known as “Derrick’s theorem” [14, 17–19].

The fact that the vortices have infinite energy would naively seem to forbid their existence in the real world. An important distinction to make is that eq. (1.4) applies to the vortex configuration eq. (1.3), which describes a single vortex and therefore in particular a configuration with overall non-zero vortex number. On the other hand, vortex configurations with overall zero vortex number, which are formed by pairs of vortices and antivortices, still have finite energy in the infinite volume limit. Such configurations are therefore “naturally occurring”, and studying the system without accounting for them would give incorrect results. On the other hand, configurations with overall non-zero vortex number have infinite mass in the infinite volume and therefore do not occur naturally. However, they do occur experimentally if they are somehow forced into the system. In fact, if one imparts an angular momentum to a superfluid, it prefers to absorb it by producing a configuration of vortices *with vorticity pointing in the same direction* to match the imparted angular momentum. The resulting vortex configuration has overall non-zero vortex number. This is the type of vortex configurations that we study in this chapter. As we will see, in the quantum theory configurations with different overall vortex number live in different superselection sectors of the Hilbert space. Working in different sectors corresponds to different experimental situations.

1.2 Quantum theory

In the previous section, we discussed the classical vortices in the $O(2)$ model. But since, as we have seen, superfluidity is a quantum phenomenon it is quite natural to ask what are the *quantum* properties of topological excitations. This is a difficult topic to study because topological excitations are often a *global* phenomenon involving the collective dynamics of the field configuration. For example, one can detect the presence of a non-zero vortex number by computing the winding number of the field configuration around an *arbitrary* closed loop arbitrarily far away from the vortex. At the quantum level, such topological excitations cannot

be obtained by a small perturbation around the vacuum and are therefore, generally speaking, a strongly-coupled phenomenon. One can attempt a *semiclassical* approach instead, where one expands the perturbative series around the non-trivial vacuum of a topological excitation [19, 20]. We give an example of such a calculation in Chapter 2. But this is technically difficult, especially because analytical soliton solutions are hard to come by in dimension higher than $1 + 1$. In general, it is even difficult to understand what one means by topological excitations in a quantum theory. In the classical case, we could identify topological excitations by looking at the homotopy class of the solution of the equation of motion. But in the quantum theory, we instead integrate over all possible fields (even discontinuous ones, for which homotopy is not defined) and it is not clear how to translate the previous argument. The situation becomes even more complicated when we discretize the spacetime into a lattice. In this section, we discuss the non-perturbative construction of the partition function of the quantum $O(2)$ model. Then in Section 1.3 we discuss the duality transformation in this model, which will be a crucial ingredient for the non-perturbative construction of the quantum vortices in Section 1.4.

An important feature of quantum field theories is that the coupling constants are not constants, but rather depend on the energy scale. The change in the couplings is described by the renormalization group (RG) flow. For the $O(2)$ model in $2 + 1$ dimensions with action eq. (1.1) and partition function eq. (1.2) the RG flow can be computed perturbatively using the ϵ expansion [21, 22]. It predicts two RG fixed points, a trivial Gaussian fixed point and a non-trivial “Wilson-Fisher” fixed point [23]. This last fixed point is the one of interest in our case. Near the Wilson-Fisher fixed point, the coupling λ is *irrelevant*. This means that for any value of λ there is a value of v^2 (depending on λ) which places the theory on the critical surface. If we are interested in *universal* quantities, we can fix an arbitrary value of λ and then drive the system to the Wilson-Fisher fixed point by tuning v^2 . Many reasonable choices of λ are possible. For example, one can choose the λ at which corrections to scaling are smallest [24]. In this work, we choose the λ which leads to the simplest theory, i.e. $\lambda = +\infty$. This forces the potential term to zero, which means that the absolute value of the scalar field is now fixed, $|\Phi| \equiv v$. Thus the scalar field may be written in terms of an angular variable φ such that $\Phi = v \exp(i\varphi)$. The resulting Lagrangian is then that of the XY model (also known as the compact boson),

$$\mathcal{L} = \frac{1}{2}v^2 \partial_\mu \varphi \partial^\mu \varphi, \quad \varphi \in [0, 2\pi). \quad (1.5)$$

Once we have an action, as anticipated in the introduction to this chapter, we consider the appropriate quantum partition function

$$Z = \int D\Phi \exp\left(-\int d^3x \mathcal{L}\right). \quad (1.6)$$

Unfortunately, the partition functions of quantum field theories, such as eq. (1.6) are generally ill-defined. This is because it is not possible to assign a precise mathematical meaning to the measure $D\Phi$. In fact, it can be shown that there is no Lebesgue measure on an infinite dimensional space [25] such as a space of functions. While this statement is often considered merely a technicality, it is actually a fact of great physical significance. In particular, the symmetries of a classical theory can be broken by quantum effects, a phenomenon known as a quantum *anomaly* [26]. The presence of anomalies can be tied to the regularization of the measure $D\Phi$, and therefore the existence of a naive Lebesgue measure would forbid quantum anomalies, which is physically incorrect. Moreover, the definition of a quantum field theory is deeply intertwined with the renormalization group flow (in perturbative language, to regulate infinities), and thus a rigorous definition of the continuum measure needs to somehow incorporate

the RG flow. As we see in the next paragraph as well as several times in the rest of this thesis, this is evident from the way one takes the continuum limit on the lattice.

The only known way to *define* the partition function of a quantum field theory is via a lattice discretization. In other words, the infinite spacetime is sampled at a finite set of points; then the integral in the partition function simply becomes a finite number of ordinary integrals. The finite lattice also provides a regulator for both UV and IR divergences. Since in the end we want to recover continuum physics, it is important to understand in general what is the relation between lattice and continuum physics. A lattice theory is described by a partition function $Z(g^2, a, N)$ which, schematically, is a well-defined function of the lattice spacing a (which appears in the action), the number of lattice points N and one or more couplings g^2 . Similarly, on the lattice one can compute various quantity of interest F which are again well-defined functions of the same variables, i.e. $F \equiv F(g^2, a, N)$. Since N is a pure number, one can take the “infinite volume” or “thermodynamic” limit unambiguously, to obtain

$$F(g^2, a) \equiv \lim_{N \rightarrow \infty} F(g^2, a, N) . \quad (1.7)$$

Of course, one needs to make sure that F is appropriately normalized so that a finite limit exists. Theoretically, proving the existence of the thermodynamic limit is usually not so difficult. In practice $F(g^2, a, N)$ is computed numerically for several values of N and extrapolated to infinite volume either by fitting to a theoretical prediction for its volume scaling or by going to a large enough value of N where one observes a plateau. We also note that one can extract interesting quantities directly from the finite volume behaviour of certain observables [27].

The final limit to take is the *continuum limit*. There are two different equivalent points of view for this limit:

1. From the condensed matter point of view, the lattice is *physical* (for example, it could be a crystal). Then the lattice spacing a is a fixed physical number, and the continuum limit is achieved by tuning the coupling g^2 to a point in its phase diagram where a continuous transition occurs. One then constructs appropriate ratios of quantities which are finite as the limit is taken. In this point of view, the continuum physics is merely an effective description of the underlying discrete degrees of freedom. In Chapter 1, we will adopt this point of view.
2. From the high-energy point of view, the lattice is merely a regularization artefact and one wants to send the lattice spacing $a \rightarrow 0$. On the lattice one can compute a quantity $F(g^2, a)$ (for example, the mass of a particle) and compare it to its real-life physical value F_{phys} . This then defines a particular renormalization trajectory where the continuum limit is taken by sending $a \rightarrow 0$ while the coupling $g^2 = g^2(a)$ is varied as a function of a such that $F(g^2, a) \equiv F_{\text{phys}}$ remains constant. We will adopt this point of view in Chapter 2.

For a practical example of the two approaches, suppose that our physical theory allows us to compute the mass of a particle X . On the lattice, we can only access dimensionless combinations (this is most evident in numerical simulations); therefore the lattice theory allows us to compute the dimensionless mass $m_X^{(L)}(g^2, a)$ as a function of a and g^2 . In the high-energy point of view, we would compare the lattice mass with the physical mass by setting

$$m_X^{(L)}(g^2, a) = a m_X^{(\text{phys})} , \quad (1.8)$$

which can be interpreted as either a definition of the (dimensionful) lattice spacing a as a function of g^2 , or an implicit definition of g^2 as a function of a . Note that, since $m_X^{(\text{phys})}$ is fixed,

taking the continuum limit $a \rightarrow 0$ requires the existence of a point in the phase diagram where the lattice mass $m_X^{(L)}(g^2, a) \rightarrow 0$. This is precisely a point where a continuous phase transition occurs. From the condensed matter point of view instead, one would simply consider the mass of another particle, say Y . Its ratio with the mass of the X particle is expected to have a finite continuum limit

$$\lim_{g^2 \rightarrow g_c^2} \frac{m_Y^{(L)}(g^2)}{m_X^{(L)}(g^2)} = \frac{m_X^{(\text{phys})}}{m_Y^{(\text{phys})}}, \quad (1.9)$$

as g^2 is tuned to a continuous phase transition located at the critical value g_c^2 .

Lattice calculations are usually performed in a Euclidean path integral formulation. In many cases, this is not a major limitation; as long as the action satisfies certain reasonable assumptions, Wick rotation back to a theory defined in Minkowski space can be rigorously performed [28, 29]. In practice, numerical simulations are sometimes hindered by the so-called *sign problem*. We will see one such example in Chapter 3. Moreover, working in the Euclidean path integral approach prevents access to the real-time dynamics of the theory. Both these problems can potentially be solved by simulating such theories with quantum hardware.

In practice, similar to the infinite-volume limit, the continuum limit is typically obtained by extrapolating via a known theoretical scaling form. However, because of these complexities, the existence of the continuum limit is hard to prove mathematically. It has been shown for scalar field theories in two and three spacetime dimensions as interacting theories [30–38] and in four [39] and higher dimensions as trivial theories [40, 41]. In two dimensions, some fermion-scalar theories [42] as well as the Abelian Higgs model [43–45] have been constructed. Proving the existence of the continuum limit (as defined above) for lattice Yang-Mills theory in four spacetime dimensions is part of one of the Millennium Prize problems [46]. See also [47, 48] for reviews of these issues, as well as [49–55] for recent developments. Let us also note that these issues do not only affect the path integral approach to quantum theory; also canonical quantization (at least in its naive form) is ill-defined [56].

As usual in analysis, the fact that a limit exists does not mean that it is equal to the value that we expect naively. In particular, it is possible that the continuum limit of a lattice field theory which naively discretizes a certain continuum action *does not* reproduce the correct continuum physics. This problem plagues in particular the lattice discretization of fermionic fields as the “fermion doubling” problem [57, 58]. In some cases, no lattice discretization is known which reproduces the correct continuum physics. These include most importantly non-Abelian chiral gauge theories [59], with some important exceptions [60–62].

Another important fact is that limits are “many-to-one”: different lattice theories may have the same continuum limit. The different discretizations may have different advantages over each other. We will encounter this situation many times over this thesis, especially in Chapter 2. From a Wilsonian perspective, one expects that two different lattice theories with the same symmetries (or a sufficiently large subgroup thereof) should describe the same continuum physics. We will discuss this further in Chapter 3.

Going back to the $O(2)$ model, our lattice discretization will involve one angle $\varphi_x \in [0, 2\pi)$ per site x of the lattice. The partition function is a simple discretization of the XY model Lagrangian eq. (1.5) and takes the form

$$Z = \left(\prod_x \frac{1}{2\pi} \int_{-\pi}^{\pi} d\varphi_x \right) \exp \left(- \sum_{\langle xy \rangle} s(\varphi_x, \varphi_y) \right), \quad (1.10)$$

where $\langle xy \rangle$ are nearest neighbours. As discussed above, there are several equivalent lattice

actions s which reproduce the same continuum physics. A natural choice would be

$$s(\varphi_x, \varphi_y) = \frac{1}{g^2}(1 - \cos(\varphi_x - \varphi_y)) . \quad (1.11)$$

Here we choose instead a different action, known as the Villain action, because it will lead to a simpler dual theory:

$$e^{-s(\varphi_x, \varphi_y)} = \sum_{n_{\langle xy \rangle} \in \mathbb{Z}} \exp \left[-\frac{1}{2g^2} (\varphi_x - \varphi_y + 2\pi n_{\langle xy \rangle})^2 \right] . \quad (1.12)$$

Here g^2 is the bare coupling and periodicity over 2π is enforced by the summation over the n variable.

The phase diagram of this model is well understood. With the action eq. (1.12), for small g^2 the $O(2)$ symmetry is broken, resulting in one massless Goldstone boson. On the other hand, for large g^2 the $O(2)$ symmetry is unbroken. The two phases are separated by a second-order phase transition. The exact location of the transition depends on the choice of action. For the Villain action eq. (1.12), it is located at [63]

$$g_c^2 = 3.00239(6) . \quad (1.13)$$

1.3 Duality transformation

In order to study this model, it is useful to perform a duality transformation. This is particularly useful because, as we will see in a moment, computing the properties of the vortex is easier in the dual formulation. In this context, a duality is a change of variables in the partition function which relates two apparently different theories. Suppose that we start from a partition function of the form:

$$Z = \left(\prod_x \frac{1}{2\pi} \int_{-\pi}^{\pi} d\varphi_x \right) \exp \left(-\sum_{\langle xy \rangle} s(\varphi_x - \varphi_y) \right) . \quad (1.14)$$

By hypothesis, the action s , and therefore the Boltzmann weight, are periodic with period 2π . Moreover, they depend only on the difference $\varphi_x - \varphi_y$. Therefore the Boltzmann weight can be expanded in a Fourier series,

$$e^{-s(\varphi_x - \varphi_y)} = \sum_{k_{\langle xy \rangle} \in \mathbb{Z}} e^{-\tilde{s}(k_{\langle xy \rangle})} e^{i(\varphi_x - \varphi_y)k_{\langle xy \rangle}} . \quad (1.15)$$

The coefficients of the Fourier series must be positive by reflection positivity [64], so they can be written as an exponential. Then it is simplest to use the language of lattice differential forms (see for example [12, 65] for the details). In this language φ_x is a 0-form and applying the derivative operator one obtains the 1-form $(\delta\varphi)_{\langle xy \rangle} = \varphi_x - \varphi_y$ which lives on lattice links. Then, when plugging the Fourier expansion back into the partition function, we can integrate by parts to find

$$\sum_{\langle xy \rangle} (\varphi_x - \varphi_y)k_{\langle xy \rangle} = \sum_x \varphi_x (\delta k)_x , \quad (1.16)$$

where δ is the co-differential, which can be thought of as a sort of “divergence”. Therefore the partition function becomes

$$Z = \left(\prod_x \frac{1}{2\pi} \int_{-\pi}^{\pi} d\varphi_x \right) \left(\prod_{\langle xy \rangle} \sum_{k_{\langle xy \rangle} \in \mathbb{Z}} \right) e^{-\sum_{\langle xy \rangle} \tilde{s}(k_{\langle xy \rangle})} e^{i \sum_x \varphi_x (\delta k)_x} . \quad (1.17)$$

Now the integration over the φ_x can be performed directly, and it leads (up to some prefactors) to a delta function on δk , which is thus forced to be zero everywhere. In infinite volume the Poincaré lemma guarantees that if $\delta k = 0$, where k is a 1-form, then there exists a 2-form A such that $k = \delta A$ [66]. The new form A lives on the 2-cells of the lattice, i.e. the plaquettes. Then we find the partition function

$$Z = \left(\prod_{\square} \sum_{A_{\square} \in \mathbb{Z}} \right) \exp \left(- \sum_{\langle xy \rangle} \tilde{s}(\delta A_{\langle xy \rangle}) \right). \quad (1.18)$$

In this formula, \square denotes the lattice plaquettes. This partition function can be rewritten in terms of more convenient variables which live on the dual lattice. An n -cell of the original lattice is dual to a $d - n$ cell of the dual lattice. Therefore in the dual lattice A lives on the lattice links, and we can therefore write the final dual partition function

$$Z = \left(\prod_{\langle xy \rangle} \sum_{A_{\langle xy \rangle} \in \mathbb{Z}} \right) \exp \left(- \sum_{\square} \tilde{s}(dA_{\square}) \right), \quad (1.19)$$

where now all quantities refer to the *dual* lattice. Here $dA_{\square} = A_1 + A_2 - A_3 - A_4$ is a non-compact plaquette variable for the four links in plaquette \square . This is just the partition function of a non-compact integer-valued lattice gauge theory.

For the Villain partition function eq. (1.12) of the original theory, the Fourier expansion is found to be, apart from an overall prefactor,

$$e^{-s(\varphi)} \equiv \sum_{n \in \mathbb{Z}} \exp \left[-\frac{1}{2g^2} (\varphi + 2\pi n)^2 \right] = \sum_{n \in \mathbb{Z}} e^{-\frac{g^2}{2} n^2} e^{in\varphi}, \quad (1.20)$$

and therefore the dual partition function is particularly simple:

$$Z = \left(\prod_{\langle xy \rangle} \sum_{A_{\langle xy \rangle} \in \mathbb{Z}} \right) \exp \left(-\frac{g^2}{2} \sum_{\square} (dA_{\square})^2 \right). \quad (1.21)$$

In general terms, as is clear from the above discussion, exact lattice dualities preserve the partition function up to constant prefactors. They are simply a rewriting of the same theory in terms of different variables. It is not however clear what is the relationship between the original variables φ and the dual variables A . As mappings between quantum states, dualities are generally *not* unitary transformations, and not even one-to-one maps [67–69]. This is most easily seen in the case of the 2-dimensional Ising model, which is self-dual, and the duality maps the broken phase (where the ground state is degenerate) to the symmetric phase (where the ground state is unique). Generally speaking, a duality maps a theory consisting of n forms living in an Abelian group G in d dimensions to a theory consisting of $d - n - 2$ forms living in its Pontryagin dual \hat{G} on the dual lattice [70, 71]. Intuitively, the Pontryagin dual \hat{G} is the space of the Fourier coefficients of G , which is again an Abelian group if G is Abelian, i.e. Pontryagin duality relates Abelian groups as follows:

$$\mathbb{R} \leftrightarrow \mathbb{R}, \quad \text{U}(1) \leftrightarrow \mathbb{Z}, \quad \mathbb{Z}_N \leftrightarrow \mathbb{Z}_N. \quad (1.22)$$

Respectively, these are the familiar cases of the Fourier transform, the Fourier series and the discrete Fourier transform. More generally, for an arbitrary (possibly non-Abelian) group G ,

the coefficients of the Fourier transform (which appear in the first step of dualization) are the irreducible group characters, i.e. the traces of irreducible representations of G [72]. The Pontryagin dual \hat{G} may thus also be defined as the space of the irreducible characters of G . Unfortunately, however, \hat{G} only forms a group if G is Abelian. For example, the irreps of $U(1)$ are of the form $e^{in\theta}$ for $\theta \in [0, 2\pi)$ and integer n and the product of two irreps is again an irrep i.e. $e^{in\theta}e^{im\theta} = e^{i(n+m)\theta}$. Thus for $G = U(1)$ the dual group is again a group, i.e. the integers $\hat{G} = \mathbb{Z}$, as we already saw. On the other hand, for a non-Abelian group like $SU(2)$, the (tensor) product of two irreps is not an irrep but only a direct sum of irreps. Thus \hat{G} does not have a group structure. This is at least part of the reason why exact duality transformations are not known for non-Abelian theories. The corresponding notion of duality for non-Abelian groups is known as Tanaka-Krein duality [73, 74], but it is unclear if it is useful in this context.

Another interesting consideration is to note the fate of the symmetries on the two sides of the duality. On one side, we had a theory with a *global* $O(2)$ symmetry and on the other side we found a theory with a *local* \mathbb{Z} symmetry. There is no obvious relation between the two. This is a demonstration of the fact that there are important subtleties in saying that a certain theory has a local symmetry, or even a global symmetry, and that such statements are somewhat ambiguous [75].

As we noted during the derivation, the duality transformation is exact only in the infinite volume. In finite volume, the Poincaré lemma is not necessarily true as stated and, depending on the boundary conditions, may need to be appropriately modified. Also the integration by parts may pick up some boundary terms. Generally speaking, for a partition function Z in finite volume, the duality is of the form

$$Z = \sum_i Z^{(i)}, \quad (1.23)$$

where the $Z^{(i)}$ are partition functions for the *same* theory with *different* boundary conditions. However, the finite-volume effects arising from the duality are typically exponentially suppressed [76]. Dualities in general preserve all *local properties* (such as expectation values of local operators) but not *global properties* such as the ground state degeneracy. For a modern perspective on dualities, see [67–69].

To give a taste of dualities in finite volume, we sketch the derivation of the above duality in finite volume. The finite-volume duality in the other direction, i.e. starting from the integer gauge theory with C -periodic boundaries, has been worked out in [10, 11]. Suppose that we start from the partition function of the XY model eq. (1.14) on a finite lattice with periodic boundaries. The first step of the duality transformation, Fourier expansion, is unchanged since this is performed locally on each link. With periodic boundaries (but not in general), integration by parts is exact and therefore this step is also unchanged. However, after integrating out the φ , we obtain the condition $\delta k = 0$. In infinite volume, we could solve this by setting $k = \delta A$. This is not true in finite volume. Instead, the Poincaré lemma on a finite periodic lattice states that a 1-form k such that $\delta k = 0$ can be written as $k = \delta A + \Delta k$, where A is a 2-form and Δk is a 1-form which is supported only on the boundary of the lattice [77]. The Δk term is necessary because configurations on a finite periodic lattice can have non-trivial winding $\sum k$, but $\sum \delta A = 0$. Thus the dual partition function takes the form

$$Z = \left(\prod_{\square \in \text{boundary}} \sum_{\Delta k_{\square} \in \mathbb{Z}} \right) \left(\prod_{\langle xy \rangle} \sum_{A_{\langle xy \rangle} \in \mathbb{Z}} \right) \exp \left(-\frac{g^2}{2} \sum_{\square} (dA_{\square} + \Delta k_{\square})^2 \right). \quad (1.24)$$

The underlying dual lattice again has periodic boundary conditions. Alternatively, the shifts Δk can be absorbed in the boundary conditions for the field. The finite volume dual partition

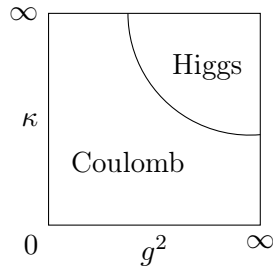


Figure 1.2: Phase diagram of non-compact 3D scalar QED. The integer gauge theory eq. (1.21) corresponds to $\kappa = \infty$.

	O(2) model	Integer gauge theory
small g^2	Broken	Coulomb
large g^2	Symmetric	Higgs

Table 1.1: Phases of the dual models.

function is then of the general form eq. (1.23). Going through the proof of the Poincaré lemma in [77] it is possible to work out a more explicit form for the shifts Δk .

Finally, we note that since the duality is a change of variables within the partition function, it also allows to relate operators in the original theory to operators in the dual theory. For example, the massless photon in the Coulomb phase of the integer gauge theory is dual to the massless Goldstone boson in the broken phase of the O(2) model. As we will see in the next section, the vortex in the O(2) model is dual to the charged particle in the integer gauge theory.

1.4 The phase diagram and the vortex operator

In order to better understand the integer gauge theory eq. (1.21), it is useful to note that it can be obtained as a particular limit of non-compact scalar QED. Consider the following lattice action for a compact scalar $\Phi \in U(1)$ and a real-valued gauge field $A \in \mathbb{R}$:

$$S[A, \Phi] = \frac{g^2}{2} \sum_{\square} (F_{\square})^2 - \kappa \sum_{\langle xy \rangle} \text{Re} (\Phi_x e^{2\pi i A_{\langle xy \rangle}} \Phi_y^*) . \quad (1.25)$$

Then to recover the integer gauge theory eq. (1.21), we can first choose the unitary gauge $\Phi \equiv 1$. Then taking the limit $\kappa \rightarrow \infty$ forces the gauge field to become integer-valued, i.e. $A_{\langle xy \rangle} \in \mathbb{Z}$ and one obtains eq. (1.21).

The phase diagram of non-compact scalar QED [78, 79] is shown in Fig. 1.2. In the integer gauge theory limit $\kappa \rightarrow \infty$, one then simply has a Coulomb phase for small g^2 and a Higgs phase for large g^2 . In the Higgs phase, the photon acquires a mass. The duality maps the Coulomb phase of the integer gauge theory to the broken phase of the original O(2) model and the Higgs phase to the symmetric phase. This is summarized in Table 1.1. It is important to note that in the Coulomb phase the O(2) vortex exists as a particle, while it is condensed in the Higgs phase.

It is also interesting to consider the opposite limit, i.e. the limit $\kappa \rightarrow 0$ where the scalar field decouples and one is left with a pure gauge theory with gauge group \mathbb{R} . This theory is found in a Coulomb phase for all values of the coupling g^2 . On the other hand, in the second chapter of this thesis we will consider the pure gauge theory with gauge group U(1) (i.e. the “compact” gauge theory). As we will see, this theory is found in a *confining* phase for all values of the

coupling [80, 81]. This is again a manifestation of topology: the U(1) theory admits “monopoles” which are responsible for confinement. We can see this already in the classical theory in the continuum, with similar arguments to those presented in Section 1.1. Mathematically, a gauge field should be understood as a connection on a fiber bundle. We can then proceed as in the previous section; consider a two-sphere $S^2 \in \mathbb{R}^3$ and restrict a classical U(1) gauge field to it. This defines a U(1) connection on S^2 , which are classified by the first Chern number $c_1 \in \mathbb{Z}$ [14]. Here c_1 is nothing but the magnetic flux through the sphere. Given a classical U(1) gauge field, we can detect a monopole at a point if a sufficiently small two-sphere surrounding the point has non-zero c_1 . Much like vorticity, this also admits a natural analog on the lattice, whereby one sums the excesses above 2π of the plaquettes belonging to each cube [82].

The importance of topology is a theme of this thesis. It can have striking consequences for the behaviour of the lattice theory. Nonetheless, from a continuum perspective, only the Lie algebra is visible and therefore both the \mathbb{R} and the U(1) gauge theories have the same naive continuum limit. How their difference should be understood from a continuum perspective is a matter of debate [75, 83].

Now the “moral” of the duality is that the vortex in the original picture may be interpreted as a charged particle in the dual picture [10, 12, 78]. In order to obtain a gauge-invariant operator, one needs to combine the scalar field with some other term involving the gauge field. Under a gauge transformation, $\Phi_x \rightarrow e^{2\pi i \alpha_x} \Phi_x$ and $A_{\langle xy \rangle} \rightarrow A_{\langle xy \rangle} + \alpha_y - \alpha_x$. Even though it may seem paradoxical, gauge-invariant operators can be obtained by gauge-fixing the scalar field according to various prescriptions. For example, we can gauge-fix to Landau gauge where $\delta A = 0$. Given an arbitrary starting gauge field configuration A , the Landau gauge-fixing is achieved by the choice $\alpha = -\square^{-1} \delta A$ where $\square \equiv d\delta + \delta d$ is the three-dimensional Laplacian. Then the scalar field gauge-fixed to Landau gauge is given by the operator

$$\Phi_L(x) = \exp(-2\pi i \square^{-1} \delta A) \Phi_x . \quad (1.26)$$

One can check explicitly that the operator in eq. (1.26) is actually gauge-invariant. Therefore, it has a well-defined expectation value. Nonetheless, other choices of gauge are possible. In fact, eq. (1.26) may be interpreted as a scalar field, which has been “dressed” with an appropriate cloud of photons. In eq. (1.26), the photon cloud spreads in the three-dimensional lattice. This would be an appropriate operator for example for the study of “monopoles”. On the other hand, in this work we are interested in vortices, which are point-like defects living on a two-dimensional spatial timeslice. Therefore the correct operator has a photon cloud lying entirely within a single timeslice. Therefore the correct operator, which we call the “vortex operator”, is equivalent to gauge-fixing to the Coulomb gauge:

$$\Phi_V(x) = \exp(-2\pi i \Delta^{-1} \delta_2 A) \Phi_x , \quad (1.27)$$

where now δ_2 is the *spatial* divergence and Δ the *spatial* Laplacian. Again, the operator eq. (1.27) is gauge invariant and therefore a valid observable. In this case, the prefactor of eq. (1.27) represents a Coulomb cloud extending in the spatial directions, consistent with its interpretation as a vortex operator. In the $\kappa \rightarrow \infty$ limit in which scalar QED reduces to the integer gauge theory, the vortex operator (1.27) becomes

$$\Phi_V(x) = \exp(-2\pi i \Delta^{-1} \delta A) , \quad (1.28)$$

where now A is integer-valued. Rigorous mathematical work has shown that the operator (1.28) gives rise to topological sectors [78]. Because of its Coulomb cloud, the vortex operator is non-local in space (but still local in time). In fact, the vortex is an *infraparticle* [12, 78, 84–86] which is especially infrared sensitive. We will discuss this further in Section 1.7.

In our case the various choices of gauge have a physical interpretation and therefore we simply consider one, gauge-invariant operator (i.e. eq. (1.28)). Nonetheless, the issue of the choice of gauge has received significant attention in the context of a rigorous interpretation of the Higgs mechanism [79, 87–89]. Perturbatively, one considers the expectation value of the scalar field Φ , which is not gauge-invariant. In the Higgs phase, Φ is supposed to acquire a vacuum expectation value. However since it is not a gauge-invariant operator, this statement is gauge dependent. For example, it does in Landau gauge [87] but not in axial gauge [89]. In Coulomb gauge, which is the one corresponding to the vortex operator, a non-zero vacuum expectation value has been rigorously shown in the relevant phase of scalar QED in four dimensions [78]. In three dimensions, we are not aware of rigorous results, but our work provides numerical evidence for a non-zero vacuum expectation value in the Higgs phase.

We note that it is in fact entirely possible to describe the Higgs mechanism in a non-perturbative gauge-invariant manner [89]. Moreover, the Higgs phase can be distinguished from a Coulomb phase by the fact that it is massive (i.e. gapped) as opposed to massless. In fact the Higgs phase is often analytically connected to another massive phase, the confining phase, and there is therefore no local order parameter distinguishing the two [90]. Very recently, it has been argued that the two phases can nonetheless be distinguished as symmetry-protected topological (SPT) phases [91, 92].

In what follows, we will mostly be interested in correlation functions of the vortex operator,

$$\langle \Phi_V(x) \Phi_V(y)^* \rangle, \quad (1.29)$$

from which all quantities of interest in this work can be computed. To further understand the duality correspondence between the vortex and the charged particle, it is then interesting to ask what the vortex correlation function corresponds to in the original theory.

To this end, we derive a different representation of the partition function of the $O(2)$ model. See also [11, 78, 93]. In particular, starting from the usual partition function in Villain form,

$$Z = \left(\prod_x \frac{1}{2\pi} \int_{-\pi}^{\pi} d\varphi_x \right) \left(\prod_l \sum_{n_l \in \mathbb{Z}} \right) \exp \left[-\frac{1}{2g^2} \sum_l (d\varphi_l + 2\pi n_l)^2 \right], \quad (1.30)$$

we perform a Hodge decomposition of the Villain field n_l :

$$n = \delta \square^{-1} dn + d \square^{-1} \delta n. \quad (1.31)$$

Instead of summing over n we can then instead sum over $k = \square^{-1} \delta n$ and $m = dn$, as long as we impose the constraints $\delta k = 0$ and $dm = 0$. Since k is a 0-form, the first such constraint is trivial. Thus we find,

$$Z = \left(\prod_x \sum_{k_x \in \mathbb{Z}} \frac{1}{2\pi} \int_{-\pi}^{\pi} d\varphi_x \right) \left(\prod_l \sum_{\substack{m_l \in \mathbb{Z} \\ dm=0}} \right) \exp \left[-\frac{1}{2g^2} \sum_l (d\varphi_l + 2\pi dk_l + 2\pi \delta \square^{-1} m_l)^2 \right]. \quad (1.32)$$

Now we replace $\Phi = \varphi + 2\pi k$. This is a non-compact zero form; summing over l and integrating over φ is equivalent to integrating Φ over the whole real axis, so the partition function is

$$Z = \left(\prod_x \int_{-\infty}^{\infty} d\Phi_x \right) \left(\prod_l \sum_{\substack{m_l \in \mathbb{Z} \\ dm=0}} \right) \exp \left[-\frac{1}{2g^2} \sum_l (d\Phi_l + 2\pi \delta \square^{-1} m_l)^2 \right]. \quad (1.33)$$

The two partition functions actually completely decouple, since (using the inner product between forms and integration by parts) the cross term vanishes,

$$(d\Phi, \delta\Box^{-1}m) = (\Phi, \delta^2\Box^{-1}m) = 0. \quad (1.34)$$

Thus we see that the partition function factorizes into a “spin wave” part and a “vortex part”,

$$Z = Z_{\text{sw}}Z_{\text{vortex}}, \quad (1.35)$$

where

$$Z_{\text{sw}} = \left(\prod_x \int_{-\infty}^{\infty} d\Phi_x \right) \exp \left[-\frac{1}{2g^2} (d\Phi, d\Phi) \right]. \quad (1.36)$$

and, simplifying the expression using integration by parts (note that $\Box m = d\delta m$ since $dm = 0$),

$$Z_{\text{vortex}} = \left(\prod_l \sum_{\substack{m_l \in \mathbb{Z} \\ dm=0}} \right) \exp \left[-\frac{2\pi^2}{g^2} (m, \Box^{-1}m) \right]. \quad (1.37)$$

This decomposition is familiar from the analytical treatment of the BKT transition. We see that Z_{sw} describes simply a real massless scalar, has no phase transition, and is rather uninteresting. On the other, the vortex partition function is the partition function for a Coulomb gas. Here m is a 2-form (thus living on plaquettes) which can be interpreted as the vorticity associated with plaquettes. Since the φ are angular variables, we have $d^2\varphi = 0 \pmod{2\pi}$, while the equality would have been exact if the φ were genuine non-compact variables. For each link, the excess above 2π is absorbed by the Villain variable n . Then $m = dn$ is just the sum of the excesses around a plaquette, and is thus a natural definition of vorticity. This is a lattice analog of the continuum definition of vorticity, where we integrate the derivative of the angular field around a small closed loop. The constraint $dm = 0$ is a conservation law, i.e. there are no sources of vorticity. In the dual picture, m is a 1-form and is then interpreted as a vortex worldline. The conservation law is $\delta m = 0$, which implies that the vortex lines are closed [11]. It is interesting that the Villain formulation allows direct access to the vorticity via the auxiliary field n ; while the physics is the same as in the cosine formulation, it is less clear how to define the vorticity in that case. This property of the Villain action has been used recently to construct novel lattice discretizations with desirable properties [94, 95].

Since, as we already mentioned, the duality provides a dictionary between the two theories, we can use it to relate observables on the two sides of the transition. For the vortex correlation function, we obtain in the vortex gas representation

$$\langle \Phi_V(x) \Phi_V(y)^* \rangle = \frac{\left(\prod_l \sum_{\substack{m_l \in \mathbb{Z} \\ dm = -dB}} \right) \exp \left[-\frac{2\pi^2}{g^2} ((m+B), \Box^{-1}(m+B)) \right]}{\left(\prod_l \sum_{\substack{m_l \in \mathbb{Z} \\ dm=0}} \right) \exp \left[-\frac{2\pi^2}{g^2} (m, \Box^{-1}m) \right]}, \quad (1.38)$$

where $B = B_{\tilde{x}} - B_{\tilde{y}}$ and $B_{\tilde{x}} = \delta_2 \Delta^{-1} \delta_{\tilde{x}}$ is the spatial Coulomb field arising from a point-like source located on the cube \tilde{x} dual to the dual lattice point x . Thus $\delta_{\tilde{x}}$ is a 3-form on the original lattice. Then $B_{\tilde{x}}$ is a 2-form which satisfies $dB_{\tilde{x}} = \delta_{\tilde{x}}$. The vortex correlation function is actually a ratio of partition functions (note that the state space sampled in the numerator and denominator are different), as is standard with the construction of topological defects via disorder operators [96]. In the dual interpretation, the vortex correlator introduces an open vortex worldline in the sea of closed vortex worldlines.

Finally, an expression for the expectation value of the vortex correlation function can also be derived directly in the original formulation. One finds again a ratio of partition functions [11]

$$\langle \Phi_V(x) \Phi_V(y)^* \rangle = \frac{1}{Z} \left(\prod_x \frac{1}{2\pi} \int_{-\pi}^{\pi} d\varphi_x \right) \left(\prod_l \sum_{n_l \in \mathbb{Z}} \right) \exp \left[-\frac{1}{2g^2} \sum_l (d\varphi_l + 2\pi n_l - D_l)^2 \right], \quad (1.39)$$

where D is the defect,

$$D = 2\pi\delta\Box^{-1}(B - \omega). \quad (1.40)$$

In this formula, ω is (the dual of) an integer-valued 1-form (i.e. the ‘‘Dirac string’’) which connects x and y . Expanding the square, we can also interpret this as an observable in the original theory, where the compact scalar couples to the vortex defect D .

Let us also now clarify an important distinction which may be a source of confusion. Our interest is studying the vortex in the original $O(2)$ model. From the duality, the vortex can be studied as the charged particle in the dual model, which is the integer gauge theory. On the other hand the scalar QED theory may also be interpreted as the Landau-Ginzburg theory describing the superconducting phase transition [63]. In this language, the Higgs phase is the superconducting phase, where the photon is massive. In this phase there is a *superconducting* vortex, which is *not* the one we are interested in, which is a stable particle with finite energy in the infinite volume. From the dual point of view, we shall only be concerned with the charged particle, which corresponds to the $O(2)$ vortex in the original model.

Finally, we also mention that one often encounters in the literature a different kind of duality. This is known as a ‘‘low-energy duality’’ and *cannot* be obtained via a change of variables in the partition function. It is *not* an exact duality. Rather, it is the statement that two different continuum theories flow to the same RG fixed point. In this context ‘‘particle-vortex duality’’ predicts that in three dimensions the $O(2)$ model eq. (1.1) is dual to the Abelian Higgs model (i.e. scalar QED) with gauge group $U(1)$ [97–99]. There is some numerical evidence for this duality, as long as one is extremely close to the phase transition [100]. Many other low-energy dualities have been conjectured [101].

1.5 Boundary conditions and symmetries

To perform numerical simulations, the theory is placed on a finite lattice, which therefore must be supplemented with appropriate boundary conditions. The most obvious choice is periodic boundaries, which preserve translation invariance. However, this choice is unsuitable in this case. As we have seen, we are interested in configurations with overall non-zero vortex number. In the dual picture, the vortex becomes the charged particle, and we thus care about configurations with non-zero charge. But the topology of periodic boundary conditions is that of a torus, which, as a surface, has no boundary. Thus by Gauss’ law, the overall charge on a torus must be zero. Because of this phenomenon, the vortex operator eq. (1.28) is ill-defined with periodic boundaries. We can see this explicitly. On 0-forms such as δA , the Laplacian acts as

$$\Delta f(\vec{x}) \equiv (d\delta + \delta d)f(\vec{x}) = \sum_i \left[f(\vec{x} + \hat{i}) + f(\vec{x} - \hat{i}) - 2f(\vec{x}) \right], \quad (1.41)$$

where the sum is over the spatial directions only, since Δ is the spatial Laplacian. To define the vortex operator eq. (1.28) we need the inverse Laplacian Δ^{-1} which can be obtained by solving for the Green’s function G such that

$$\Delta G(\vec{x}) = \delta(\vec{x}), \quad (1.42)$$

where $\delta(\vec{x})$ is the Kronecker delta. This equation can be easily solved by going to momentum space. For periodic boundaries the momentum takes values $k_i = \frac{2\pi n_i}{L}$ if the spatial size is L , where n_i is an integer. Then the Green's function is (for 2 spatial dimensions)

$$G(\vec{k}) = \frac{1}{2 \sum_i \cos k_i - 2} . \quad (1.43)$$

In particular, the momentum $\vec{k} = 0$ is allowed and therefore $G(0)$ is divergent. This means that the Laplacian Δ is not invertible, and the vortex operator eq. (1.28) is ill-defined.

To remedy this issue, we modify the boundary conditions. The most general boundary conditions on the fields which preserve translation invariance are schematically of the form

$$\phi(x + L\hat{\mu}) = S\phi(x) , \quad (1.44)$$

where S is a symmetry operation. Among this class of boundary conditions, we choose C -periodic boundary conditions [12, 102, 103], where we perform charge conjugation C as we go across the boundary. This acts as

$$C : A_\mu(x) \rightarrow -A_\mu(x) , \quad (1.45)$$

and therefore, on the vortex operator eq. (1.28), as

$$C : \Phi_V(x) \rightarrow \Phi_V(x)^* , \quad (1.46)$$

consistent with the action of charge conjugation on a complex scalar. Since the Laplacian is spatial, we apply C -periodic boundary conditions only in the spatial directions. In the time direction, we choose to apply standard periodic boundary conditions in order to maintain the thermodynamic interpretation of the partition function. Thus we work with boundary conditions such that

$$A_\mu(x + L\hat{t}) = -A_\mu(x) . \quad (1.47)$$

In the time direction all quantities remain periodic. Since the Laplacian is applied to δA , which sees antiperiodic boundary conditions if we choose C -periodic boundary conditions, then the expression for the Green's function eq. (1.43) remains unchanged, but the allowed momenta for antiperiodic functions are instead $k_i = \frac{\pi(2n_i+1)}{L}$ for integer n_i . Thus $\vec{k} = 0$ is not allowed and the Laplacian is indeed invertible.

We also discuss another technical issue, this time directly with the partition function of the integer gauge theory. For a thorough discussion of this problem, see [104, 105]. Due to the non-compactness of the height variables, the partition function is technically infinite, i.e. $Z = \infty$, even in a finite volume. This infinity is due in the first place to the gauge symmetry; the summation over some of the gauge field variables is redundant, and since they are non-compact they give rise to infinities. One should then appropriately gauge-fix the partition function so that integrations occur only over a minimal set of gauge fields. However, this is not an issue in practice when computing gauge-invariant observables, which schematically take the form

$$\langle O \rangle = \frac{\int DA e^{-S} O}{\int DA e^{-S}} . \quad (1.48)$$

As long as O is gauge-invariant, the redundant summations are the same in both the numerator and denominator and therefore simply contribute an irrelevant, even though infinite, constant prefactor which can be cancelled out. However, even gauge-fixing is not sufficient to make the partition function finite. In fact, with periodic boundaries the action is invariant under a shift symmetry

$$A_\mu(x) \rightarrow A_\mu(x) + n_\mu , \quad (1.49)$$

where n_μ is an integer which depends only on the direction μ . This symmetry may also be seen as arising from the fact that the gauge-fixed action is actually independent of one or more gauge field values (equal to the number of periodic directions). Thus again one has infinite summations over the integers, leading to $Z = \infty$. However this is not a problem in practice. First of all, C -periodicity in a direction forbids the shift symmetry eq. (1.49) in that direction, so the issue only affects the periodic directions (which is only one in our case). Even then, this will again contribute simply equal, constant infinite prefactors in the numerator and denominator of any gauge-invariant, shift-invariant observable which cancel each other. Thus such operators are thus not affected by this issue. In fact the vortex operator is invariant under the shift symmetry eq. (1.49). While this is an acceptable resolution of this “zero mode” problem for pure gauge theories, with the inclusion of matter fields it is not sufficient and one must resort to different methods [105].

Finally, we discuss the symmetries of the action with our chosen C -periodic boundaries. The action of the integer gauge theory is in principle invariant under generic \mathbb{Z} -valued gauge transformations, which are the remnant of the original \mathbb{R} -valued gauge transformations of scalar QED after sending $\kappa \rightarrow \infty$. In the original $O(2)$ model the phase transition is characterized by the breaking of the $O(2)$ symmetry; on the other hand in the dual theory the same transition is characterized by the “breaking” of the gauge symmetry (in the sense of a Higgs phase). As is clear in this case, and as we have already remarked, it is not possible to directly relate symmetries on the two sides of a duality. In any case, under a \mathbb{Z} -valued gauge transformation,

$$A_\mu(x) \rightarrow A_\mu(x) + \alpha(x + \hat{\mu}) - \alpha(x) . \quad (1.50)$$

But in a finite volume, consistency with C periodic boundary conditions also requires the gauge transformation α_x to be antiperiodic up to a constant integer,

$$\alpha(x + L\hat{i}) = -\alpha(x) + m_i , \quad (1.51)$$

where m_i depends only on the direction. This can be easily seen by translating the gauge transformation eq. (1.50) and applying the boundary condition eq. (1.47). Of course in the time direction we have periodic boundaries, so α is *periodic* up to a constant integer,

$$\alpha(x + N_T\hat{0}) = \alpha(x) + m_0 . \quad (1.52)$$

Here N_T is the number of lattice spacings in the time direction. The antiperiodicity in the space directions implies that the *global* part of the gauge symmetry is rather different with periodic vs C -periodic boundary conditions. In the C -periodic case, the only constant gauge transformations allowed are those which are half-integer valued, $\alpha(x) \equiv \alpha \in \frac{1}{2}\mathbb{Z}$. It is easy to check that under such a transformation,

$$\Phi_V \rightarrow -\Phi_V . \quad (1.53)$$

Therefore we call this \mathbb{Z}_2 symmetry “vortex field reflection”. In fact, as we will see, the two phases of the model can be characterized in terms of this \mathbb{Z}_2 symmetry. In the Coulomb phase, where the vortices exist as particles, the \mathbb{Z}_2 symmetry is unbroken and the vortex operator has zero vacuum expectation value. On the other hand, in the Higgs phase the vortex operator acquires a vacuum expectation value and therefore the vortices are condensed, and the \mathbb{Z}_2 vortex field reflection symmetry is broken. This *does not* mean that the phase transition is in the \mathbb{Z}_2 universality class. By the duality, it is clear that it is in the $O(2)$ universality class and in fact the \mathbb{Z}_2 vortex field reflection symmetry is really only a finite volume effect. Interestingly, from

the point of view of the dual theory, even in infinite volume (where one has the full \mathbb{Z} gauge invariance), it would not be clear that the transition is in the $O(2)$ universality class.

As we mentioned before, it is not possible to directly relate symmetries on the two sides of the duality. However, given its action on the vortex field eq. (1.53), it is quite natural to identify the global part of the \mathbb{Z} symmetry with vortex number. After all, the vortex is dual to the charged particle whose charge is determined by the \mathbb{Z} symmetry.

We end this section by noting the following fact. We've seen that under charge conjugation the vortex field transforms by complex conjugation

$$C : \Phi_V \rightarrow \Phi_V^* . \quad (1.54)$$

Therefore, its real and imaginary parts transform differently,

$$C : \text{Re } \Phi_V \rightarrow \text{Re } \Phi_V , \quad \text{Im } \Phi_V \rightarrow -\text{Im } \Phi_V . \quad (1.55)$$

Therefore with C -periodic boundary conditions, $\text{Re } \Phi_V$ sees periodic boundaries, while $\text{Im } \Phi_V$ sees antiperiodic boundaries. Therefore the allowed momenta for the real part of the vortex field are of the form $2n\pi/L$ for $n \in \mathbb{Z}$, while for the imaginary part they are instead $(2n+1)\pi/L$ for $n \in \mathbb{Z}$. As such, the lowest momentum state one can form with the real part of the vortex field has momenta $(0, 0)$ in both spatial directions; on the other hand, the lowest momentum state one can form with the imaginary part of the vortex field has momenta $(\pi/L, \pi/L)$, assuming that both spatial directions have L sites.

1.6 Numerical calculations and results

We simulated the integer gauge theory with a standard Metropolis algorithm on lattices with $L^2 N_T$ sites, with equal size in the space directions. In this work, we focused on the zero-momentum sector and we thus projected the vortex operator according to the prescription in the previous section,

$$\Phi_V(t) \equiv \frac{1}{L^2} \sum_{\vec{x}} \text{Re } \Phi_V(t, \vec{x}) , \quad (1.56)$$

where $x = (t, \vec{x})$. Then all quantities of interest can be extracted from the correlation function of the vortex operator,

$$C(t) \equiv \langle \Phi_V(0) \Phi_V(t) \rangle . \quad (1.57)$$

At the theoretical level, in Euclidean space, correlation functions of operators can be expanded in the so-called spectral decomposition,

$$\langle \Phi_V(0) \Phi_V(t) \rangle = \frac{1}{Z} \sum_{n,m} |\langle n | \Phi_V | m \rangle|^2 e^{-tE_m + (t-N_T)E_n} . \quad (1.58)$$

This can be obtained by writing $\Phi_V(t) = e^{tH} \Phi_V(0) e^{-tH}$ and then inserting appropriate energy eigenstates. The partition function itself can be expanded in a similar manner, i.e.

$$Z = \sum_{n=0}^{\infty} e^{-N_T E_n} . \quad (1.59)$$

In particular, the correlation function $C(t)$ of eq. (1.57) is computed numerically via Monte Carlo simulations, and then fitted to eq. (1.58) (truncated to a certain order) in order to extract quantities of interest such as matrix elements or energies. Importantly, one only has access to

states whose corresponding matrix elements are non-zero. As we will see in a moment, these are mostly determined by symmetry.

In the Coulomb phase the vortices exist as particles. Thus, we expect a unique vacuum state with vortex number zero (i.e. no vortices). The same sector with zero vortex number also contains states which correspond to vortex-antivortex pairs. However, we are interested in states with overall non-zero vortex number. As explained in the previous section, in finite volume the boundary conditions break vortex number down to \mathbb{Z}_2 vortex field reflection, and it is therefore only conserved modulo 2. In particular, the vortex operator Φ_V is odd under vortex field reflection and therefore it couples only to states with non-zero vortex number. For example, by symmetry all matrix elements $\langle n | \Phi_V | 0 \rangle$ where 0 is the vacuum and $|n\rangle$ is \mathbb{Z}_2 -even are zero. Thus, in this phase, the lowest-lying state in the vortex field reflection-odd sector can be naturally identified with the state corresponding to a single vortex. Since the operator $\Phi(t)$ has zero momentum, the corresponding energy can be naturally identified with the vortex mass m_V . This calculation was performed in [10] (see also [11] for more details) and it was found that the mass behaves as

$$m_V \sim |t|^{\nu_V} \log \frac{L}{L_0} , \quad (1.60)$$

where $t = g^2 - g_c^2$ is the distance from the phase transition. In particular, much like in the classical theory, the vortex mass is logarithmically divergent with the spatial volume. In the continuum limit, it scales with a critical exponent ν_V which is found to be numerically equal to the critical exponent for the ordinary field, $\nu_V = \nu$ [10].

Here we are mostly concerned with the behaviour of the vortex in the Higgs phase. In particular, since the vortices are condensed, the natural quantity to study is the vortex condensate. In this phase the \mathbb{Z}_2 vortex field reflection symmetry is spontaneously broken and therefore the structure of the Hilbert space is more complicated [106, 107]. In infinite volume, one expects two exactly degenerate ground states $|0_{\pm}\rangle$ related by the \mathbb{Z}_2 symmetry. These define two superselection sectors, where all matrix elements between the two sectors are zero. In finite volume, however, there is no true spontaneous symmetry breaking. In particular, the vacuum is always unique and invariant under the symmetry. One expects that on top of the finite-volume ground state $|+\rangle$ (which is \mathbb{Z}_2 even) one finds another almost degenerate state $|-\rangle$ which is \mathbb{Z}_2 -odd. Their energy difference is exponentially small in the volume. One can then form appropriate linear combinations which are finite-volume versions of the infinite-volume ground states,

$$|0_+\rangle = \frac{|+\rangle + |-\rangle}{\sqrt{2}} , \quad |0_-\rangle = \frac{|+\rangle - |-\rangle}{\sqrt{2}} . \quad (1.61)$$

As expected, under vortex field reflection $|0_{\pm}\rangle \rightarrow |0_{\mp}\rangle$. Since the gap between $|\pm\rangle$ is exponentially small in the volume, $|0_{\pm}\rangle$ become degenerate in infinite volume. In infinite volume, one would want to compute the vortex condensate

$$\langle 0_+ | \Phi_V | 0_+ \rangle = - \langle 0_- | \Phi_V | 0_- \rangle , \quad (1.62)$$

as the two states are related by the \mathbb{Z}_2 symmetry. However, in finite volume $|0_{\pm}\rangle$ are not energy eigenstates and therefore they are not accessible from the spectral decomposition eq. (1.58). Therefore, we work with $|\pm\rangle$ instead. By symmetry,

$$\langle + | \Phi_V | + \rangle = \langle - | \Phi_V | - \rangle = 0 . \quad (1.63)$$

On the other hand, one has

$$\langle - | \Phi_V | + \rangle = \langle 0_+ | \Phi_V | 0_+ \rangle + \frac{1}{2} \langle 0_+ | \Phi_V | 0_- \rangle + \frac{1}{2} \langle 0_- | \Phi_V | 0_+ \rangle , \quad (1.64)$$

where we used eq. (1.62). Because of the superselection structure, the mixed terms are exactly zero in infinite volume and exponentially small in finite volume. Thus $\langle -|\Phi_V|+\rangle$ may be taken as the definition of the vortex condensate in finite volume. To avoid issues with the sign, we define the *vortex condensate* to be

$$\Sigma_V \equiv |\langle -|\Phi_V|+\rangle| , \quad (1.65)$$

which can be extracted from the spectral decomposition eq. (1.58).

As we will see in a moment, in order to renormalize the vortex condensate we will need to compute another quantity *in the Coulomb phase*. This is the *vortex susceptibility*

$$\chi_V \equiv \frac{1}{2L^2 N_T} \sum_{x,y} \langle \text{Re } \Phi_V(x) \text{Re } \Phi_V(y) \rangle , \quad (1.66)$$

where $L^2 N_T$ is the spacetime volume. This was defined in analogy with the susceptibility of the ordinary O(2) field [24]. In the Coulomb phase the vortex has zero vacuum expectation value. Therefore its dynamics is roughly a random walk, which has variance of order volume. Thus the order volume prefactor of eq. (1.66) ensures that the susceptibility is finite in the infinite volume limit. Plugging in the spectral decomposition eq. (1.58) into the expression for the vortex susceptibility, eq. (1.66), one finds in the infinite time extent limit $N_T \rightarrow \infty$ (or zero temperature limit)

$$\chi_V \rightarrow \frac{L^2}{2} \sum_{n>0} |\langle n|\Phi_V|0\rangle|^2 \coth\left(\frac{E_n}{2}\right) . \quad (1.67)$$

In the infinite volume limit, the vortex mass is divergent and therefore $E_n \rightarrow \infty$, so that $\coth E_n \rightarrow 1$. Therefore the fact that the vortex has infinite mass in the Coulomb phase does not make the susceptibility χ_V ill-defined (note that the matrix elements $|\langle n|\Phi_V|0\rangle|^2$ are L -dependent).

As we have noted several times, the vortex operator is non-local. Most of the theory of statistical mechanics relies on the locality of operators, and it is therefore a priori unclear if one can assume that the vortex operator behaves in the same way as standard local operators. In what follows, we will assume functional forms typical of the scaling theory of local operators, and we find that the vortex operator, despite being non-local, can be adequately fitted with this choice. In particular, after performing an infinite volume extrapolation, one can fit the condensate and susceptibility to the scaling forms

$$\Sigma_V \sim |t|^{\beta_V} , \quad (1.68)$$

and

$$\chi_V \sim |t|^{-\gamma_V} , \quad (1.69)$$

where $t = g^2 - g_c^2$ is the distance from the phase transition and β_V, γ_V are critical exponents associated with the vortex.

These exponents are related to each other by scaling relations. In particular, our theory can be driven to a continuous phase transition by tuning *one* appropriate coupling t . Suppose that we are interested in the behaviour of an observable which is coupled via a coupling h . Then the free energy of the system is a function $f(t, h)$ of the two couplings. In the simplest examples h is a magnetic field coupled to the system's magnetization, but in principle it could be any local operator. Again it is a priori not clear if standard scaling theory applies to the vortex operator, which is non-local. But as we will see, if we *do* apply it, its predictions are in excellent agreement with the numerical data. Therefore in this case we choose h to couple to the vortex

operator. Now, according to the *scaling hypothesis* [108], the free energy near the transition is assumed to be a homogeneous function of the two couplings, i.e. for any positive λ one has

$$f(\lambda^{\Delta_t} t, \lambda^{\Delta_h} h) = \lambda^d f(t, h) . \quad (1.70)$$

Here d is the (spacetime) dimension of the system and Δ_t and Δ_h are the scaling dimensions of the two couplings (the scaling dimensions of the corresponding operators are then simply $d - \Delta_t$ and $d - \Delta_h$). Homogeneity implies that f can be described in terms of a function g of a single variable, i.e.

$$f(t, h) = t^{d/\Delta_t} g\left(\frac{h}{t^{\Delta_h/\Delta_t}}\right) . \quad (1.71)$$

Then, for example, the expectation value of the operator coupled to h can be obtained by differentiating. So if h couples to the vortex operator, we find

$$\Sigma_V \sim \left. \frac{\partial f}{\partial h} \right|_{h=0} \sim t^{\frac{d-\Delta_h}{\Delta_t}} . \quad (1.72)$$

Therefore the critical exponent for the condensate is

$$\beta_V = \frac{d - \Delta_h}{\Delta_t} . \quad (1.73)$$

On the other hand, for the susceptibility one has

$$\chi_V \sim \left. \frac{\partial^2 f}{\partial h^2} \right|_{h=0} \sim t^{\frac{d-2\Delta_h}{\Delta_t}} , \quad (1.74)$$

so that

$$\gamma_V = \frac{2\Delta_h - d}{\Delta_t} . \quad (1.75)$$

Finally, as usual the free energy at $h = 0$ scales as $f \sim \xi^{-d}$ where ξ is the correlation length (i.e. the inverse mass) [21] so that

$$\nu_V = \nu = \frac{1}{\Delta_t} . \quad (1.76)$$

Therefore, the three critical exponents can be determined in terms of only two quantities, the scaling dimensions of the two operators. Equivalently, the critical exponents satisfy the ‘‘scaling relation’’

$$\gamma_V + 2\beta_V = \nu d . \quad (1.77)$$

As we will see in a moment, the numerically computed critical exponents γ_V and β_V indeed satisfy this scaling relation. Thanks to this scaling relation we can construct a quantity which is finite as we approach the transition. This is the universal amplitude ratio

$$R_V \equiv \frac{\Sigma_V^2(t)\xi(t)^3}{\chi_V(-t)} , \quad (1.78)$$

which is finite as we take the continuum limit by tuning the coupling to the critical point. Here ξ is the usual (second-moment) correlation length in the symmetric phase of the original O(2) model, which scales as $\xi \sim |t|^{-\nu}$. We choose to work with ξ because it is finite in the infinite volume limit, unlike the vortex mass m_V . The correlation length can be computed to a high precision using the Wolff cluster algorithm [109]. As the transition is approached, i.e. $t \rightarrow 0$, the universal amplitude ratio eq. (1.78) becomes a universal number characterizing the

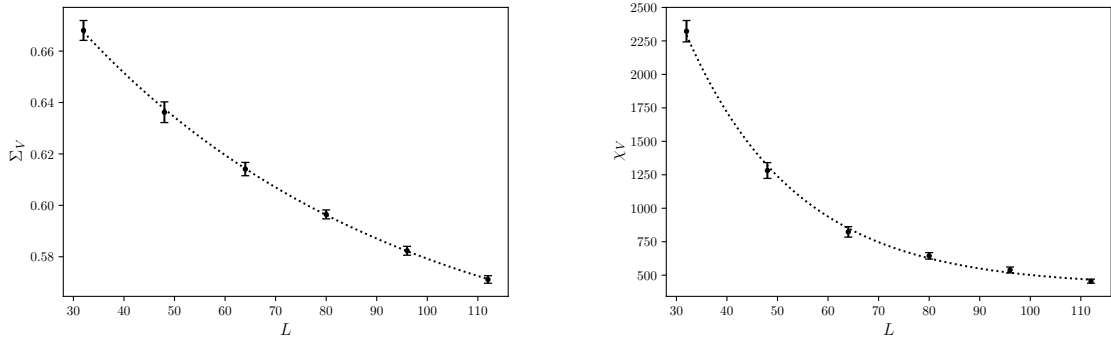


Figure 1.3: Finite volume scaling of the condensate (*left*) and susceptibility (*right*), at couplings in the two phases at the same distance from the phase transition, with $|g^2 - g_c^2| = 0.015103$. The dotted line is the exponential fit. Reprinted from [1].

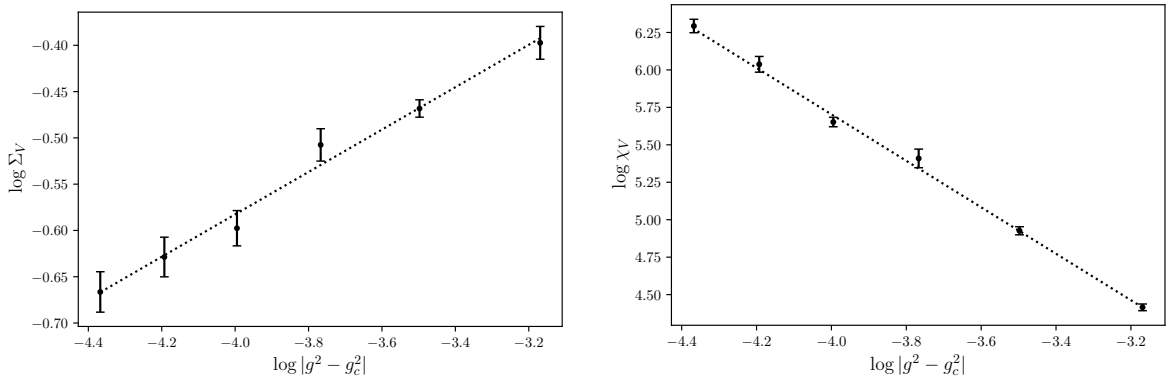


Figure 1.4: Continuum scaling for the condensate (*left*) and susceptibility (*right*) on a logarithmic scale, together with a linear fit (dotted line). Reprinted from [1].

behaviour of the vortex near the Wilson-Fisher fixed point. In particle physics language, it may also be interpreted as a renormalized vortex condensate. We note that an attempt to obtain a renormalized condensate for monopoles in four-dimensional U(1) gauge theory was made in [13] using similar techniques. In that case, a renormalized condensate could not be obtained, possibly because in four dimensions U(1) gauge theory only has a first-order phase transition and therefore no continuum limit.

The parameters and results of the numerical simulations are given in Table 1.2. The couplings in the two phases were chosen to lie at the same distance from the transition. For each coupling, the simulations were performed at fixed time extent N_T and increasing spatial sizes L . Note that for the condensate we found a small but significant error from the finite N_T extrapolation; therefore we repeated each simulation for five increasing values of N_T and included the difference in the error budget. Note that more statistics were required in the Coulomb phase in order to sufficiently resolve the finite-volume behaviour.

For the determination of the condensate, one has to keep in mind the more complicated structure of the Hilbert space due to symmetry breaking. In particular, the presence of almost-degenerate states needs to be accounted for. For the susceptibility, no fitting is required. Thus both quantities were determined for each spatial size L and coupling g^2 . They were then extrapolated to infinite volume by fitting to an exponential form, as shown in Fig. 1.3. As is clear

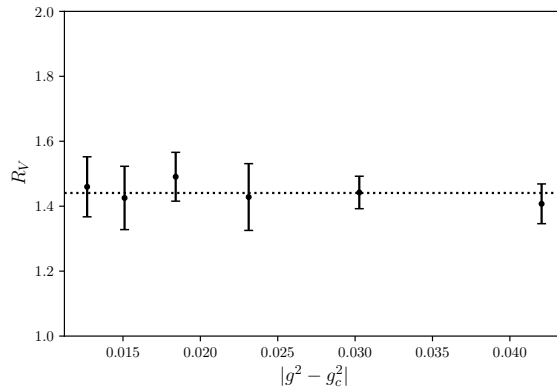


Figure 1.5: Continuum scaling of the amplitude ratio eq. (1.78), together with a constant fit (dotted line). Reprinted from [1].

Both		Coulomb			Higgs			
$ g^2 - g_c^2 $	L_{\max}	g^2	sweeps	χ_V	g^2	sweeps	Σ_V	ξ
0.042051	64	2.960331	$2 \cdot 10^6$	83(2)	3.044449	$5 \cdot 10^5$	0.67(1)	6.36(2)
0.030270	80	2.972112	$2 \cdot 10^6$	138(4)	3.032668	$5 \cdot 10^5$	0.626(6)	7.97(3)
0.023123	80	2.979259	$2 \cdot 10^6$	223(13)	3.025521	$5 \cdot 10^5$	0.60(1)	9.59(3)
0.018407	112	2.983975	$4 \cdot 10^6$	285(9)	3.020805	$1 \cdot 10^6$	0.55(1)	11.20(4)
0.015103	112	2.987278	$4 \cdot 10^6$	419(22)	3.017502	$1 \cdot 10^6$	0.53(1)	12.80(4)
0.012683	128	2.989699	$8 \cdot 10^6$	541(24)	3.015081	$2 \cdot 10^6$	0.51(1)	14.41(5)

Table 1.2: Parameters and results of the simulations in the Coulomb and Higgs phases. The couplings in the two phases are chosen so that they are at the same distance from the phase transition, which is located at $g_c^2 = 3.00239(6)$. The maximum spatial lattice size is the same for corresponding couplings. The quoted values for Σ_V , χ_V and ξ refer to their extrapolation to infinite volume.

from the figure, the susceptibility overall has much stronger finite volume effects. Unfortunately, no theoretical predictions are available for the finite-volume scaling, but we found good agreement with the exponential fits. Other fitting forms, such as power laws, were found to be incompatible with the data.

Finally, the quantities were extrapolated to the continuum limit by fitting to the assumed scaling forms (1.68) and (1.69). This is shown (on a logarithmic scale) in Fig. 1.4. As is clear from the plots, the data fit accurately the predicted scaling form, with $\chi^2/\text{d.o.f.} \approx 0.59$ for the condensate and $\chi^2/\text{d.o.f.} \approx 0.93$ for the susceptibility. On the other hand, the amplitude ratio is shown in Fig. 1.5. Again, the result is consistent with the prediction of the scaling relation eq. (1.77).

The final results are therefore found to be

$$\begin{aligned}
 \chi_V &= C_\chi |t|^{-\gamma_V} , & C_\chi &= 0.61(7) , & \gamma_V &= 1.55(3) , \\
 \Sigma_V &= C_\Sigma |t|^{\beta_V} , & C_\Sigma &= 1.40(9) , & \beta_V &= 0.23(2) , \\
 & & R_V &= 1.44(3) . & &
 \end{aligned} \tag{1.79}$$

The critical exponents and amplitudes in eq. (1.79) represent the main novel results of our work,

together with the fact that the critical exponents indeed satisfy the scaling relation eq. (1.77).

For completeness, we also list the critical exponents for the ordinary field of the O(2) model [110]

$$\nu = 0.67169(7) , \quad \gamma = 1.378(1) , \quad \beta = 0.34864(5) . \quad (1.80)$$

Note that in principle there's no reason why the critical exponents for the condensate and susceptibility should be the same for different operators. Within numerical precision, the vortex critical exponents satisfy the predicted scaling relation (1.77):

$$2\beta_V + \gamma_V = 2.01(3) , \quad (1.81)$$

$$3\nu = 2.0151(2) . \quad (1.82)$$

From standard scaling theory, as we have seen, one then obtains the scaling dimension of the vortex operator,

$$\Delta_V = \frac{\beta}{\nu} = 0.34(3) . \quad (1.83)$$

1.7 Infraparticles

As we have seen, the vortex, much like charged particles in general, cannot be created by a local operator [78, 85]. Such non-local operators, which have been referred to as ‘‘infraparticles’’ [78, 85, 86], are especially sensitive to the boundary conditions. In fact, already for simple electrodynamics in four spacetime dimensions, charged particles exhibit peculiar properties. It is clear that some non-locality is present in the theory, since by Gauss' law the total charge of the universe can be detected by an integral at infinity,

$$Q = \lim_{R \rightarrow \infty} R^2 \int_{S^2} dS \vec{n} \cdot \vec{E} , \quad (1.84)$$

where S^2 is the sphere at infinity. The total charge Q is also *conserved*. However, it is not only the *integral* of the electric field at infinity (i.e. Q) which is conserved, but also the value itself of the electric field at infinity [85, 111],

$$Q(\theta, \varphi) = \lim_{R \rightarrow \infty} R^2 \vec{n}(\theta, \varphi) \cdot \vec{E}(R, \theta, \varphi) . \quad (1.85)$$

In classical field theory, showing that the charges $Q(\theta, \varphi)$ are conserved is not hard. In particular, using Maxwell's equations we find,

$$\frac{\partial Q(\theta, \varphi)}{\partial t} = \lim_{R \rightarrow \infty} R^2 \vec{n}(\theta, \varphi) \cdot \frac{\partial \vec{E}(R, \theta, \varphi)}{\partial t} = \lim_{R \rightarrow \infty} R^2 \vec{n} \cdot \left[\nabla \times \vec{B} - \vec{J} \right] . \quad (1.86)$$

The second term is strictly zero because we're taking the infinite R limit and we can assume that the current distribution \vec{J} is localized. On the other hand, in four spacetime dimensions the electric and magnetic fields decay to infinity at most as fast as $1/R^2$. Thus $\nabla \times \vec{B}$ is at most $\mathcal{O}(1/R^3)$ and therefore the corresponding term vanishes in the limit. Therefore the electric field at each point at spacelike infinity is conserved.

Importantly, this gives rise to two qualitatively different cases: if the overall charge of the universe is zero, then the electric field decays faster than $1/R^2$ (for example an electric dipole has $E \sim 1/R^3$) and all the charges $Q(\theta, \varphi)$ are zero (in particular, replacing R^2 with a higher power would spoil charge conservation). On the other hand, if the overall charge of the universe is non-zero, then the electric field at each point at infinity is a conserved quantity. The charges

$Q(\theta, \varphi)$ are certainly not rotationally invariant, but they are not even invariant under a Lorentz boost. In particular, starting from electric and magnetic fields \vec{E} and \vec{B} and boosting to a frame with velocity \vec{v} with respect to the original frame leads to an electric field

$$\vec{E}' = \gamma(\vec{E} + \vec{v} \times \vec{B}) - (\gamma - 1)(\vec{E} \cdot \hat{v})\hat{v} , \quad (1.87)$$

which does not leave the charge $Q(\theta, \varphi)$ invariant.

These results (in an appropriate sense) can also be established in the quantum theory [85, 111]. Then the charges $Q(\theta, \varphi)$, being defined at infinity, commute with any local operator. Thus, in particular, no local operator can change the charge distribution at infinity, which means that operators which create charged particles must necessarily be non-local. Moreover, in a Lorentz-invariant quantum theory only local operators are allowed observables. For example, the operator which projects onto (say) the 42nd eigenstate of the Hamiltonian [75], despite being Hermitean, is not an observable. A restriction on the allowed operators leads to the concept of superselection sectors for the Hilbert space. In particular, two sectors A and B of the Hilbert space are different superselection sectors if, for any observable O ,

$$\langle \psi_A | O | \psi_B \rangle = 0 , \quad \psi_A \in A , \psi_B \in B . \quad (1.88)$$

This is a very strong condition. If the allowed observables had not been somehow restricted, then this condition would have been impossible. Since no observable can have a non-zero matrix element between different superselection sectors, no measurement can distinguish between a quantum superposition and a mixed state for two states in different superselection sectors. Therefore, morally speaking, superposition of states in different superselection sectors are forbidden. Since in a Lorentz-invariant theory only local operators are allowed (i.e. supported in a finite region of spacetime), and the charges Q are defined at spatial infinity, no observable can change the values of the charges. As we have seen, a Lorentz boost modifies the electric field at infinity and therefore the distribution of generalized charges. This means that to construct a state which transforms covariantly under Lorentz transformations, one must superimpose states belonging to different superselection sectors. But by definition of superselection, this should not be possible, thus one speaks of “spontaneous breaking of Lorentz symmetry” [78, 84–86, 112]. More generally, it is also not possible to construct a state which is simultaneously an eigenstate of both the charge operator and the mass operator [85, 86, 112]. Of course, this is mostly a *theoretical* issue, in that it manifests only in a situation where the overall charge of the universe is non-zero. Physically, every time that we extract a charge, we also leave behind one which is equal and opposite. Thus, as long as “initially” the charge of the universe is zero, it will remain zero at all times in the future and the issue is not a problem for our description of the physical universe.

As we have seen, the vortex is a non-local infraparticle. In fact, the impossibility of finding simultaneous eigenstates of charge and mass is also present in our case already at finite volume [12]. Under charge conjugation, a charged state is mapped to a state with opposite charge. We can construct a state by acting on the vacuum with the vortex operator, for example $\text{Re } \Phi_V |0\rangle$. This is a momentum eigenstate, however it is *not* a charge eigenstate, as it is invariant under C . On the other hand, for example the states $(\text{Re } \Phi_V \pm \text{Im } \Phi_V) |0\rangle$ are related by charge conjugation and are thus charged, but they are not momentum eigenstates. In fact it is not possible to construct a state with definite momentum and charge simultaneously.

1.8 Conclusions

In this chapter, we have discussed the fully quantum non-perturbative construction of vortices in the $O(2)$ model. As we have seen, both these aspects are non-trivial. Along the way, we've also learned an important lesson. Despite the fact that the vortex operator is non-local, it can be treated via standard scaling theory much like local operators. We have obtained results on the critical exponents of the vortex which can in principle be checked experimentally. From a more theoretical perspective, we have obtained the scaling dimension of the vortex operator at the Wilson-Fisher fixed point. It would be interesting to understand whether the vortex operator admits a reasonable interpretation in the context of conformal field theories. In principle, similar calculations could also be performed in the context of other models which support topological excitations, such as the $U(1)$ Abelian Higgs model or the quantum XY model.

2

Confinement in U(1) gauge theory

This chapter is based on:

M. Caselle, A. Mariani, M. Panero and A. Smecca, “Equation of state of U(1) gauge theory in three dimensions”, *to appear*.

In this chapter, we study the standard U(1) gauge theory in three dimensions. This theory is well-understood both analytically and numerically. In particular, it has been rigorously shown to be confining at all values of the coupling [80, 81]. The analytical predictions have been validated numerically [113–116]. Several studies have also been performed at finite temperature [117–122]. We first discuss the confining string and its description in terms of effective string theory. We then discuss the known results on the three-dimensional U(1) gauge theory, which will also be useful in Chapter 3.

Our main novel result is the computation of the finite temperature equation of state in this theory. By comparing it with the prediction for a gas of glueballs, we can learn some interesting facts about confinement in this theory.

As we have seen in Chapter 1, several possible lattice discretizations are possible for each continuum action. In the case of U(1) gauge theory, the two main actions are the Wilson and Villain actions, which describe the same continuum physics [93, 123, 124]. We have seen a rather similar situation in Chapter 1. In both cases, the partition function takes the form

$$Z = \left(\prod_{l \in \text{links}} \int_0^{2\pi} \right) \exp \left[- \sum_p s(d\varphi_p) \right]. \quad (2.1)$$

Here φ is a U(1)-valued 1-form, i.e. it lives on lattice links, and $d\varphi_p$ is the associated plaquette variable on plaquette p . The Wilson action takes the form

$$s(\varphi_p) = \beta(1 - \cos \varphi_p), \quad (2.2)$$

while the Villain action is given instead by

$$e^{-s(\varphi_p)} = \sum_{n \in \mathbb{Z}} e^{-\frac{\beta}{2}(\varphi_p + 2\pi n)^2}. \quad (2.3)$$

In both cases β is a dimensionless coupling, which may be expressed as $\beta = 1/e^2$ with e^2 dimensionless (which we will use in Chapter 3) as well as $\beta = 1/(ag^2)$ where g^2 is a dimensionful coupling with dimensions of energy (this will be useful later in this chapter).

Dualization proceeds much in the same way as in Chapter 1, and we will not repeat the details. The crucial step is the expansion of the Boltzmann weight in its Fourier series. In Chapter 1, we've seen already how this works for the Villain action. For the Wilson action, the corresponding expression is

$$e^{\beta \cos \varphi} = \sum_{n \in \mathbb{Z}} I_n(\beta) e^{in\varphi} , \quad (2.4)$$

where $I_n(\beta)$ is a modified Bessel function of the first kind. The dual theory corresponding to the Wilson action then has partition function

$$Z = \left(\prod_x \sum_{h_x \in \mathbb{Z}} \right) \prod_{l=\langle xy \rangle} I_{|h_x - h_y|}(\beta) , \quad (2.5)$$

where the product is over links l connecting sites x and y . The absolute value is not strictly necessary because in fact $I_n = I_{-n}$. On the other hand, with the Villain action the dual partition function is given by

$$Z = \left(\prod_x \sum_{h_x \in \mathbb{Z}} \right) \exp \left[-\frac{1}{2\beta} \sum_{\langle xy \rangle} (h_x - h_y)^2 \right] . \quad (2.6)$$

In this chapter, we will make use of both actions. In the original formulation, it is easier to use the Wilson action, and in fact most finite temperature studies in the literature have been performed with this choice of action. On the other hand, in the dual picture the Villain action is simplest, and in fact this is the action most commonly used for analytical manipulations.

Let us also note here the crucial fact that this is a $U(1)$ gauge theory, rather than an \mathbb{R} gauge theory. In fact, the partition function for the dual Villain model contains a simple quadratic term. It is only non-trivial because the scalar fields take values in the integers \mathbb{Z} ; if instead they took values in the reals \mathbb{R} , then the theory would have been simply a free massless scalar field. Suppose in fact that we were considering an \mathbb{R} gauge theory; an appropriate choice of action would have been

$$S[A] = \frac{\beta}{2} \sum_p (dA_p)^2 , \quad (2.7)$$

where dA is the plaquette variable for the non-compact real valued variable gauge field $A \in \mathbb{R}$. Then dualization of the corresponding partition function leads to a scalar field theory with a real valued scalar field $\Phi \in \mathbb{R}$ and action

$$\tilde{S}[\Phi] = \frac{2\pi^2}{\beta} \sum_{\langle xy \rangle} (\Phi_x - \Phi_y)^2 . \quad (2.8)$$

This is indeed simply the theory of a free massless scalar, which is mostly uninteresting. We had already seen this in Chapter 1 in the context of scalar QED. Thus in this case the difference between $U(1)$ and \mathbb{R} is crucial: in the former case the theory is, as anticipated, always confining, while in the latter case it is always in a Coulomb phase. This may seem particularly strange from a continuum point of view, where the distinction between $U(1)$ and \mathbb{R} is immaterial. How can an Abelian theory, which is not self-interacting, be confining? Much like in Chapter 1, the crucial difference between the two is that $U(1)$ admits topological excitations known as “monopoles”, while \mathbb{R} doesn't. Due to this non-perturbative effect, the $U(1)$ theory is actually self-interacting via monopoles. In fact, in Chapter 1 we had already seen how monopoles arise classically in this theory. We will see this in more detail in the rest of this chapter. It is also interesting to note that the situation is rather different in four dimensions: in that case, while the \mathbb{R} gauge theory

is still free, the $U(1)$ gauge theory admits two phases, a confining phase where monopoles are relevant and a Coulomb phase where they are irrelevant. Since one is interested in this latter phase, calculations with either gauge group lead to the same results in the region of interest. Finally, we note that as we have already seen in Chapter 1, the three-dimensional \mathbb{R} gauge theory can still be interesting when coupled to matter fields.

2.1 The confining string

Pure gauge theories without matter only describe gauge bosons. Nonetheless, one can introduce static external charges and study the behaviour of the gauge bosons in their presence. A natural choice is to insert a pair of charges with equal and opposite charge. Due to confinement, the electric field will only be appreciably different from the vacuum in a small region between the static charges. In particular, it will take the shape of a “flux tube” connecting the two static charges. The flux tube is also known as a “confining string”. The existence of the confining string can be seen quite clearly in the Hamiltonian picture in the strong coupling limit [125].

Another intuitive explanation for the formation of the flux string is the “dual superconductor model” [126, 127]. Ordinary superconductors exhibit the so-called Meissner effect, whereby they expel magnetic fields in the bulk [2]. More quantitatively, an external magnetic field can penetrate only an exponentially small region of a superconducting sample. If one imagines placing a monopole-antimonopole pair inside a superconductor, most of their magnetic field would be expelled, leaving simply a thin magnetic flux string between the two monopoles. In the context of gauge theories, (chromo)electric charges are confined instead, so this is referred to as a “dual” superconductor. In the three-dimensional $U(1)$ gauge theory, as we will soon see in more detail, confinement is indeed due to monopoles. However, in non-Abelian theories (due to the fact that exact dualities are not known) it is less clear if these ideas can be made precise.

As explained in detail in Chapter 3, it is possible to define a local version of the electric field as well as a local energy, associated to each lattice link. Both quantities can be measured via Monte Carlo simulations. This way, one can measure the local energy distribution in the presence of static charges for the three-dimensional $U(1)$ gauge theory. The results are shown in Fig. 2.1. From the pictures, it is clear that in all three directions the energy is highly concentrated in a string-like region between the two charges. Similarly, the electric field is on average non-zero only in a small region connecting the two charges, and virtually parallel to the line connecting them.

Mathematically, a static unit charge located at a spatial position \vec{x} is described by a “Polyakov loop”, i.e. a product of the gauge field variables at \vec{x} across all timeslices, in the time direction,

$$P(\vec{x}) = \prod_{t=0}^{N_T-1} e^{i\varphi(t,\vec{x})_0} . \quad (2.9)$$

A pair of static charges of equal and opposite charge located at \vec{x} and \vec{y} is then described by the Polyakov loop correlator $P(\vec{x})P(\vec{y})^*$. Its expectation value is actually a ratio of two partition functions,

$$\langle P(\vec{x})P(\vec{y})^* \rangle = \frac{Z_{q,-q}}{Z} . \quad (2.10)$$

This can be seen as follows [128]. As we will see in more detail in Chapter 3, in the Hamiltonian formulation of gauge theories one needs to project onto the appropriate Gauss law sector. In fact the usual partition function can be written in terms of the Hamiltonian H as

$$Z = \text{tr} \left(e^{-N_T H} \mathbb{P} \right) , \quad (2.11)$$

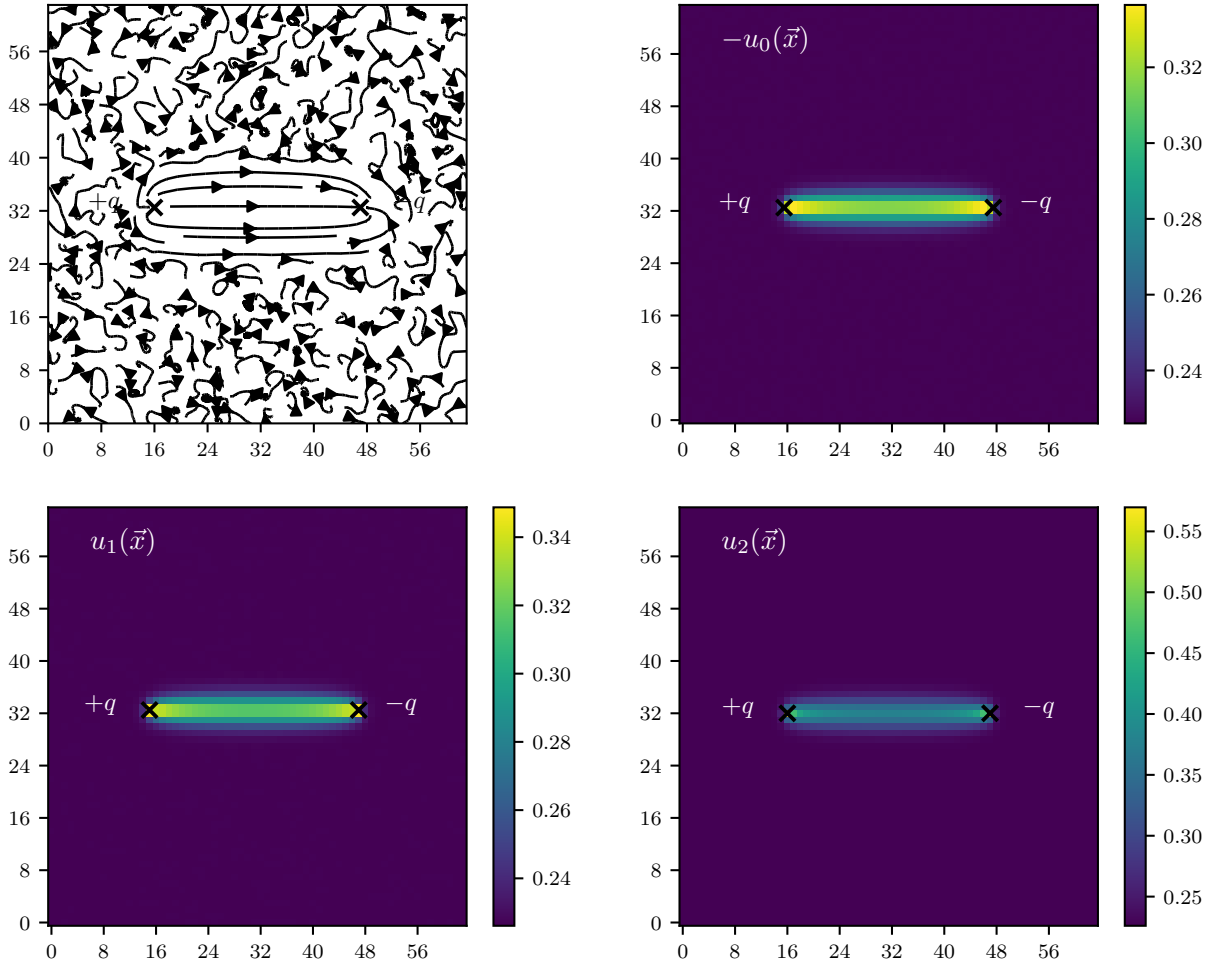


Figure 2.1: Time-averaged local energies and electric field on a spatial $L \times L$ lattice with $L = 64$ measured in the presence of two static charges, for $\beta = 1.0$. The first figure (top left) shows the field lines of the electric field \vec{E} defined in eq. (3.57). The last three figures (top right through bottom right) show the local energy defined in eq. (3.55) in the three spacetime directions.

where \mathbb{P} is the projector onto the Hilbert space sector where all states are invariant under the Gauss law. Inserting static charges at locations \vec{x} and \vec{y} corresponds to violating the Gauss law at those two lattice points. Thus the theory with static charges is defined by the *same Hamiltonian*, but a different projector $\mathbb{P}_{q,-q}$ which projects onto the sector where the Gauss law is satisfied everywhere except at \vec{x} and \vec{y} where it is violated by the appropriate charge amount. Thus

$$Z_{q,-q} = \text{tr} \left(e^{-N_T H} \mathbb{P}_{q,-q} \right). \quad (2.12)$$

Each partition function can be expanded in terms of energy eigenstates in the appropriate sector, for example

$$Z = \sum_{n=0}^{\infty} d_n e^{-E_n N_T}, \quad (2.13)$$

where in both cases the coefficients d_n are positive integers, since they are the degeneracy of eigenstate n . In particular on general grounds one expects in finite volume that the ground state

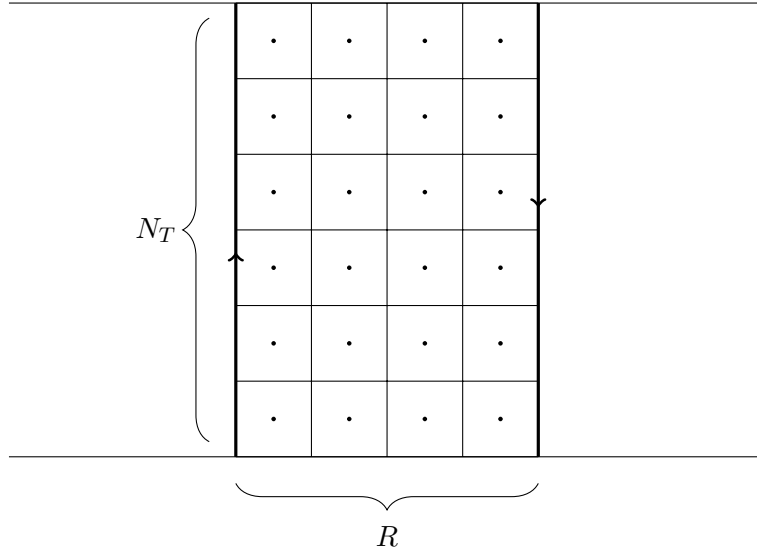


Figure 2.2: A cross-section of the lattice showing the two Polyakov loops (*thick lines*) together with the minimal surface in between, as well as the links in the dual lattice dual to each plaquette (the dots).

is non-degenerate, $d_0 = 1$. Thus the ratio of partition functions can be expanded as a series of the form

$$\langle P(\vec{x})P(\vec{y})^* \rangle = \frac{Z_{q,-q}}{Z} = \sum_{n=0}^{\infty} w_n e^{-\tilde{E}_n N_T} , \quad (2.14)$$

where the w_n are integer-valued and \tilde{E}_n are some coefficients. Most importantly, $\tilde{E}_0 = E_0^{q,-q} - E_0$ is the energy difference between the ground state energy in the sector with static charges and the ground state energy with no static charges. This can be interpreted as the potential energy $V(R)$ between the static charges, where $R = |\vec{x} - \vec{y}|$ (assuming rotational invariance for simplicity). Since we expect $w_0 = 1$, we can extract the potential directly without fits,

$$V(R) = -\frac{1}{N_T} \log \langle P(\vec{x})P(\vec{y})^* \rangle . \quad (2.15)$$

This expression is correct up to exponentially small corrections in N_T .

The expectation value of the Polyakov loop correlator can be nicely expressed in the dual theory. As we have seen in Chapter 1, the duality provides a dictionary between observables in the two theories. The dualization is not hard and we quickly show it for the Wilson action. Each Polyakov loop can be written as

$$P(\vec{x}) = e^{i(\varphi, \gamma_{\vec{x}})} , \quad (2.16)$$

where $\gamma_{\vec{x}}$ is a lattice 1-form equal to one on the links belonging to the non-contractible loop defining $P(\vec{x})$ and zero otherwise. The Polyakov loop correlator can then be written as

$$P(\vec{x})P(\vec{y}) = e^{i(\varphi, \gamma_{\vec{x}} - \gamma_{\vec{y}})} . \quad (2.17)$$

Since the action of the gauge theory depends only on plaquette variables, we want to rewrite the Polyakov loop correlator also in terms of plaquette variables only. To this end, we pick an arbitrary surface S (i.e. a connected collection of plaquettes) bounded by the Polyakov loops and

define a 2-form s by setting $s_p = \pm 1$ if $p \in S$ (depending on the orientation) and zero otherwise. The surface S is arbitrary and the result is independent of the choice of S . The natural choice is the “minimal” surface (i.e. the $R \times N_T$ rectangle between the Polyakov loops), as shown in Fig. 2.2. We then tile the surface with plaquettes. In practice, we have $\gamma_{\vec{x}} - \gamma_{\vec{y}} = \delta s$, so that the Polyakov loop observable can be written as (using integration by parts)

$$P(\vec{x})P(\vec{y}) = e^{i(d\varphi, s)}. \quad (2.18)$$

The dualization then proceeds very easily for any observable of this form (which includes for example also the plaquette). The end result is that one simply replaces each $h_x - h_y$ with $h_x - h_y + s_{\langle xy \rangle}$ where s is the dual of the s field on the original lattice, i.e. it equals ± 1 on the links of the dual lattice dual to a plaquette in S and zero otherwise. With the Wilson action we find

$$\langle P(\vec{x})P(\vec{y})^* \rangle = \frac{1}{Z} \left(\prod_x \sum_{h_x \in \mathbb{Z}} \right) \prod_{l=\langle xy \rangle} I_{|h_x - h_y + s_{\langle xy \rangle}|}(\beta) = \left\langle \prod_{l=\langle xy \rangle} \frac{I_{|h_x - h_y + s_{\langle xy \rangle}|}(\beta)}{I_{|h_x - h_y|}(\beta)} \right\rangle, \quad (2.19)$$

while with the Villain action,

$$\begin{aligned} \langle P(\vec{x})P(\vec{y})^* \rangle &= \frac{1}{Z} \left(\prod_x \sum_{h_x \in \mathbb{Z}} \right) \exp \left[-\frac{1}{2\beta} \sum_{\langle xy \rangle} (h_x - h_y + s_{\langle xy \rangle})^2 \right] = \\ &= \left\langle \exp \left[-\frac{1}{\beta} \sum_{\langle xy \rangle} \left(s_{\langle xy \rangle}^2 + s_{\langle xy \rangle} (h_x - h_y) \right) \right] \right\rangle. \end{aligned} \quad (2.20)$$

In both cases, we have reinterpreted the ratio of partition functions as an observable in the theory without Polyakov loops.

From eq. (2.20) it is clear that since $s_{\langle xy \rangle}$ is non-zero only on links dual to the surface S , the Polyakov loop correlator scales as $\exp(-\text{const} \times A(S))$ where $A(S)$ is the area of the surface S . Thus it makes sense to pick the surface with the *least* area, i.e. the minimal surface, which is simply the $R \times N_T$ rectangle bounding the Polyakov loops (note that this is the minimal surface only if $R < L/2$, so we restrict to this case; otherwise the minimal surface would be the one which wraps around the boundary). Nonetheless, even with this choice, the Polyakov loop correlator is exponentially small in RN_T , which is typically large. This leads to a signal-to-noise problem which makes the correlator hard to measure. To circumvent this problem, one can employ the so-called “snake algorithm” [129–131]. Let $Z_{q,-q} \equiv Z(R)$ if the Polyakov loops are separated by a distance R . We are interested in computing $Z(R)/Z$ for several values of R , so that we can extract the potential $V(R)$ according to eq. (2.15). The ratio of partition functions can be factored as

$$\frac{Z(R)}{Z} = \prod_{r=0}^{R-1} \frac{Z(r+1)}{Z(r)}. \quad (2.21)$$

With this factorization, one could compute each ratio $Z(r+1)/Z(r)$ as an observable in the ensemble generated according to the partition function $Z(r)$. This is certainly an improvement, since now the observable is exponentially small in N_T rather than RN_T , but not resolved. Thus we perform a further factorization of each factor. In particular, define the intermediate partition function $Z(r, M)$ defined as above, but where the surface S is chosen as in Fig. 2.3, i.e. the last column of plaquettes is not complete. More concretely, suppose that we are on a $L^2 N_T$ lattice and the two Polyakov loops are located at spatial positions $(x_0, L/2)$ and $(x_0 + R, L/2)$. Then

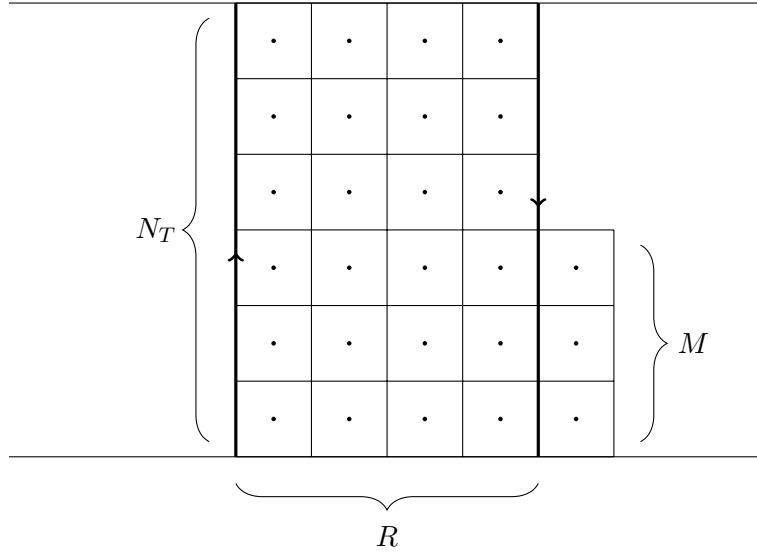


Figure 2.3: Illustration of the snake algorithm. A cross-section of the lattice at $y = L/2$. The dots denote dual lattice links in the y direction piercing the plaquettes between the two Polyakov loops. The M links represent an unfinished column of links.

the links dual to plaquettes in S are those in the y direction starting at (t, x, y) where $y = L/2$ and $x_0 \leq x < x + R$ and t satisfies

$$\begin{cases} 0 \leq t < M & x = x_0 + R, \\ 0 \leq t < N_T & \text{otherwise.} \end{cases} \quad (2.22)$$

This is illustrated in Fig. 2.3. Note that $Z(r+1) = Z(r+1, 0) = Z(r, N_T)$. Then we can perform the further factorization,

$$\frac{Z(r+1)}{Z(r)} = \prod_{M=0}^{N_T-1} \frac{Z(r, M+1)}{Z(r, M)}. \quad (2.23)$$

Now each factor $Z(r, M+1)/Z(r, M)$ can be expressed as an observable in an ensemble generated by $Z(r, M)$ which is supported only on *one single link*. Therefore each of these ratios can be efficiently evaluated via an arbitrary algorithm (for example, Metropolis). Then the potential can be reconstructed as

$$V(R) = -\frac{1}{N_T} \sum_{r=0}^{R-1} \sum_{M=0}^{N_T-1} \log \frac{Z(r, M+1)}{Z(r, M)} \quad (2.24)$$

Since each measurement is independent, the total error on $V(R)$ can be computed as the mean squared error of each factor, which in itself can be computed by error propagation. Note also that one does not need to recompute $V(R)$ for each R , but rather one can fix an R_{\max} and by summing over fewer elements we get all the $V(R)$ for $0 \leq R \leq R_{\max}$.

In practice, however, to avoid the accumulation of errors in eq. (2.24) it is better to work directly with the force

$$Q(R) = -\frac{1}{N_T} \log \frac{Z(R+1)}{Z(R)} = -\frac{1}{N_T} \sum_{M=0}^{N_T-1} \log \frac{Z(R, M+1)}{Z(R, M)}. \quad (2.25)$$

In this case, the advantage is that the sum contains always an equal number of independently computed quantities, so that the error on $Q(R)$ is roughly independent of R (on the other hand, the error on $V(R)$ rises roughly linearly with R). The two quantities are connected as $Q(R) = V(R + 1) - V(R)$.

The final step is to express each ratio as observables which can be measured. We do this only for the Wilson action, as the expressions for the Villain action can be obtained by simply replacing the Bessel function with the appropriate Boltzmann weight. Suppose that $Z(r, M)$ is described by an auxiliary field s , while $Z(r, M + 1)$ is described by s' . Then their ratio is given by

$$\frac{Z(r, M + 1)}{Z(r, M)} = \frac{\sum_{\{h\} \in \mathbb{Z}} \prod_{\langle xy \rangle} I_{|h_x - h_y + s'_{xy}|}(\beta)}{Z(r, M)} = \quad (2.26)$$

$$= \left\langle \prod_{\langle xy \rangle} \frac{I_{|h_x - h_y + s'_{xy}|}(\beta)}{I_{|h_x - h_y + s_{xy}|}(\beta)} \right\rangle_{r, M} = \left\langle \frac{I_{|h_{\tilde{x}} - h_{\tilde{y}} + 1|}(\beta)}{I_{|h_{\tilde{x}} - h_{\tilde{y}}|}(\beta)} \right\rangle_{r, M} \quad (2.27)$$

where the expectation value is taken with respect to the partition function $Z(r, M)$. The last equality follows because by construction s and s' differ only on *one* link and therefore most terms in the above ratio cancel out. This is the link in the y direction starting from (t, x, y) where $t = M$, $x = x_0 + R$, $y = L/2$, which we call $\tilde{l} = \langle \tilde{x}\tilde{y} \rangle$. On this link $s'_{\tilde{l}} = 1$ (in the standard orientation), but $s_{\tilde{l}} = 0$.

2.2 Effective string theory

Since, as we have seen, the energy flux in the presence of static charges forms a confining string, it is quite natural that the dynamics of the system can be described as a string theory. This should be understood as an *effective* theory which describes the long-range dynamics of the confining string, whose fundamental behaviour is determined by the underlying gauge theory. Effective string theory is useful because it provides analytical predictions for various quantities, which can be compared with the results of lattice simulations.

While effective string theory has many features in common with the (bosonic version of) its more famous sister, string theory as a fundamental theory of nature, the two should not be confused. In particular, while it is famously known that bosonic string theory is only consistent in $d = 26$ dimensions [132], since our string theory is only an effective theory we can unashamedly use it in $d = 3$ or $d = 4$. See also [133] on this point.

Effective string theory was introduced in [134, 135]. Mathematically, the fluctuations of a string can be described by a “displacement vector” $X^\alpha(z)$ with $\alpha = 1, 2, \dots, d - 2$ which is a function of the worldsheet coordinates $z = (z_0, z_1)$ and describes the transverse components of the string fluctuations. The worldsheet parametrizes time z_0 and position along the string z_1 (so that $0 \leq z_1 \leq R$). In the time direction, one imposes periodic boundaries ($0 \leq z_0 \leq N_T$). The string action is written in terms of an infinite series,

$$S = \sigma R N_T + \mu N_T + S_0 + S_1 + \dots, \quad (2.28)$$

where the first two terms correspond the “classical” case where the string does not fluctuate. The first correction to the linear behaviour is Gaussian,

$$S_0 = \frac{\sigma}{2} \int d^2 z \partial_a X^\alpha \partial_a X^\alpha, \quad (2.29)$$

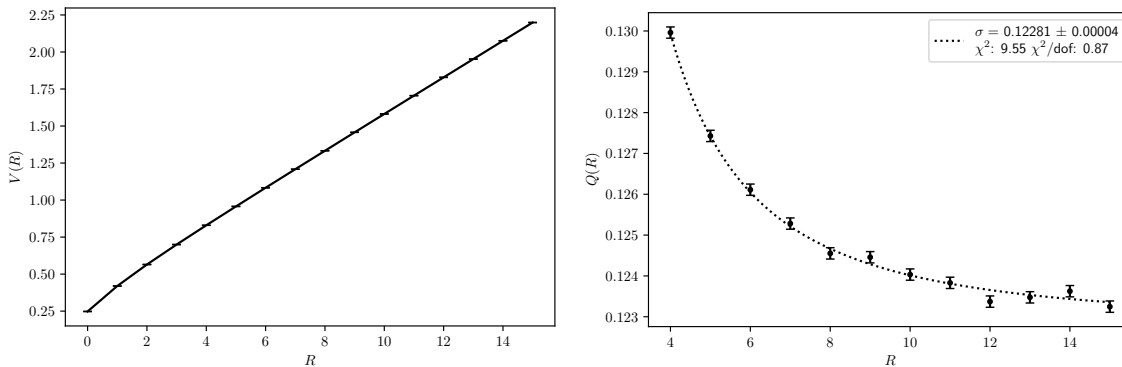


Figure 2.4: Potential $V(R)$ (*left*) and force $Q(R)$ (*right*) between two static charges in the three-dimensional U(1) gauge theory with the Wilson action, at $\beta = 1.7$ and $N_T = L = 32$. The force $Q(R)$ was fitted against the Nambu-Goto prediction (the best fit is shown *dotted*) eq. (2.34).

for $a = 0, 1$. The higher-order corrections can be organized in terms of a derivative expansion [128]. Then the string partition function

$$Z = \int DX e^{-S[X]}, \quad (2.30)$$

is expected to be proportional to the partition function with the static charges inserted $Z_{q,-q}$ [128]. For example, with the Gaussian correction term S_0 one can compute the lowest-order correction to the potential, which is (up to a constant)

$$V(R) = \sigma R - \frac{\pi(d-2)}{24} \frac{1}{R} + \mathcal{O}(1/R^3). \quad (2.31)$$

The $1/R$ correction is known as the Lüscher term. Interestingly, it is *universal*, in that it is independent of any low-energy constants which enter the partition function, including the string tension. In particular, as is usual in effective theories, higher-order terms enter the action with appropriate coefficients known as low-energy constants. These can be constrained in various ways, such as symmetry, but are otherwise not predicted by the effective theory. To lowest order, the only low-energy constant is the string tension, which is not predicted by the effective theory. It can be extracted by determining $V(R)$ numerically for the system of interest (for example using the snake algorithm which we discussed in the previous section) and fitting to the analytical prediction from effective string theory, for example eq. (2.31).

Interestingly, while the value of the low-energy constants such as the string tension depends on the gauge theory and the dimension of spacetime, the general form of the prediction is independent of other details of the underlying system. In $SU(N)$ gauge theories, the value of the string tension actually depends only on the N -ality of the representation of the static quarks [136], although higher-order corrections generally involve low-energy constants which may have a more complicated dependence on the representation. Attempts to further understand string tensions have been made recently in the context of non-invertible symmetries [137, 138].

Later, it was been realized that the requirement of Poincaré invariance of the underlying theory strongly constrains the various low-energy constants appearing in the effective string action [133, 139–142]. See also the reviews [143, 144] as well as [145] for effective string theory at finite temperature. The various corrections are related to the induced metric on the worldsheet

$$g_{ab} = \partial_a X_\alpha \partial_b X^\alpha. \quad (2.32)$$

In particular, all terms which depend solely on the string tension and contain no other low-energy constant can be organized as the Nambu-Goto action,

$$S_{\text{NG}} = \sigma \int d^2z \sqrt{\det g}, \quad (2.33)$$

which to lowest order in a derivative expansion reproduces the linear potential as well as the Gaussian correction eq. (2.29). The resulting potential with the full Nambu-Goto action can be computed exactly [146],

$$V(R) = \sigma R \sqrt{1 - \frac{\pi(d-2)}{12\sigma R^2}}. \quad (2.34)$$

A fit of snake algorithm data to the Nambu-Goto prediction for U(1) gauge theory in three dimensions is shown in Fig. 2.4. Note that the string tension is the only fit parameter. There are two types of corrections to the Nambu-Goto action: bulk terms and boundary terms. The bulk terms can be organized in terms of geometric quantities in an expansion familiar from general relativity. In $d = 3$ target dimensions, one finds [147]

$$S = \int d^2z \sqrt{\det g} [\sigma + \gamma_1 R + \gamma_2 K^2 + \gamma_3 K^4 + \dots]. \quad (2.35)$$

Here R is the Ricci scalar and K is the extrinsic curvature. The integral of the Ricci scalar is a topological invariant in two dimensions and therefore does not contribute to the potential (since we do not expect large, topology-changing fluctuations). The K^2 term introduces a ‘‘rigidity’’ in the confining string. This term is exponentially small in R in principle and can therefore also be neglected, unless its coefficient is unusually large. In fact this is exactly what happens in the three-dimensional U(1) gauge theory [116]. An extrinsic curvature term for the confining string in 3D U(1) gauge theory was in fact first proposed in [148], where it was argued that $\gamma_2 \sim \sigma/m^2$, where m is the mass gap of the theory [148, 149]. As we will see in the next chapter, this ratio is divergent in a continuum limit where the string tension is held fixed. Thus in this case the string is dominated by the K^2 term. From the expansion eq. (2.35), bulk corrections beyond Nambu-Goto arise at order $1/R^7$. Apart from bulk terms, one should also consider contributions localized at the boundaries. The lowest order such contribution turns out to lead to a correction in the potential of order $1/R^4$ [150], and is therefore much larger than the lowest order bulk correction. Interestingly, boundary corrections are suppressed at finite temperature, where it is then possible to detect the bulk corrections [147, 150].

2.3 Known results on the 3D U(1) gauge theory

Based on the dual partition function in the Villain formulation, it is possible to perform a sequence of analytical manipulations which lead to an effective theory for the three-dimensional U(1) gauge theory near the continuum [80, 81, 93]. With this formulation, it has been rigorously shown that the theory is confining for all values of the coupling g^2 [81]. In the rest of this section, we review this calculation and discuss its consequences. We follow in part [137] for a simpler presentation of the results in [81]. We start from the dual Villain partition function,

$$Z = \left(\prod_x \sum_{h_x \in \mathbb{Z}} \right) \exp \left[-\frac{1}{2\beta} \sum_{\langle xy \rangle} (h_x - h_y)^2 \right]. \quad (2.36)$$

The main idea is to attempt to replace the discrete variables h with real-valued variables σ , and attempt to control the error that one introduces by doing so [151]. Initially we simply introduce

δ functions,

$$Z = \left(\prod_x \int_{-\infty}^{+\infty} d\sigma_x \right) \left(\prod_x \sum_{h_x} \delta(\sigma_x - 2\pi h_x) \right) \exp \left[-\frac{1}{8\pi^2\beta} \sum_{\langle xy \rangle} (\sigma_x - \sigma_y)^2 \right]. \quad (2.37)$$

Exploiting the Poisson summation formula, we find

$$\sum_{h_x \in \mathbb{Z}} \delta(\sigma_x - 2\pi h_x) = \sum_{q_x \in \mathbb{Z}} e^{iq_x \sigma_x}, \quad (2.38)$$

apart from some prefactors. Therefore the partition function becomes

$$Z = \left(\prod_x \int_{-\infty}^{+\infty} d\sigma_x \right) \left(\prod_x \sum_{q_x \in \mathbb{Z}} \right) \exp \left[-\frac{1}{8\pi^2\beta} \sum_{\langle xy \rangle} (\sigma_x - \sigma_y)^2 + i \sum_x q_x \sigma_x - i \sum_x q_x B_x \right]. \quad (2.39)$$

Here we have introduced a “magnetic field” B_x which couples to the q . This will turn out to be useful for a calculation which we perform in Chapter 3. For the standard U(1) theory $B_x \equiv 0$, but its presence barely affects the calculation.

It is important to note that the partition function for the height model eq. (2.36) is invariant under a global integer shift of the height variables, $h_x \rightarrow h_x + n$, with $n \in \mathbb{Z}$. We call this the “global” \mathbb{Z} symmetry. In particular, it should be understood as a sort of redundancy in our description of the system. The overall height around which the height variables fluctuate should not matter and therefore all observables are required to be invariant under the \mathbb{Z} symmetry [81]. Note further that the global \mathbb{Z} symmetry is related to a zero-mode problem, similar to the one encountered in Chapter 1. In particular the partition function eq. (2.36) is infinite, i.e. $Z = \infty$, even in finite volume. This is because, with open or periodic boundaries, the integrand in the partition function is actually independent of one of the height variables, which manifests itself by the presence of the global \mathbb{Z} invariance. This can be seen most easily by considering the one-dimensional case with one or two links. One therefore has an unconstrained sum over the non-compact space \mathbb{Z} , which leads to the infinity. Again, this is very similar to the problem encountered in Chapter 1. Several resolutions are possible; in particular, one could fix one of the height variables to an arbitrary value, or alternatively employ C -periodic boundary conditions. Here we note that, similarly to Chapter 1, the infinity of the partition function does not translate to observables (in which case the infinity cancels between numerator and denominator). Therefore we simply choose periodic boundaries; as long as we only consider observables which are invariant under the global \mathbb{Z} symmetry, no issue arises. The global \mathbb{Z} invariance has implications for the real scalar field σ that we just introduced. In particular, physically we should identify configurations which differ by a global 2π difference, i.e. $\sigma_x \sim \sigma_x + 2\pi$. Thus, while $\sigma \in \mathbb{R}$, it is in some sense compactified.

To proceed, we want to integrate out the σ , whose action is basically Gaussian. To this end, for ease of notation we rewrite the expression in terms of lattice differential forms, in which case the above action may be rewritten as

$$Z = \left(\prod_x \int_{-\infty}^{+\infty} d\sigma_x \right) \left(\prod_x \sum_{q_x \in \mathbb{Z}} \right) \exp \left[-\frac{1}{8\pi^2\beta} (d\sigma, d\sigma) + i(q, \sigma) - i(q, B) \right], \quad (2.40)$$

where σ, q, B are 0-forms and $d\sigma_{\langle xy \rangle} = \sigma_x - \sigma_y$, while (\cdot, \cdot) is the inner product on k -forms. Then note that, using integration by parts,

$$(d\sigma, d\sigma) = (\sigma, \delta d\sigma) = (\sigma, \square \sigma), \quad (2.41)$$

where $\square = d\delta + \delta\sigma$ is the three-dimensional lattice Laplacian and $\delta\sigma = 0$ since σ is a 0-form. Standard Gaussian integration then gives (up to constant prefactors)

$$Z = \left(\prod_x \sum_{q_x \in \mathbb{Z}} \right) \exp \left[-2\pi^2 \beta(q, \square^{-1}q) - i(q, B) \right]. \quad (2.42)$$

For the relevant case $B \equiv 0$ this is the partition function for a Coulomb gas of *monopoles* interacting via a Coulomb force. This expression should be compared with the very similar expression for the vortex gas which we obtained in Chapter 1.

Now the monopole partition function receives both short-ranged contributions and long-range contributions; for an effective theory near the continuum we're interested in the latter. To separate the two we perform a Pauli-Villars regularization, setting

$$\begin{aligned} \square^{-1} &= \square^{-1} - (\square + M^2)^{-1} + (\square + M^2)^{-1} = \\ &= \square^{-1}(1 + \square/M^2)^{-1} + (\square + M^2)^{-1} \equiv \square_{\text{PV}}^{-1} + \square_M^{-1} \end{aligned} \quad (2.43)$$

where the mass M is arbitrary. Here the massive propagator \square_M^{-1} corresponds to the short-range contributions, while the regularized Pauli-Villars propagator corresponds instead to the long-ranged physics. The partition function then becomes

$$Z = \left(\prod_x \sum_{q_x \in \mathbb{Z}} \right) \exp \left[-2\pi^2 \beta(q, \square_{\text{PV}}^{-1}q) - 2\pi^2 \beta(q, \square_M^{-1}q) - i(q, B) \right]. \quad (2.44)$$

Now we reintroduce the scalar field σ , but only for the long-range degrees of freedom; the short range contributions will be integrated out. Undoing the transformation simply leads to

$$Z = \left(\prod_x \int_{-\infty}^{+\infty} d\sigma_x \right) \left(\prod_x \sum_{q_x \in \mathbb{Z}} \right) \exp \left[-\frac{1}{8\pi^2 \beta} (\sigma, \square_{\text{PV}} \sigma) + i(q, \sigma - B) - 2\pi^2 \beta(q, \square_M^{-1}q) \right]. \quad (2.45)$$

Finally, we sum away the short-ranged contributions given by the remaining q variables. First of all, note that the mass M in the Pauli-Villars regularization is arbitrary. However, it must be chosen to scale appropriately with the other quantities in the system in order to obtain a valid limit. In particular, if a is the lattice spacing and m is the physical mass of the system (or any other quantity which is taken as the standard of length), one must choose M to scale such that $M/m \rightarrow \infty$ while $aM \rightarrow 0$ in the continuum limit $a \rightarrow 0$ [81].

In particular, the massive propagator $\square_M^{-1} \equiv v_M(x-y)$ scales as $e^{-M|x-y|}$. If the mass m is taken as the standard of length, then as one approaches the continuum, $v_M(x-y) \sim e^{-(M/m)(m|x-y|)}$. Since we have chosen M/m large, then as the continuum limit is approached the propagator is exponentially peaked around $x \approx y$ and therefore $(q, \square_M^{-1}q)$ can be approximated by $(q, \square_M^{-1}q) \approx v_M(0) \sum_x (q_x)^2$. But since $aM \rightarrow 0$, in lattice units $v_M(0) \approx v(0) + \mathcal{O}(aM)$. The inverse lattice Laplacian was computed in Chapter 1 in two dimensions. On a d -dimensional infinite hypercubic lattice, the formula is quite similar,

$$v(x-y) = \left(\frac{a}{2\pi} \right)^d \int_{BZ} d^d \vec{k} \frac{e^{ik \cdot (x-y)}}{2 \left(d - \sum_{\mu} \cos(k_{\mu}) \right)} \quad (2.46)$$

where the Brillouin zone is $[-\frac{\pi}{a}, \frac{\pi}{a}]^d$. Therefore in three spacetime dimensions at zero separation it takes the value [152]

$$\begin{aligned} v_0 \equiv v(0) &= \frac{1}{2\pi^3} \int_0^\pi \int_0^\pi \int_0^\pi \frac{du dv dw}{3 - \cos(u) - \cos(v) - \cos(w)} = \\ &= \frac{\sqrt{6}}{192\pi^3} \Gamma\left(\frac{1}{24}\right) \Gamma\left(\frac{5}{24}\right) \Gamma\left(\frac{7}{24}\right) \Gamma\left(\frac{11}{24}\right) \approx 0.252731 \dots \end{aligned} \quad (2.47)$$

Note that this part of the argument is crucially connected to three spacetime dimensions [153]. For example, in two dimensions the corresponding integral is divergent [154],

$$\frac{1}{2\pi^2} \int_0^\pi \int_0^\pi \frac{du dv}{2 - \cos(u) - \cos(v)} = \infty. \quad (2.48)$$

More precisely, $v_M(0)$ diverges as $v_M(0) \sim \log(aM)$ [153]. Therefore, as stated, the argument fails in two dimensions. Interestingly, the fact that the inverse Laplacian at zero separation is divergent on a square lattice but finite on a cubic lattice is responsible for the fact that random walks are recurrent on the square lattice, but transient on the cubic lattice [155].

At this point we can integrate out the short-range monopole contributions. For large β , the monopoles with $|q_x| > 1$ are subleading, thus one can make the ‘‘dilute gas approximation’’ where $q_x = 0, \pm 1$. Then we find

$$\begin{aligned} \left(\prod_x \sum_{q_x \in \mathbb{Z}} \right) \exp [i(q, \sigma - B) - 2\pi^2 \beta(q, \square_M^{-1} q)] &\approx \prod_x \left[\sum_{q=0, \pm 1} \exp (iq(\sigma_x - B_x) - 2\pi^2 \beta v(0) q^2) \right] = \\ &= \prod_x \left[1 + 2e^{-2\pi^2 \beta v(0)} \cos(\sigma_x - B_x) \right] = \\ &\approx \prod_x \exp \left[2e^{-2\pi^2 \beta v(0)} \cos(\sigma_x - B_x) \right]. \end{aligned} \quad (2.49)$$

Therefore the partition function becomes

$$Z = \left(\prod_x \int_{-\infty}^{+\infty} d\sigma_x \right) \exp \left[-\frac{1}{8\pi^2 \beta} (\sigma, \square_{\text{PV}} \sigma) + 2e^{-2\pi^2 \beta v(0)} \sum_x \cos(\sigma_x - B_x) \right]. \quad (2.50)$$

As we approach the continuum, we can replace the Pauli-Villars Laplacian \square_{PV} with the standard Laplacian; then canonically normalizing the kinetic term and setting $B_x \equiv 0$ for the standard U(1) theory, one finds

$$Z = \left(\prod_x \int_{-\infty}^{+\infty} d\phi_x \right) \exp \left[-\frac{1}{2} \sum_{\langle xy \rangle} (\phi_x - \phi_y)^2 + 2e^{-2\pi^2 \beta v(0)} \sum_x \cos(2\pi \sqrt{\beta} \phi_x) \right]. \quad (2.51)$$

Note that this expression is valid for large β . Therefore, this analytical method cannot show the absence of phase transitions in other regions of coupling space. This possibility is however excluded numerically.

From here we can take the continuum limit where one sends $\beta \rightarrow \infty$. For clarity, we restore the lattice spacing a . Let $\tilde{\phi} = \phi/\sqrt{a}$ be a dimensionful field with the correct dimensions for a scalar field in three dimensions (this is dictated by the kinetic term in the action). Defining a dimensionful coupling $\tilde{\beta} = a\beta$, as we approach the continuum the action can be written as

$$S \approx \int d^3x \left[\frac{1}{2} \partial_\mu \tilde{\phi} \partial_\mu \tilde{\phi} - \frac{1}{a^3} 2e^{-2\pi^2 \beta v(0)} \cos \left(2\pi \sqrt{\tilde{\beta}} \tilde{\phi}_x \right) \right]. \quad (2.52)$$

Now we need a renormalization prescription for the running of the coupling β as the continuum limit is taken. One possibility is to fix a mass m and let

$$a^2 m^2 = 8\pi^2 \beta \exp[-2\pi^2 v_0 \beta]. \quad (2.53)$$

This provides a prescription for the continuum limit, with a different trajectory for each fixed value of m . As $a \rightarrow 0$, $am \rightarrow 0$ and since the effective theory assumes β large, this then forces $\beta(a) \rightarrow \infty$ as $a \rightarrow 0$. A more precise relationship can be obtained by inverting eq. (2.53) (using the Lambert W function) whereby one finds,

$$\beta(a) \sim -\log a \rightarrow +\infty \quad \implies \quad \tilde{\beta}(a) \equiv a\beta(a) \sim -a \log(a) \rightarrow 0. \quad (2.54)$$

as the continuum limit $a \rightarrow 0$ is taken. Substituting the mass definition eq. (2.53) into the action, one finds

$$S \approx \int d^3x \left[\frac{1}{2} \partial_\mu \tilde{\phi} \partial_\mu \tilde{\phi} - \frac{m^2}{4\pi^2 \tilde{\beta}} \cos \left(2\pi \sqrt{\tilde{\beta}} \tilde{\phi}_x \right) \right]. \quad (2.55)$$

Therefore as we approach the continuum, since $\tilde{\beta} \rightarrow 0$, the potential difference separating different minima of the cosine becomes infinite. The minima are all physically equivalent because they are related by a global shift of the scalars; thus we expand the field around an arbitrary minimum. In particular, this also means that the field ϕ decompactifies, and becomes a proper scalar field as the continuum limit is approached. One can then expand the cosine in a Taylor series, and since $\tilde{\beta} \rightarrow 0$ only the second-order term survives in the continuum limit (up to a constant) and one finds,

$$S \approx \int d^3x \left[\frac{1}{2} \partial_\mu \tilde{\phi} \partial_\mu \tilde{\phi} + \frac{1}{2} m^2 \tilde{\phi}^2 \right]. \quad (2.56)$$

Thus the theory has become a theory of a free real-valued scalar field with a non-perturbatively generated mass m .

The fact that the continuum physics is described by a massive free scalar has interesting implications for the spectrum of the theory. Naively, one would expect simply a massless photon. However, as we've seen, due to non-perturbative self-interactions via monopoles the photon is itself confined. Nonetheless, the situation cannot be simply described as the photon acquiring a mass, because the effective theory predicts that the long-range physics is described by a *scalar* particle. Instead, the intuitive picture is that photons are packed together by monopoles into forming “glueballs”, or “photoballs”, which are scalar particles. In fact in the continuum the mass of the lowest glueball coincides with the mass of the continuum scalar [81]. In more general terms, one can construct glueball states in various microscopic channels and study the scaling of their masses. One finds that, as the continuum is approached, the glueball masses in various channels become integer multiples of the mass gap [115]. Thus, the various microscopic glueball states should be interpreted as excitations of a single non-interacting free scalar, which is precisely the effective theory description of this model.

The form of the mass gap for the U(1) theory eq. (2.53) is quite reminiscent of the formula for the mass gap in non-Abelian gauge theories. Nonetheless, interestingly, in that case the coefficient in the exponent is *universal*. Here, instead, it is peculiarly dependent on the underlying lattice. If one discretizes the theory on a different three-dimensional lattice, then one would expect the mass gap to scale with the v_0 corresponding to the zero-separation limit of the Green's function for the corresponding lattice.

From the effective theory eq. (2.51) a semiclassical approach allows the calculation of the string tension σ [80, 81, 156], which is found to scale as

$$a^2 \sigma = \frac{\tilde{c}}{4\pi^2} \frac{am}{\beta}, \quad (2.57)$$

where \tilde{c} is a dimensionless constant. These results have found numerical confirmation [113–116, 157, 158], and the constant $\tilde{c}/4\pi^2 \approx 0.21$ was estimated for the Wilson action in [115]. We postpone the derivation of eq. (2.57) until the end of this section since it is somewhat involved.

The scaling of the string tension vs the mass is rather peculiar. In non-Abelian Yang-Mills theories, the string tension and mass are commensurate, in that the ratio $\sqrt{\sigma}/m$ is finite in the continuum limit [159, 160]. On the other hand, in this case eq. (2.57) predicts the scaling

$$\frac{\sigma}{m^2} \rightarrow \infty, \quad \frac{(a^2\sigma)\beta}{(am)} \rightarrow \frac{\tilde{c}}{4\pi^2}. \quad (2.58)$$

Therefore this theory has inequivalent length scales, in the sense that one can choose to keep fixed either the mass or the string tension, but not both. Therefore, depending on what quantity is taken as the standard of length, one can take three different continuum limits:

1. If the mass m is taken as the standard of length, the string tension becomes infinite in the continuum limit. As we have seen, the theory is equivalent to a free massive scalar (the “photoball”).
2. If the string tension σ is taken as the standard of length, the mass goes to zero in the continuum limit.
3. A third continuum limit may also be obtained by noting that the dimensionless coupling β may also be expressed in terms of the usual dimensionful coupling g^2 as $\beta = 1/(ag^2)$. One may then take g^2 as the standard of length; with this choice, both the mass and string tension go to zero. The resulting theory has been rigorously shown to be free electrodynamics [161].

Because of these three different options, lattice U(1) gauge theory is capable of describing different continuum theories depending on how the limit is taken. This is an interesting fact which makes clear the difficulty outlined in Chapter 1 in defining a continuum limit. One *cannot* assign an unambiguous meaning to the limit $a \rightarrow 0$, because the result depends on the renormalization prescription that is chosen. Because of this ambiguity, it is even unclear what a continuum path-integral measure “should” even mean if it were possible to rigorously define it.

The existence of the three continuum limits also has consequences for the finite temperature physics in this model. In particular, as we will see, even the existence of the finite temperature deconfinement transition depends on how the limit is taken.

A fact which to our knowledge has gone unnoticed in the literature is that it is actually not necessary to perform the dilute gas approximation. The monopole sum can be performed to all orders, leading to a formula for the higher-monopole corrections to the mass gap formula eq. (2.53). In particular, the monopole sum can be performed exactly, whereby

$$\sum_{q \in \mathbb{Z}} \exp [iq\sigma - 2\pi^2\beta v_0 q^2] = \theta(z; \tau), \quad (2.59)$$

where θ is the Jacobi theta function and

$$\begin{cases} z = \frac{\sigma}{2\pi}, \\ \tau = 2i\pi\beta v_0. \end{cases} \quad (2.60)$$

Then the action takes the form

$$S = \frac{1}{8\pi^2\beta} (\sigma, \square_{\text{PV}}\sigma) + \sum_x V(\sigma_x), \quad (2.61)$$

where the potential is given by $\exp(-V(\sigma)) = \theta(z; \tau)$. The Jacobi theta function can also be expressed as [162]

$$\theta(z; \tau) = \prod_{m=1}^{\infty} (1 - e^{2\pi im\tau}) \left(1 + e^{(2m-1)\pi i\tau + 2\pi iz}\right) \left(1 + e^{(2m-1)\pi i\tau - 2\pi iz}\right). \quad (2.62)$$

Therefore

$$V(\sigma) = -\log \theta(z; \tau) = -\sum_{m=1}^{\infty} \left[\log(1 - \lambda^{2m}) + \log(1 + \lambda^{2m-1} e^{i\sigma}) + \log(1 + \lambda^{2m-1} e^{-i\sigma}) \right] \quad (2.63)$$

where we set $\lambda \equiv e^{-2\pi^2\beta v_0}$. Since $\lambda < 1$ we can expand the logarithm in a series, and we find

$$V(\sigma) = \sum_{m=1}^{\infty} \sum_{n=1}^{\infty} \frac{\lambda^{2mn}}{n} \left[1 + 2 \frac{(-1)^n}{\lambda^n} \cos(\sigma n) \right]. \quad (2.64)$$

The first term is simply a constant which we ignore. The lowest order term is obtained for $m = n = 1$ and reproduces the cosine potential in the previous case. Again since $|\lambda| < 1$ the series is absolutely convergent and we can therefore swap the two summations, leading to

$$V(\sigma) = \sum_{n=1}^{\infty} \frac{1}{n} \frac{(-1)^n}{\sinh(2\pi^2\beta v_0 n)} \cos(\sigma n). \quad (2.65)$$

From this expression we can extract the mass of the particle by repeating the previous calculation. In particular, we canonically normalize the kinetic term by setting $\sigma = 2\pi\sqrt{\beta}\phi$. The mass can be identified by the same procedure as in the standard case (alternatively, simply by Taylor expansion) and one finds (restoring the lattice spacing a)

$$a^2 m^2 = 4\pi^2\beta \sum_{n=1}^{\infty} \frac{1}{n} \frac{(-1)^{n-1}}{\sinh(2\pi^2\beta v_0 n)}. \quad (2.66)$$

For large x , $\sinh x \approx \frac{1}{2}e^x$ and therefore the leading-order term reduces to the standard result eq. (2.53).

Finally, we describe the semiclassical derivation of the string tension formula eq. (2.57). See also [80, 93, 156, 163]. The starting point is the partition function with the insertion of a current,

$$Z[s] = \left(\prod_x \sum_{h_x} \right) \exp \left[-\frac{1}{2\beta} \sum_{\langle xy \rangle} (h_x - h_y + s_{\langle xy \rangle})^2 \right]. \quad (2.67)$$

We have seen in eq. (2.20) that this is the form of the partition function with the insertion of Polyakov loops. Since the derivation of the effective theory is performed in infinite volume, it is easier to see $s_{\langle xy \rangle}$ as the current arising from the insertion of a rectangular Wilson loop in the original theory. Then $s_{\langle xy \rangle} = \pm 1$ on links dual to plaquettes in the minimal surface bounded by the Wilson loop and 0 otherwise. One can repeat the derivation of the effective theory in the presence of the current s . Since the calculation is rather similar, we skip most steps and highlight only the differences. Again we replace the discrete $h \in \mathbb{Z}$ with real $\sigma \in \mathbb{R}$ and get

$$Z[s] = \left(\prod_x \int_{-\infty}^{+\infty} d\sigma_x \right) \left(\prod_x \sum_{q_x \in \mathbb{Z}} \right) \exp \left[-\frac{1}{8\pi^2\beta} \sum_{\langle xy \rangle} (\sigma_x - \sigma_y + 2\pi s_{\langle xy \rangle})^2 + i \sum_x q_x \sigma_x \right]. \quad (2.68)$$

Expanding the quantity in the square and writing everything in form notation (also integrating by parts) leads to

$$Z[s] = \left(\prod_x \int_{-\infty}^{+\infty} d\sigma_x \right) \left(\prod_x \sum_{q_x \in \mathbb{Z}} \right) \exp \left[-\frac{1}{8\pi^2\beta} (\sigma, \square\sigma) - \frac{1}{2\beta} (s, s) + \left(iq - \frac{1}{2\pi\beta} \delta s, \sigma \right) \right]. \quad (2.69)$$

It is now rather simple to perform the Gaussian integration over σ and obtain the monopole gas representation

$$Z[s] = \left(\prod_x \sum_{q_x \in \mathbb{Z}} \right) \exp \left[2\pi^2\beta \left(\left(iq - \frac{1}{2\pi\beta} \delta s \right), \square^{-1} \left(iq - \frac{1}{2\pi\beta} \delta s \right) \right) - \frac{1}{2\beta} (s, s) \right]. \quad (2.70)$$

This is the partition function for a Coulomb gas of monopoles in the presence of sources. The sources δs are a 0-form which is non-zero on the sites directly on the two sides of the Wilson loop, equal to $+1$ on one side and -1 on the other. Thus the monopoles arrange themselves in order to screen the electric charge. This partition function is actually rather similar to the partition function for the gas of vortex lines which we encountered in Chapter 1. Now expanding the quantity in brackets, using Pauli-Villars regularization, reintroducing the σ field for the long-range contributions and summing over the q s in the dilute gas approximation, we arrive at

$$Z[s] = \left(\prod_x \int_{-\infty}^{+\infty} d\sigma_x \right) \exp \left[-\frac{1}{8\pi^2\beta} (\sigma, \square\sigma) + 2\lambda \sum_x \cos(\sigma_x - B_x) + \right. \\ \left. - \frac{1}{2\beta} (s, s) + \frac{1}{2\beta} (\delta s, \square^{-1} \delta s) \right], \quad (2.71)$$

where $\lambda = e^{-2\pi^2\beta v_0}$ and $B = 2\pi\square^{-1}\delta s$ is the Coulomb potential due to the monopole sources δs . The leading-order contribution to the partition function is due to the classical solution of the equations of motion. This is the semi-classical approximation. We are only interested in extracting area-law terms in the ratio $Z[s]/Z$.

The first observation is that while the two terms in the second line of eq. (2.71) are individually proportional to the area of the Wilson loop, their combination is actually only proportional to the perimeter, and can thus be discarded in the calculation. In fact, from the Hodge decomposition, we have $s = d\square^{-1}\delta s + \delta\square^{-1}ds$ so that, using integration by parts,

$$(s, s) - (\delta s, \square^{-1}\delta s) = (ds, \square^{-1}ds). \quad (2.72)$$

Now ds is a 2-form and thus lives on plaquettes. It is only supported on plaquettes on the border of the Wilson loop, and it is thus reasonable that the corresponding term is perimeter-behaved.

Now we turn to the two terms in the first line of eq. (2.71). Since the effective theory is valid near the continuum, we approximate the action in terms of continuum variables:

$$S \approx \int d^3x \left[\frac{1}{8\pi^2\beta} (\partial_\mu \sigma)^2 + 2\lambda(1 - \cos(\sigma - B)) \right], \quad (2.73)$$

where we added a constant to ensure that the final results are finite. When going to the continuum, we need to be careful not to introduce divergences. From the lattice definition of δs , it is clear how to define it in the continuum. Suppose that the Wilson loop (assumed to be very large) is located on the plane $y = 0$. Then in the continuum $\delta s = -\delta'(y)\theta_W(x, t)$ where δ' is the

derivative of the Dirac delta function and $\theta_W(x, t) = 1$ if (x, t) is inside the Wilson loop (i.e. $0 \leq x \leq R$ and $0 \leq t \leq N_T$) and zero otherwise. The classical equations of motion arising from the above action are

$$\partial_\mu^2 \sigma = 8\pi^2 \beta \lambda \sin(\sigma - B) . \quad (2.74)$$

Defining $\chi = \sigma - B$ and recalling that $m^2 = 8\pi^2 \beta \lambda$, we find

$$\partial_\mu^2 \chi = 2\pi \delta s + m^2 \sin \chi . \quad (2.75)$$

This is just the three-dimensional Sine-Gordon equation. We solve it by setting (recall that the Wilson loop is in the $y = 0$ plane)

$$\chi(t, x, y) = \theta_W(t, x) \xi(y) . \quad (2.76)$$

Ignoring the effect of the boundary, the equation of motion reduces to

$$\xi''(y) = -2\pi \delta'(y) + m^2 \sin(\xi(y)) . \quad (2.77)$$

For $y \neq 0$ this is simply the one-dimensional Sine-Gordon equation, which is one of those theories admitting exact soliton solutions. In this case, we have the kink (domain wall) solutions $\xi(y) = 4 \arctan(e^{\pm my})$ [14, 19]. Note that since this is a non-linear equation, the normalization (apart from the overall sign) is not arbitrary. To avoid mistakes, it is important to take a step back. Assuming that $\sin \xi$ is well-behaved, we can integrate eq. (2.77) once to obtain (schematically)

$$\xi'(y) + 2\pi \delta(y) = m^2 \int \sin(\xi(y)) . \quad (2.78)$$

This tells us that ξ' has a delta function singularity at $y = 0$, and it is only the combination $\xi'(y) + 2\pi \delta(y)$ that is well-behaved around $y = 0$. Integrating once more around a small domain near $y = 0$ then implies that ξ jumps by -2π across $y = 0$ (note that under the jump, $\sin \xi$ remains continuous). The other boundary condition is simply that $\xi \rightarrow 0$ at infinity. To achieve both conditions, we can combine two kinks [80],

$$\xi(y) = \begin{cases} -4 \arctan(e^{-my}) & y > 0 , \\ 4 \arctan(e^{my}) & y < 0 . \end{cases} \quad (2.79)$$

Miraculously, this solution correctly jumps by -2π at $y = 0$ (since $\arctan(1) = \pi/4$) and solves the Sine-Gordon equation.

We can then go back to evaluate the action on the classical solution. Note that $\cos(\sigma - B) = \cos(\chi)$ is actually continuous across $y = 0$, so this term poses no issue. On the other hand, the evaluation of the kinetic term requires the calculation of the derivative of χ , which, as we have seen, contains a δ singularity. In fact for $y \neq 0$,

$$\xi'(y) = \frac{4me^{my}}{e^{2my} + 1} . \quad (2.80)$$

On the other hand, ξ' is divergent at $y = 0$ due to the discontinuity. Then from eq. (2.78) we see that for all y ,

$$\xi'(y) + 2\pi \delta(y) = \frac{4me^{my}}{e^{2my} + 1} . \quad (2.81)$$

Plugging back into the action, we then see that θ_W gives rise immediately to the area law, and we find

$$S \approx \text{Area} \int_{-\infty}^{+\infty} dy \left[\frac{1}{8\pi^2 \beta} (\xi'(y) + 2\pi \delta(y))^2 + 2\lambda(1 - \cos \xi) \right] . \quad (2.82)$$

Both integrals are elementary and equal to $m/(\pi^2\beta)$ so that

$$S \approx \frac{2m}{\pi^2\beta} \text{Area} . \quad (2.83)$$

Therefore, to leading order in the semiclassical calculation, the Wilson loop shows area-law behaviour

$$\frac{Z[s]}{Z} \sim \exp(-\sigma \text{Area}) , \quad (2.84)$$

with the string tension

$$\sigma = \frac{2m}{\pi^2\beta} . \quad (2.85)$$

Restoring lattice units, this is just the string tension prediction eq. (2.57) with an explicit constant $\tilde{c}/(4\pi^2) = 2/\pi^2 \approx 0.20$.

The semiclassical scaling of the string tension is lent further credit since it can be rigorously shown to be a lower bound for the string tension. For sufficiently large β , one has [81]

$$a^2\sigma \geq \text{const} \times \frac{am}{\beta} . \quad (2.86)$$

Moreover, a similar upper bound has also been shown [164],

$$a^2\sigma \leq \text{const} \times \frac{am}{\sqrt{\beta}} \left(1 + \mathcal{O}\left(\frac{\log \beta}{\beta}\right) \right) . \quad (2.87)$$

The semiclassical calculation also makes it clear that in the dual picture the string tension should be interpreted as an interface tension. The presence of a Wilson loop in a certain plane is captured by the insertion of the current s ; however, it can be equivalently captured by a boundary condition, whereby the field jumps by 2π across the Wilson loop plane. In fact the presence of the source δs in the Sine-Gordon equation of motion (2.77) precisely enforces this boundary condition. Thus the string tension can be seen as the interface tension for the global \mathbb{Z} symmetry across the Wilson loop. This method has also been explicitly used to compute the string tension in a lattice calculation [113].

2.4 U(1) gauge theory at finite temperature

The Euclidean partition function of a quantum field theory with periodic boundary conditions in the time directions can be interpreted as the partition function of a thermal system in the canonical ensemble with temperature

$$T = \frac{1}{aN_T} . \quad (2.88)$$

Suppose that we perform a simulation with spatial extent L and time extent N_T . To perform a simulation at zero temperature, a simple prescription would be to take $N_T = L$ and then extrapolate to the thermodynamic limit $L \rightarrow \infty$. Then one takes the continuum limit as explained in Chapter 1 by tuning the system to a continuous transition.

On the other hand, to perform a simulation at finite temperature the infinite volume limit is taken only in the space directions. One performs simulations at fixed N_T and increasing L with $L \gg N_T$. Then the continuum limit $a \rightarrow 0$ is taken together with the limit $N_T \rightarrow \infty$, while holding fixed the temperature T in eq. (2.88). In practice, one expresses the temperature as a

dimensionless ratio which can be determined on the lattice. Usually, one considers a ratio with the string tension σ (computed at zero temperature), i.e.

$$\frac{T}{\sqrt{\sigma}} = \frac{1}{\sqrt{a^2\sigma}N_T} . \quad (2.89)$$

In particular, the right-hand side can be determined on the lattice, as N_T is a parameter of the simulation and the string tension in lattice units $a^2\sigma$ can be determined by numerical simulations as discussed in the previous sections. However, as we have seen, in the three-dimensional U(1) gauge theory one has three possible continuum limits. Measuring T in units of $\sqrt{\sigma}$ and then taking $N_T \rightarrow \infty$ corresponds to a continuum limit where the string tension is taken as the standard of length. Note that this requires tuning the theory to a point where $a^2\sigma \rightarrow 0$, which is simply a point where a continuous transition takes place. On the other hand, if the mass gap m (at zero temperature) is taken as the standard of length, then one considers a ratio

$$\frac{T}{m} = \frac{1}{(am)N_T} . \quad (2.90)$$

A third continuum limit may be obtained where the dimensionful coupling g^2 is taken as the standard of length. The corresponding temperature ratio is

$$\frac{T}{g^2} = \frac{\beta}{N_T} , \quad (2.91)$$

where $\beta = 1/(ag^2)$ is the dimensionless coupling which appears in the action.

At sufficiently high temperature, gauge theories undergo a deconfinement transition. An order parameter for deconfinement is the Polyakov loop expectation value $\langle P \rangle$, typically averaged over space:

$$P = \frac{1}{L^2} \sum_{\vec{x}} P(\vec{x}) . \quad (2.92)$$

An argument for why this is an order parameter of the deconfinement transition goes as follows. On general grounds, one expects that the expectation value of the Polyakov loop correlator factorizes at large distances,

$$\lim_{R \rightarrow \infty} \langle P(\vec{x})P(\vec{y})^* \rangle = |\langle P \rangle|^2 , \quad (2.93)$$

since $\langle P(\vec{x}) \rangle = \langle P(\vec{y}) \rangle$ by translational invariance. But we know that the Polyakov loop correlator is related to the interquark potential as

$$\langle P(\vec{x})P(\vec{y})^* \rangle = e^{-N_T V(R)} . \quad (2.94)$$

In the confining phase, the interquark potential takes the form

$$V(R) = \sigma R + \text{const} + \mathcal{O}(1/R) . \quad (2.95)$$

This we have seen from the effective string theory, and in fact it can be rigorously shown that $V(R)$ cannot grow faster than linearly [165]. In the confining phase the string tension is non-zero and therefore $V(R) \rightarrow \infty$ as $R \rightarrow \infty$.

In the deconfined phase the theory is massless and one expects static charges to interact via a Coulomb potential. In four spacetime dimensions, this goes like $V(R) \sim 1/R$, so that

$V(R) \rightarrow \text{const}$ as $R \rightarrow \infty$. Thus seeing $|\langle P \rangle|^2$ as the $R \rightarrow \infty$ limit of the Polyakov loop correlator, we see that

$$\text{confinement} \implies \langle P \rangle = 0 , \quad (2.96)$$

$$\text{deconfinement} \implies \langle P \rangle \neq 0 . \quad (2.97)$$

Thus the Polyakov loop is an order parameter for the finite-temperature deconfinement transition.

In three spacetime dimensions, the situation is more complicated, because (at least for electrodynamics) the Coulomb potential is logarithmic, $V(R) \sim \log R$. Then in both phases $V(R) \rightarrow 0$ as $R \rightarrow \infty$, although the rate of decay is different:

$$\text{confinement} \implies \langle P(\vec{x})P(\vec{y})^* \rangle \rightarrow 0 \text{ exponentially} , \quad (2.98)$$

$$\text{deconfinement} \implies \langle P(\vec{x})P(\vec{y})^* \rangle \rightarrow 0 \text{ as a power law} . \quad (2.99)$$

In this case, the “deconfined” phase is really another confined phase, but only logarithmically so. The string tension is therefore zero in this phase. Even though the Polyakov loop does not acquire a vacuum expectation value, it can still be used to identify the location of the phase transition. In fact at the transition the functional form of the decay changes abruptly; thus one expects a sharp rate of change in $\langle P \rangle$ at the transition point. The decay of the Polyakov loop correlator eq. (2.98) is reminiscent of the decay of the spin correlator on the two sides of the BKT transition in the two-dimensional XY model. As we will see in a moment, this is not by chance.

As long as the Polyakov loop acquires a vacuum expectation value, the deconfinement transition may also be interpreted as the spontaneous breaking of a symmetry. In fact, the action of pure gauge theories is actually invariant under a 1-form symmetry known as “center symmetry” which acts by multiplying all gauge field variables on links in the time direction in one timeslice by a center element $z \in Z(G)$. Under such a transformation, the Polyakov loop transforms as

$$P \rightarrow zP . \quad (2.100)$$

Thus the deconfinement transition is associated with the spontaneous breaking of the center symmetry. This also leads to a heuristic argument which predicts the universality class of the deconfinement transition. The relevant variables for deconfinement are the Polyakov loops $P(\vec{x})$. Since they extend across all timeslices and at finite-temperature $L \gg N_T$, the system can be thought of as being effectively dimensionally-reduced to one dimension less. The Polyakov loops can then be thought of as spin variables which interact via nearest-neighbour interactions (intuitively, since the underlying theory has plaquette interactions) and global symmetry group $Z(G)$. This then leads to the prediction, known as the Svetitsky-Yaffe conjecture [166], that the deconfinement transition of a gauge theory with gauge group G in d spacetime dimensions should be in the same universality class of the transition of the spin model with symmetry $Z(G)$ in $d - 1$ dimensions. This should be true at least if the transition has universal features, i.e. it is continuous. Thus, for example, SU(2) gauge theory in three spacetime dimension is expected to have a deconfinement transition in the two-dimensional Ising universality class. Moreover, since a crucial role in this argument is played by the center of the gauge group, we also mention that it is especially interesting to study gauge groups without a center [167, 168].

A heuristic for the order of the deconfinement transition is that the transition will be continuous if the mismatch between the number of degrees of freedom on the two sides is small [169]. For U(1) in three dimensions, on one side we have a massless photon, and on the other a massive photoball. Thus one expects a continuous transition. Moreover, the center of U(1) is simply U(1), so by the Svetitsky-Yaffe conjecture the transition should be in the BKT universality

N_T	L_{\max}	β_{pc}
4	80	2.11(1)
6	80	2.35(5)
8	104	2.55(1)

Table 2.1: Location of the deconfinement transition for $N_T = 4, 6, 8$. The pseudo-critical coupling β_{pc} refers to the peak of the Polyakov loop susceptibility for the largest volume that we considered.

class. Lattice calculations provide support to these statements [114, 117, 120–122]. In fact, as we have seen in eq. (2.98), gauge theory arguments predict that the Polyakov loop correlator behaves in the same way as the spin correlator in the two-dimensional XY model, with the confined phase mapped to the disordered phase and the deconfined phase mapped to the quasi-long range ordered phase. Therefore in the 3D U(1) case, the deconfinement transition is not associated with spontaneous symmetry breaking. Intuitively, the at finite temperature the U(1) gauge theory monopoles are “squashed” in the time direction and become the two-dimensional BKT vortices. These arguments are also supported by RG calculations [166, 170]. In three dimensions, it is also interesting to contrast the U(1) gauge theory with the SU(2) gauge theory. Naively, in the deconfined phase of SU(2) gauge theory one might expect again a logarithmic Coulomb potential (much like in U(1)) due to the deconfined plasma of gluons. This would then again imply the absence of a vacuum expectation value for the Polyakov loop and thus no spontaneous symmetry breaking. However, the Svetitsky-Yaffe conjecture predicts that the transition in SU(2) gauge theory is in the two-dimensional Ising universality class. This is characterized by the spontaneous breaking of the \mathbb{Z}_2 symmetry and by a spontaneous magnetization in the broken phase (which corresponds to the deconfined case). Presumably, this then implies that the potential between static charges due to the SU(2) gluon plasma is not logarithmic, but rather at most a power law.

In practice, in any numerical simulation at finite volume, $\langle P \rangle = 0$. Thus one often considers $\langle |P| \rangle$ instead. For each N_T, L , the pseudocritical coupling β_{pc} can be identified as the location of the peak of the Polyakov loop susceptibility

$$\chi_P = L^2 \left(\langle |P|^2 \rangle - \langle |P| \rangle^2 \right). \quad (2.101)$$

In our case, there is no spontaneous symmetry breaking, but χ_P peaks at the location of sharpest change in the Polyakov loop, which is the phase transition. As usual, one then needs to extrapolate β_{pc} to infinite volume in order to obtain the critical coupling β_c . Due to the BKT nature of the transition, large lattices are required to obtain reliable data. The critical coupling also depends on the details of the infinite-volume extrapolation. Previous studies have found that to leading order the critical coupling scales as $\beta_c = \mathcal{O}(N_T)$ [118, 120, 121], which is also expected on theoretical grounds [115]. However, there is some disagreement over the actual values of β_c . This issue is not central to our work and we have therefore chosen to simply work with the pseudocritical couplings computed at the largest volume we considered. An example of the Polyakov loop susceptibility for $N_T = 6$ and increasing L is shown in Fig. 2.5, and the computed pseudocritical couplings are given in Table 2.1.

The above scaling of the critical coupling has important implications for the continuum limit of the theory. In particular, as $N_T \rightarrow \infty$ we have that $\beta_c \rightarrow \infty$ and therefore both $am \rightarrow 0$ and $a^2\sigma \rightarrow 0$ exponentially in N_T . Thus from eqs. (2.90) and (2.89), we find

$$\frac{T_c}{m} \rightarrow \infty, \quad \frac{T_c}{\sqrt{\sigma}} \rightarrow \infty. \quad (2.102)$$

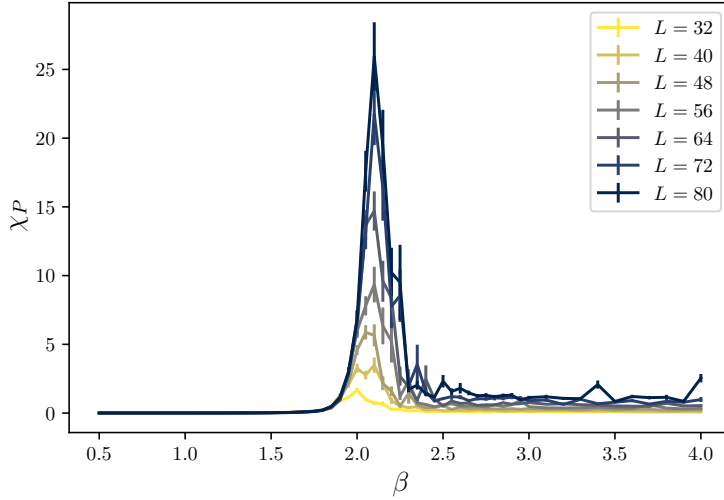


Figure 2.5: Polyakov loop susceptibility for $N_T = 6$ as a function of β , for increasing spatial extents L .

Therefore if either the mass or string tension are held fixed in the continuum, the deconfinement transition disappears and even at finite temperature the theory is always confining. On the other hand, if g^2 is held fixed, since $\beta_c = \mathcal{O}(N_T)$, from eq. (2.91) in the continuum limit one finds

$$\frac{T_c}{g^2} = \text{constant} . \quad (2.103)$$

Therefore in this case, there is a deconfinement transition. This is somewhat surprising, because in this limit the theory reduces simply to ordinary free electrodynamics.

2.5 The equation of state

The equation of state is the dependence of the pressure $p(T)$ on the temperature T . It can be computed via the so-called “integral method” [171], which is rather simple. From standard thermodynamic identities, one can express

$$p(T) = - \left. \frac{\partial F}{\partial V} \right|_T = T \left. \frac{\partial}{\partial V} \log Z \right|_T = T \frac{\log Z}{V} \quad \text{as } V \rightarrow \infty . \quad (2.104)$$

Here the free energy F is related to the canonical partition function Z by $Z = \exp(-F/T)$ as usual. Note that the last equality is a non-trivial identity valid in the infinite (spatial) volume limit $V \rightarrow \infty$.

For the Wilson action eq. (2.2), we can differentiate $\log Z$ with respect to the coupling to obtain,

$$\frac{\partial \log Z}{\partial \beta} = \left\langle \sum_p \cos \theta_p \right\rangle \equiv 3L^2 N_T \square , \quad (2.105)$$

where we denoted the average plaquette expectation value as \square , and $3L^2 N_T$ is the number of plaquettes in a three-dimensional lattice. In particular, \square can be computed on the lattice via numerical simulations. Integrating this equation between two points β_0 and β , we find

$$\log Z|_{\beta} - \log Z|_{\beta_0} = 3L^2 N_T \int_{\beta_0}^{\beta} d\beta' \square(\beta') . \quad (2.106)$$

A natural choice is to set $\beta_0 = 0$, where it is possible to compute the partition function exactly,

$$Z|_{\beta_0} = (2\pi)^{3N_T L^2} . \quad (2.107)$$

Here $3N_T L^2$ is the number of links on a three-dimensional cubic lattice. The spatial volume V is given by $V = a^2 L^2$, while the temperature is $T = 1/(aN_T)$, thus

$$p(T) = \frac{T}{V} \log Z|_{\beta(T)} = \frac{3 \log(2\pi)}{a^3} + \frac{3}{a^3} \int_0^{\beta(T)} d\beta' \square(\beta') , \quad (2.108)$$

where $\beta(T)$ is the value of β at which one has temperature T according to the definition of the temperature; in this case either eq. (2.90), (2.89) or (2.91). In practice one simply computes the right-hand side as a function of β and then rescales the x -axis so that it is expressed as a function of T instead (with the chosen length standard).

We are actually interested in the pressure $p(T)$ above the zero-temperature contribution $p(0)$. Then we see that the integration constant cancels and

$$p(T) - p(0) = \frac{3}{a^3} \int_{\beta_0}^{\beta(T)} d\beta' (\square_T(\beta') - \square_0(\beta')) , \quad (2.109)$$

where \square_T is computed at temperature T , while \square_0 is computed at zero temperature. In fact the subtraction is necessary because $p(0)$ is divergent. In what follows we will drop $p(0)$ and simply refer to the above quantity as $p(T)$. Expressing the equation in terms of dimensionless ratios which can be computed on the lattice, we find

$$\frac{p(T)}{T^3} = 3N_T^3 \int_0^{\beta(T)} d\beta' (\square_T(\beta') - \square_0(\beta')) . \quad (2.110)$$

On the lattice, we compute $\square_T(\beta')$ on a $N_T \times L^2$ lattice with $L \gg N_T$ and $\square_0(\beta')$ on a L^3 lattice with the *same* L and β . The plaquette expectation values have weak finite volume effects and therefore their difference is independent of L even for relatively small values of L . Thus the infinite volume extrapolation is not difficult. With this method, we obtain various pressure curves for different values of N_T ; we then repeat the calculation for increasing N_T to reach the continuum limit.

Gauge theories are expected to deconfine at large T . For a pure gauge theory, the degrees of freedom are then massless gauge bosons. The equation of state for a non-interacting gas of massless bosons can be computed via elementary methods [172]. The partition function for a single massless boson of frequency ω is given by

$$Z_\omega = \sum_{N=0}^{\infty} e^{-\beta\hbar\omega N} = \frac{1}{1 - e^{-\beta\hbar\omega}} . \quad (2.111)$$

The full partition function is then given by integrating over all frequencies,

$$\log Z = \int_0^{\infty} d\omega g(\omega) \log Z_\omega , \quad (2.112)$$

where $g(\omega)$ is the density of states. Then extracting the pressure from the partition function is elementary, and one finds in three dimensions

$$\frac{p(T)}{T^3} = \frac{\zeta(3)}{2\pi} \approx 0.1913 , \quad (2.113)$$

where ζ is the Riemann zeta function. Since for U(1) gauge theory, the only degree of freedom in the deconfined phase is the massless photon, this is the result of interest in our case. The limit in which the equation of state reduces to eq. (2.113) is referred to as the ‘‘Stefan-Boltzmann limit’’.

For finite N_T , only the ‘‘Matsubara frequencies’’ $\omega_n = 2\pi n/N_T$ are allowed, so one replaces the integral over ω with the appropriate summation, which leads to the finite- N_T correction to the Stefan-Boltzmann law [145]

$$\frac{p(T)}{T^3} = \frac{\zeta(3)}{2\pi} \left[1 + \frac{7}{4} \frac{1}{N_T^2} \frac{\zeta(5)}{\zeta(3)} + \frac{227}{32} \frac{1}{N_T^4} \frac{\zeta(7)}{\zeta(3)} + \frac{8549}{128} \frac{1}{N_T^6} \frac{\zeta(9)}{\zeta(3)} + \dots \right]. \quad (2.114)$$

On the other hand, in the confined phase the equation of state can be compared with the prediction of a gas of non-interacting *massive* bosons, which in three dimensions is [173]

$$\frac{p(T)}{T^3} = 2 \left(\frac{m}{2\pi T} \right)^{3/2} \sum_{n=1}^{\infty} \frac{1}{n^{3/2}} K_{3/2}(nm/T), \quad (2.115)$$

where K_ν is a modified Bessel function of the second kind. This formula applies to each species of glueball of mass m (computed at zero temperature); if the glueballs are non-interacting, then one can simply add the contribution from each glueball species. The expression on the right-hand side can be computed on the lattice, since $m/T = (am)N_T$ where am is computed at zero temperature at $\beta = \beta(T)$. In the zero mass limit $m \rightarrow 0$, eq. (2.115) reduces to the Stefan-Boltzmann law eq. (2.113) as expected.

It has been argued that the density of hadrons in QCD increases exponentially with the mass [174, 175]. Such a phenomenon is known as ‘‘Hagedorn spectrum’’. There is some evidence that this is true at least at large N_c [176, 177]. A Hagedorn spectrum arises naturally in string theories [132]. In pure gauge theories, we’ve seen that an open string connects two static quarks. On the other hand, glueballs are associated with closed flux strings [178, 179]. Thus it is conceivable that a Hagedorn spectrum might arise in pure gauge theories.

A direct comparison of the prediction of a Hagedorn spectrum with lattice measurements of the spectrum of the theory is quite difficult. On the other hand, one can compare the equation of state computed via the integral method with the prediction for a gas of non-interacting glueballs, including the first few glueball states. From eq. (2.115) we see that the contribution of a glueball of mass m is exponentially small in m . Thus one expects to find good agreement between the two methods, unless the density of glueballs itself increases exponentially with the mass. This method was employed for SU(2) and SU(3) gauge theories in both three and four spacetime dimensions, where it was found that the contributions of the first few glueballs lead to much smaller values of the pressure compared to the integral method [173, 180–184]. This provides evidence that non-Abelian pure gauge theories may indeed have a Hagedorn spectrum.

In our work, we perform the same comparison for U(1) gauge theory in three dimensions. The simulations were performed with the Wilson action for $N_T = 4, 6, 8$ and various values of L with $L \leq 80$ for $N_T = 4, 6$ and $L \leq 104$ for $N_T = 8$. The simulations were performed directly in the original theory with a heat bath algorithm combined with overrelaxation. The values of the mass and string tension were taken directly from the literature [115].

The equation of state, together with a comparison with the glueball gas prediction, is shown in Fig. 2.6 for $N_T = 4, 6, 8$ as a function of β . The three curves are shown in the same plot in Fig. 2.7. For small β the theory is in the confining phase and the pressure is essentially zero. For large β , on the other hand, the theory is deconfined and saturates quickly to a plateau in excellent agreement with the finite- N_T correction to the Stefan-Boltzmann limit eq. (2.114). Already at $N_T = 8$, the pressure is quite close to the continuum Stefan-Boltzmann limit eq. (2.113).

2.5. THE EQUATION OF STATE

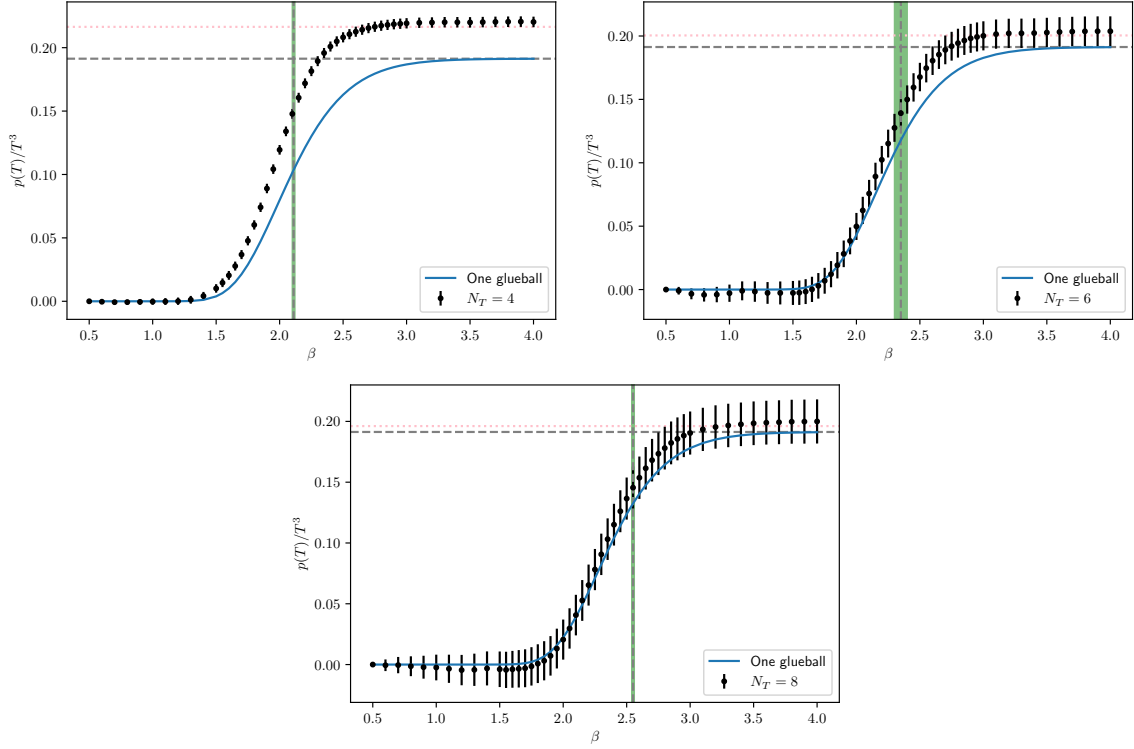


Figure 2.6: Equation of state $p(T)/T^3$ as a function of β for $N_T = 4$ (top left), $N_T = 6$ (top right) and $N_T = 8$ (bottom). In each of the three cases, the lattice results are indicated as dots with error bars. The continuous curve (blue) is the prediction for the gas of one glueball species, eq. (2.115). The horizontal dashed line (grey) is the Stefan-Boltzmann limit, eq. (2.113), while the horizontal dotted line (pink) is the finite- N_T correction to the Stefan-Boltzmann limit, eq. (2.114). Finally, the vertical line indicates the location of the pseudocritical point, together with its uncertainty (green band).

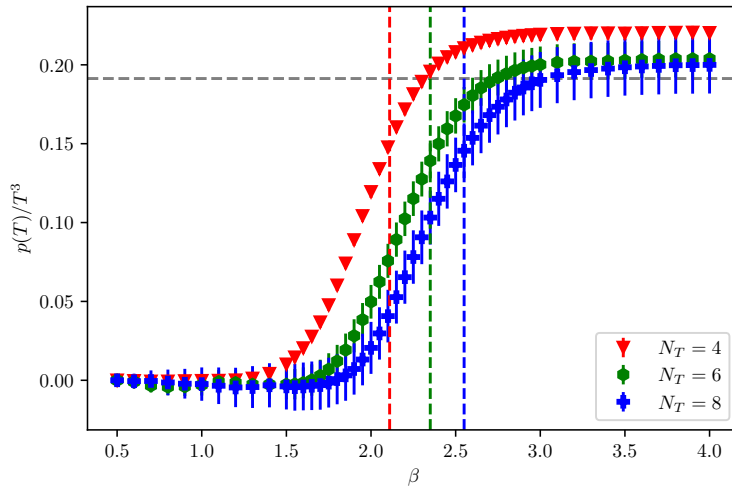


Figure 2.7: Comparison of the equation of state for $N_T = 4, 6, 8$. See also the caption of Fig. 2.6. In particular the pseudocritical coupling increases with N_T .

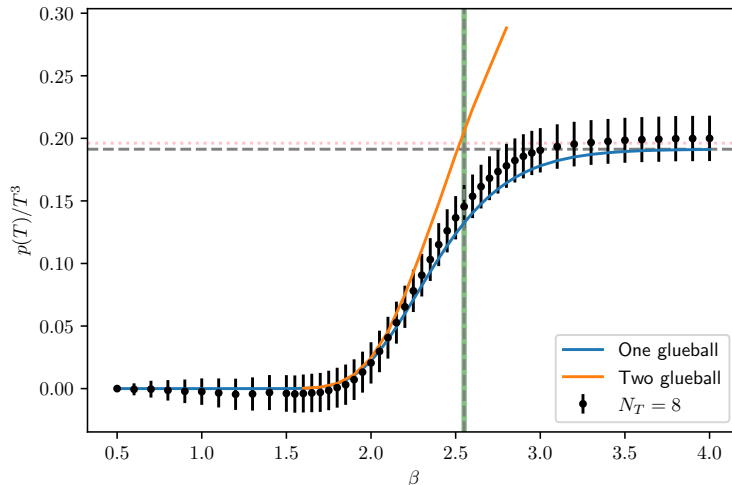


Figure 2.8: Equation of state for $N_T = 8$ together with the comparison including only one glueball species, or two glueball species. See also the caption of Fig. 2.6.

This is already an interesting result, which highlights the difference between this theory and standard non-Abelian gauge theories. In that case, in fact, the equation of state saturates only for extremely high temperatures [145, 181, 184].

As for the comparison with the glueball gas, it is clear that already at $N_T = 8$ the glueball gas with only one glueball species (with mass equal to the mass gap) is in excellent agreement with the equation of state computed with the integral method. This is another striking difference with non-Abelian gauge theories. In this theory, we therefore see no evidence of a Hagedorn spectrum. To further convince ourselves that this is the case, we can add the contribution from the second-largest glueball (which belongs to a different microscopic channel), which is shown in Fig. 2.8. But in this case, the prediction from the glueball gas is significantly larger than the pressure curve already in the confined phase where agreement would have been expected. In fact, as previously discussed, in the continuum limit the various microscopic glueball states arrange themselves in integer multiples of the mass gap [115]. Thus they should be interpreted as excitations of a *single* free massive particle, which is also predicted by the analytical treatment of the theory [81]. Then all glueball contributions are already accounted for by the lowest glueball state.

In order to avoid making a choice among the various continuum limits, we have made our plots with the bare coupling β on the x -axis. However, to discuss the continuum limit one needs to consider the temperature as defined according to eqs. (2.90), (2.89), (2.91). The plots where the mass and string tension are taken as the standard of length are given in Fig. 2.9. Since $T/g^2 = \beta/N_T$, the plots where g^2 is taken as the standard of length correspond to a simple rescaling of the previous plots and are thus omitted. In both cases, the Stefan-Boltzmann limit is saturated in a very large region, with the pressure being zero only close to zero temperature.

The interesting question is what happens to the equation of state in the continuum limit. We have seen that as N_T increases, the glueball gas prediction eq. (2.115) is in excellent agreement with the equation of state. Assuming that this remains true for larger N_T , we can use this information to extrapolate the equation of state to the continuum. In particular, it implies that the equation of state is a function of m/T only. The simplest case is the continuum limit where the mass is held fixed. Since the glueball gas prediction eq. (2.115) is independent of N_T when expressed as a function of T/m , then the curve is shown already in Fig. 2.9. In this case,

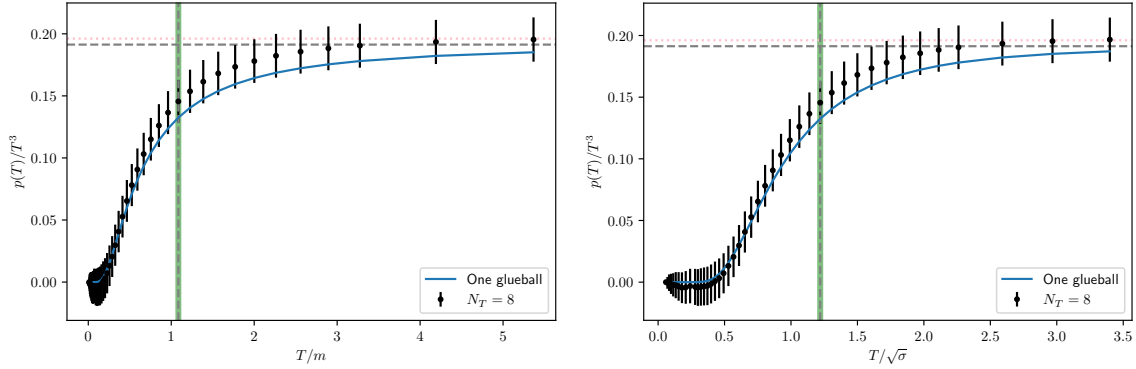


Figure 2.9: Equation of state $p(T)/T^3$ for $N_T = 8$ when either the mass (*left*) or the string tension (*right*) are held as the standard of length. See also the caption of Fig. 2.6. For clarity, several points at large β have been removed compared to the Fig. 2.6.

we've seen that $T_c/m \rightarrow \infty$, so the theory is always confining. Nonetheless, we can identify two different regimes which are separated by a simple crossover. For large T , which means $T \gg m$, the theory is effectively massless and therefore saturated at the Stefan-Boltzmann limit. On the other hand, for small T one has $T \ll m$ and the theory is effectively confined with very small pressure.

In the other two continuum limits, on the other hand, the glueball gas prediction eq. (2.115) *does* depend on N_T . In particular, we see that

$$\frac{m}{T} = \frac{m/\sqrt{\sigma}}{T/\sqrt{\sigma}}. \quad (2.116)$$

To plot $p(T)/T^3$ as a function of $T/\sqrt{\sigma}$ we fix $T/\sqrt{\sigma} = 1/(\sqrt{a^2\sigma}N_T)$ and then send $N_T \rightarrow \infty$. This requires $a^2\sigma \rightarrow 0$, which in terms of its scaling with the bare coupling eq. (2.58) means $\beta \rightarrow \infty$. But according to eq. (2.58) in this limit $m/\sqrt{\sigma} \rightarrow 0$, therefore according to the above formula, $m/T \rightarrow 0$. This means that $p(T)/T^3$ is always saturated at the massless limit, which is just the Stefan-Boltzmann limit eq. (2.113), independently of $T/\sqrt{\sigma}$. In other words, in the continuum $p(T)/T^3$ is constant as a function of $T/\sqrt{\sigma}$. In this case, we have the puzzling situation of a gauge theory which is always confining (since $T_c/\sqrt{\sigma} \rightarrow \infty$) yet it is massless and saturates the Stefan-Boltzmann limit.

A similar situation occurs if g^2 is held fixed in the continuum. In that case the appropriate ratio to consider is

$$\frac{m}{T} = \frac{m/g^2}{T/g^2}. \quad (2.117)$$

Again we take the limit $N_T \rightarrow \infty$ while fixing $T/g^2 = \beta/N_T$. This again requires $\beta \rightarrow \infty$, which implies that $m/g^2 = (am)\beta \rightarrow 0$. Thus again $p(T)/T^3$ is constant independent of T/g^2 and saturated at the Stefan-Boltzmann limit. This is less surprising since the continuum limit in this case is free electrodynamics with a simple massless photon. Yet this theory does not cease to amaze, since in this case we have a deconfinement transition at finite T_c/g^2 , yet the equation of state is *identical* on both sides of the transition.

2.6 Conclusions

In this chapter, we have studied the three-dimensional $U(1)$ gauge theory, which is interesting as a toy model for particle physics, but also in condensed matter physics as an effective gauge theory [185–190]. This theory is quite remarkable in several different ways. It can be treated analytically [80, 93, 156] and confinement has even been proven rigorously [81]. In fact, while this theory is confining, it displays remarkably different properties compared to non-Abelian gauge theories. As we have discussed, it has inequivalent length scales and therefore several continuum limits. Moreover, its confining string receives peculiarly large contributions from a “rigidity term” which is usually small [116, 143, 150].

Our contribution is the calculation of the finite-temperature equation of state of three-dimensional $U(1)$ gauge theory, which also displays peculiar differences compared to non-Abelian gauge theories. In particular, the Stefan-Boltzmann limit is saturated very quickly and we find no evidence of a Hagedorn spectrum. In terms of the three possible different continuum limits, only one leads to a non-trivial equation of state. Our results are in agreement with the analytical understanding of this theory, which predicts that, in one of the continuum limits, it is described by a free massive scalar field.

3

A new type of gauge theory

This chapter is based on:

[191] A. Banerjee, D. Banerjee, G. Kanwar, A. Mariani, T. Rindlisbacher, and U.-J. Wiese, “Broken symmetry and fractionalized flux strings in a staggered U(1) pure gauge theory”, *Phys. Rev. D* **109**, 014506 (2024), [arXiv:2309.17109](https://arxiv.org/abs/2309.17109).

In this chapter, we again investigate a three-dimensional gauge theory whose gauge group is U(1). However, contrary to Chapter 2, where we considered two standard actions in the literature, here we choose a novel action. This is interesting for many reasons. A new action may describe the same continuum physics as other actions (for example, this is the case for the Villain and Wilson actions [93, 123, 124]), or, describe a *different* continuum limit. Lattice actions describing the same continuum limit are useful because different actions may have different advantages, such as, for example, a better approach to the continuum, or they could be easier to simulate numerically, or be more suitable for theoretical manipulations, or even represent symmetries in a more useful manner. On the other hand, if the action turns out to have a different continuum limit, it is still interesting theoretically, both to map out the space of quantum field theories, but also practically for phenomenological purposes.

Generally speaking, from the Wilsonian point of view, an action is mainly determined by a choice of symmetries. Then one in principle includes all terms consistent with these symmetries. Of course, on the lattice there are several possible equivalent or inequivalent discretizations of continuum quantum field theories. In this chapter, we construct and study an alternative possible pure gauge lattice action with exact U(1) gauge invariance in three spacetime dimensions. This theory can be naturally compared with the standard U(1) gauge theory in three dimensions which we studied in Chapter 2.

The construction of the new theory has a most natural starting point in the Hamiltonian formulation. We then construct a Euclidean path integral via Trotterization, paying special attention to Lorentz invariance. We then study the properties of this theory, in particular its phase diagram, its mass gap and its confining string.

3.1 The new gauge theory action

As anticipated in the introduction, in this chapter we study a novel action with local U(1) gauge invariance in three dimensions. Actually, we consider more precisely a family of actions indexed

by an angular parameter $\alpha \in [0, 2\pi)$. The partition function is given by

$$Z = \left(\prod_l \int_0^{2\pi} d\varphi_l \right) \prod_p \left[\sum_{m \in \mathbb{Z}} e^{-i\frac{\alpha}{2\pi}(d\varphi)_p} \exp\left(-\frac{1}{2e^2}((d\varphi)_p - 2\pi m)^2\right) e^{i\alpha m} \right], \quad (3.1)$$

where we integrate over $U(1)$ variables φ_l on each link of the three-dimensional cubic lattice and $(d\varphi)_p$ is the plaquette variable associated to plaquette p . Here e^2 is a dimensionless coupling.

Several comments are in order. First of all, this is the partition function of a theory with local $U(1)$ gauge invariance. For $\alpha = 0$, it reduces to the Villain partition function eq. (2.36) for the standard $U(1)$ gauge theory, which we encountered in Chapter 2. Moreover, it is Lorentz-invariant, or rather, it is invariant under the ‘‘cubic group’’ of Lorentz transformations on the finite lattice. In what follows, we focus specifically on the case $\alpha = \pi$, which enjoys further symmetries. In particular, at this special point the theory is also invariant under parity P and charge conjugation C , which makes it especially interesting.

This partition function is rather complicated. It is not at all clear why one would consider writing down such a theory. As anticipated in the introduction, motivation for this theory comes naturally from a Hamiltonian picture. In the next section, we therefore discuss the Hamiltonian formulation of $U(1)$ gauge theory and its natural modifications which lead to the partition function eq. (3.1).

Another obvious problem for the partition function in eq. (3.1) is that it is not positive. In particular, the Boltzmann weights are in general complex; such an action is said to be affected by a ‘‘sign problem’’ and is hard to simulate. At this point of this thesis, it should not come as a surprise that the solution to this issue is dualization. As we have now seen several times, a three-dimensional gauge theory with local $U(1)$ gauge invariance is dual to a scalar field theory with a global \mathbb{Z} symmetry. As usual, the first step in the dualization is expanding in a Fourier series, which gives

$$Z = \left(\prod_l \int_0^{2\pi} d\varphi_l \right) \prod_p \left[\sum_{n \in \mathbb{Z}} e^{i(d\varphi)_p n} e^{-\frac{e^2}{2}(n + \frac{\alpha}{2\pi})^2} \right]. \quad (3.2)$$

Now, again as usual, we use integration by parts to write $\sum_p (d\varphi)_p n_p = \sum_l \varphi_l (\delta n)_l$. Integration over φ_l then simply gives δ functions which force $\delta n \equiv 0$. In infinite volume, this constraint is simply solved by writing $n = \delta h$ where h is a \mathbb{Z} -valued 3-form, therefore living on the cubes of the lattice. Finally, going to the dual lattice, h now lives on the sites of the dual lattice (the centers of each cube of the original lattice) and the partition function is given by

$$Z = \left(\prod_x \sum_{h_x \in \mathbb{Z}} \right) \exp\left(-\frac{e^2}{2} \sum_{\langle xy \rangle} (h_x - h_y + \alpha/2\pi)^2\right), \quad (3.3)$$

where all terms are now in the dual lattice. Now we note that the partition function eq. (3.1) is ambiguous in that it is not invariant under a change of orientation of each plaquette. In particular, changing the orientation of a plaquette p leads to $(d\varphi)_p \rightarrow -(d\varphi)_p$, but the obvious change of variables $m \rightarrow -m$ does not restore the partition function to its original form. This is not an issue in principle, as one simply requires a prescription defining what orientation one must use for the plaquettes. In the dual picture, one has the same ambiguity in that the partition function eq. (3.3) requires a choice of orientation for each link; it is not invariant when swapping the source and target site for each link. We choose to fix the ambiguity directly in the dual picture as follows. Each site $x = (x_0, x_1, x_2)$ is said to be even or odd based on the parity

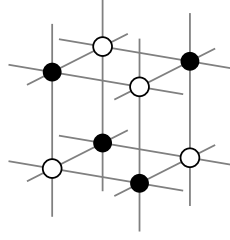


Figure 3.1: A subset of the three-dimensional dual lattice, depicting the staggered integer (black dots) and half-integer (white dots) height variables associated respectively with even and odd dual sites. Reprinted from [191].

of $x_0 + x_1 + x_2$. We then choose to orient each link $\langle xy \rangle$ so that x is always an odd site, and therefore y is always an even site. This choice preserves lattice rotational symmetry as well as translations by an even number of lattice spacing. With this choice, it is convenient to absorb the $\alpha/2\pi$ term in the scalar field on the odd sites, which leads to the partition function

$$Z = \left(\prod_{x \text{ odd}} \sum_{h_x \in \mathbb{Z} + \frac{\alpha}{2\pi}} \right) \left(\prod_{y \text{ even}} \sum_{h_y \in \mathbb{Z}} \right) \exp \left[-\frac{e^2}{2} \sum_{\langle xy \rangle} (h_x - h_y)^2 \right]. \quad (3.4)$$

This partition function is well-defined and does not suffer from ambiguities. Note that, importantly, the staggering of the height variables on even/odd sites is the same in all directions; this should be contrasted with the case of quantum link models, where the staggering is only realized in the space directions [192–195]. The staggering of the height variables is depicted in Fig. 3.1.

As mentioned above, in this work we will focus on the case $\alpha = \pi$. In this case, the height variables are integer (on the even sites) and half-integer valued (on the odd sites), and the partition function is

$$Z = \left(\prod_{x \text{ odd}} \sum_{h_x \in \mathbb{Z} + \frac{1}{2}} \right) \left(\prod_{y \text{ even}} \sum_{h_y \in \mathbb{Z}} \right) \exp \left[-\frac{e^2}{2} \sum_{\langle xy \rangle} (h_x - h_y)^2 \right]. \quad (3.5)$$

Note that the only difference compared to the standard U(1) gauge theory is the nature of the height variables on the odd sites.

The partition function for $\alpha = \pi$ enjoys the following symmetries:

1. *Global \mathbb{Z} -invariance*: $h_x \rightarrow h_x + c$ for any constant integer c .
2. *\mathbb{Z}_2 charge conjugation C* : $h_x \rightarrow -h_x$.
3. *\mathbb{Z}_2 single-site shift symmetry S* : $h_x \rightarrow h_{x+\hat{\mu}} + \frac{1}{2}$ where μ is any spacetime direction.
4. *Translations by an even number of lattice spacings*.
5. *Lattice Lorentz symmetry*, i.e. the action is fully isotropic and therefore invariant under the group of Euclidean cubic rotations and (for $\alpha = \pi$) also reflections.

Note that all symmetries are required to preserve the nature of the height variables h . In particular, integer and half-integer height variables must be mapped to height variables of the same kind. Both the global \mathbb{Z} invariance and charge conjugation naturally respect this prescription. On the other, translations by one lattice spacing in any direction (S) would

naturally swap integers and half-integers; the extra $1/2$ is added to restore the nature of the height variables. On the other hand, no such problem arises with translations by an even number of lattice spacings. Invariance under even translations is expected to be sufficient to recover full translational invariance in the continuum. Similarly, invariance under lattice Lorentz transformations is expected to be enough to recover full Lorentz invariance in the continuum. Note that while S , as defined, is not technically a \mathbb{Z}_2 symmetry (rather it squares to an even translation), it can be made so by appropriately combining it with parity P and charge conjugation C , i.e. for example $CPS : h_x \rightarrow -h_{-x+\hat{\mu}} - \frac{1}{2}$ is a proper \mathbb{Z}_2 symmetry which squares to the identity.

The staggered theory enjoys almost exactly the same lattice symmetries as the ordinary $U(1)$ theory. The only difference is the special role of the single-site shifts, which now mix with an internal transformation.

The special role played here by single-site shifts is analogous to the case of staggered fermions [125]. In that case, the fermion degrees of freedom are spread over multiple sites and, like in this case, single-site shifts are only a symmetry if combined with an appropriate internal transformation [196]. The single-site shift symmetry of staggered fermions can break spontaneously [197]. Other systems whose phase diagram is characterized by the breaking of charge conjugation C and single-site shifts S include quantum link models [192–195], as well as the quantum spin ladder regularization of $\mathbb{CP}(N-1)$ models [198, 199]. In Section 3.4.1 we will investigate the breaking of these symmetries in our model; we will find that C remains unbroken, while S is always spontaneously broken.

Finally, we note that again we have a global \mathbb{Z} symmetry much like in the standard $U(1)$ theory. We therefore remand the reader to the discussion of this symmetry in Chapter 2. In particular, it should be understood as a redundancy in our description of the system (the overall height over which the height variables fluctuate is irrelevant). Therefore all observables are required to be invariant under the \mathbb{Z} symmetry.

In the next chapter, we introduce the Hamiltonian formulation of $U(1)$ gauge theory and its natural modification which leads to the new gauge theory action in eq. (3.1). In the rest of the work, we study the new gauge theory in the $\alpha = \pi$ case. In particular, we extend to this case the effective theory for the standard $U(1)$ gauge theory which we discussed in Chapter 2 and discuss its predictions. We also perform numerical simulations to study the phase diagram of the theory, as well as its mass and its confining string.

3.2 Motivation for the new gauge theory

In this section, we explain the motivation for introducing the new gauge theory action. This is most natural in the Hamiltonian formulation, which we review. We then discuss a natural modification of the Hamiltonian and the Trotterization which leads to the partition function eq. (3.1).

Until now, we have considered lattice gauge theories in the Euclidean path-integral formulation, where spacetime is discretized as a hypercubic lattice. Alternatively, lattice gauge theories may also be formulated in the Hamiltonian picture [125]. The Euclidean path integral and Hamiltonian formulations are related by the transfer matrix formulation in temporal gauge, $A_0 = 0$ [200, 201]. In the Hamiltonian picture, the lattice theory may be thought of as a quantum mechanical system (with some caveats, see for example [202]). In particular, only *space* is discretized, while time remains continuous. Time evolution is dictated by a Hamiltonian, which acts on a Hilbert space. Classically, a gauge field configuration is given by an assignment of a group-valued variable $U_l \in U(1)$ to each spatial lattice link. In the quantum theory, then the

Hilbert space consists of wavefunctions $\psi : \mathcal{C} \rightarrow \mathbb{C}$ from the space of classical configurations \mathcal{C} which assign to each classical configuration its probability amplitude in a quantum measurement. Thus the Hilbert space is a tensor product space

$$\mathcal{H}_{\text{tot}} = \bigotimes_{l \in \text{links}} \mathcal{H}_l, \quad (3.6)$$

where each link factor \mathcal{H}_l is isomorphic to the space of square-integrable functions on $U(1)$, i.e. $\mathcal{H}_l \cong L^2(U(1))$.

Introducing coordinates on $U(1)$, we can write on each link $U_l = \exp(i\varphi_l) \in U(1)$ in terms of an angular variable $\varphi_l \in [0, 2\pi)$. On each link, the wavefunction $\psi(\varphi_l)$ is, first of all, required to be square integrable, i.e.

$$\int_0^{2\pi} d\varphi_l |\psi(\varphi_l)|^2 < \infty. \quad (3.7)$$

Moreover, they are required to have period 2π , i.e.

$$\psi(2\pi) = \psi(0). \quad (3.8)$$

This last condition is actually somewhat suspicious. In quantum mechanics, an overall phase of the wavefunction is actually irrelevant. Therefore it makes sense to require 2π -periodicity not of the wavefunction itself but only of the absolute value squared of the wavefunction,

$$|\psi(2\pi)|^2 = |\psi(0)|^2. \quad (3.9)$$

This then implies the general condition that the wavefunction comes back to itself *up to a phase*, i.e.

$$\psi(2\pi) = e^{i\alpha} \psi(0). \quad (3.10)$$

Such a modification is familiar from the quantum mechanics of a rotor (see for example [203]). In other words, the wavefunction need not be a linear representation of the $U(1)$ symmetry, but it could equally well be a *projective* representation. The angle α here is the one which will appear in the partition function for the new gauge theory eq. (3.1). We can already see that charge conjugation is broken for $\alpha \notin \{0, \pi\}$. In particular, C maps $U_l \rightarrow U_l^*$. Therefore the condition eq. (3.10) is consistent with C only if $e^{i\alpha} = e^{-i\alpha}$, which, up to periodicity, implies $\alpha \in \{0, \pi\}$.

The choice in eq. (3.10) may also be understood in a more mathematical way as a *self-adjoint extension* [204, 205]. Consider the electric field operator $E_l = -i\partial/\partial\varphi_l$ defined on the interval $[0, 2\pi]$. It is a well-known issue in quantum mechanics that such an operator, while Hermitean, cannot be self-adjoint as long as one insists that the endpoints of the interval are distinct [206, 207]. The theory of self-adjoint extensions allows one to classify the possible choices of boundary conditions for the wavefunction ψ which make E self-adjoint; the most general choice is precisely eq. (3.10). Self-adjointness is important because (unlike Hermiticity) it ensures existence of an orthonormal basis of (generalized) eigenfunctions and real eigenvalues. This is necessary so that the Hamiltonian and the Gauss law have their expected properties.

The partition function can be obtained from the Hamiltonian by appropriately Trotterizing the expression

$$Z = \text{tr}(e^{-\epsilon N_T H}), \quad (3.11)$$

where ϵ is the lattice spacing in the time direction. Modifying the Hilbert space by changing the conditions satisfied by the wavefunctions leads to a different trace and therefore a different partition function *even with the same Hamiltonian* (this is most obvious by expanding the trace in an eigenbasis of H ; the eigenvalues can certainly change with the boundary conditions).

While this is part of our construction, it is not all that is required. In particular, the resulting partition function is not Lorentz invariant. As we will see in a moment, in order to restore Lorentz invariance, we also appropriately modify the Hamiltonian.

The Hamiltonian of standard U(1) gauge theory is given by

$$H = \frac{e^2}{2} \sum_{l \in \text{links}} E_l^2 + \frac{1}{2e^2} \sum_{p \in \text{plaqs}} B^2((d\varphi)_p) . \quad (3.12)$$

Here $(d\varphi)_p$ is the plaquette variable for spatial plaquettes p , while the electric field E_l is defined on each link as the operator

$$E_l = -i \frac{\partial}{\partial \varphi_l} . \quad (3.13)$$

On each link, the theory is therefore analogous to the quantum mechanics of a particle on the circle [97, 203]: the U(1) variable $U_l = \exp(i\varphi_l)$ plays the role of “position” on the circle, while the electric field E_l plays the role of “momentum” (i.e. the conjugate momentum to position). The magnetic Hamiltonian couples the links together as a potential term. As should be familiar in this thesis by now, it may be chosen in several different ways which are equivalent in the continuum; for example one could choose the Wilson term

$$B^2((d\varphi)_p) = 1 - \cos((d\varphi)_p) , \quad (3.14)$$

or the Villain term

$$\exp(-B^2((d\varphi)_p)/2e^2) = \sum_{n \in \mathbb{Z}} \exp\left(-\frac{1}{2e^2} \sum_p ((d\varphi)_p - 2\pi n)^2\right) . \quad (3.15)$$

The last ingredient in the definition of the theory is the gauge symmetry. Among the states in the total Hilbert space \mathcal{H}_{tot} only a subset should be considered as physical. In particular, a state $|\psi\rangle$ belongs to the physical Hilbert space $\mathcal{H}_{\text{phys}}$ if it satisfies the Gauss law constraint

$$G_x |\psi\rangle = 0 , \quad G_x = \sum_i \left(E_{x,i} - E_{x-\hat{i},i} \right) , \quad (3.16)$$

where the sum over i runs over all spatial directions and \hat{i} is the unit vector oriented in the i -th spatial direction. Note that, as expected, the Hamiltonian commutes with the Gauss law.

In the above description, we have chosen to introduce the angle α in eq. (3.10) as a twist of the 2π periodicity of the wavefunction on each link. With this choice, all operators, such as the electric field and the Hamiltonian are affected only via their domain of definition. However, for simplicity, we map the Hilbert space of twisted wavefunctions eq. (3.10) to the ordinary Hilbert space of 2π -periodic wavefunctions eq. (3.9) by sending

$$\psi(\varphi) \rightarrow e^{-i\varphi\alpha/2\pi} \psi(\varphi) . \quad (3.17)$$

Under this transformation, the magnetic Hamiltonian is invariant, while the electric field is modified as

$$E_l \rightarrow E_l + \frac{\alpha}{2\pi} . \quad (3.18)$$

Therefore the family of theories indexed by the angle α can be identified with theories over the usual Hilbert space, with a modified electric field (and therefore a modified electric Hamiltonian). Note that eq. (3.18) makes it clear that the introduction of the angle α is still consistent with

the Gauss law constraint in eq. (3.16). Under the transformation eq. (3.18), the Hamiltonian is mapped to

$$H = \frac{e^2}{2} \sum_{l \in \text{links}} \left(E_l + \frac{\alpha}{2\pi} \right)^2 + \frac{1}{2e^2} \sum_{p \in \text{plaqs}} B^2((d\varphi)_p) . \quad (3.19)$$

The introduction of the angle α can be compared with another kind of topological angle, the θ angle. In particular, in $(1+1)$ dimensions, there is no magnetic field and the Hamiltonian only includes the electric part. Then the substitution in eq. (3.18) is equivalent to introducing a θ angle with $\theta = \alpha$ (or $-\alpha$ depending on the conventions). Therefore in two spacetime dimensions the α and θ angles are equivalent. On the other hand, in higher dimension this is not the case. In $(3+1)$ dimensions the θ term is introduced in the Hamiltonian by the replacement $\vec{E} \rightarrow \vec{E} - \frac{\theta}{8\pi^2} \vec{B}$, which preserves Lorentz-invariance [97]. In this sense the α angle represents one possible higher-dimensional generalization of the two-dimensional θ term. Note further that in dimension higher than $(1+1)$ eq. (3.18) only makes sense on the lattice, since E is a vector and α a scalar.

We can now discuss the Trotterization of the theory, with which we can pass from the Hamiltonian to the path-integral formulation. To this end, on each link we expand the states in the orthonormal “position basis” $\{|U\rangle\}$ indexed by the elements $U = e^{i\varphi} \in \text{U}(1)$

$$|\psi\rangle = \int_0^{2\pi} d\varphi \psi(\varphi) |U\rangle . \quad (3.20)$$

We can further introduce a dual basis $\{|m\rangle\}$ with $m \in \mathbb{Z}$ which makes the electric field diagonal,

$$\langle U|m\rangle = \frac{1}{\sqrt{2\pi}} e^{im\varphi} , \quad E|m\rangle = \left(m + \frac{\alpha}{2\pi} \right) |m\rangle . \quad (3.21)$$

On the whole lattice, the position basis is given by all tensor product states of the form

$$|\{U\}\rangle \equiv \bigotimes_{l \in \text{links}} |U_l\rangle . \quad (3.22)$$

The partition function can be written in terms of the Hamiltonian as

$$Z = \text{tr} \left(e^{-\epsilon N_T H} \right) , \quad (3.23)$$

where ϵ is the lattice spacing in the time direction and N_T is the number of lattice sites in the time direction. Then the Trotter formula gives for fixed ϵN_T ,

$$e^{-\epsilon N_T (H_E + H_B)} = \left(e^{-\epsilon H_E} e^{-\epsilon H_B} \right)^{N_T} + \mathcal{O}(\epsilon^2) . \quad (3.24)$$

We can then insert decompositions of the identity in terms of the $|\{U\}\rangle$ states between each of the N_T factors. The magnetic Hamiltonian is diagonal in this basis and is therefore easily computed. The electric Hamiltonian, on the other hand, has non-trivial matrix elements. Since H_E is a sum over all links, these can be reduced to matrix elements on each link. By inserting $\{|m\rangle\}$ states and applying Poisson summation one finds

$$\langle U' | e^{-\epsilon \frac{e^2}{2} E^2} | U \rangle = \frac{1}{\sqrt{2\pi e^2 \epsilon}} e^{-i \frac{\alpha}{2\pi} (\varphi' - \varphi)} \sum_{m \in \mathbb{Z}} \exp \left(-\frac{1}{2e^2 \epsilon} (\varphi' - \varphi - 2\pi m)^2 \right) e^{i\alpha m} . \quad (3.25)$$

Here U and U' are interpreted as link variables in two different timeslices referring to the same link; the variable $\varphi' - \varphi$ is naturally associated with the plaquette variable in the time directions,

where the links connecting the two timeslices have been set to zero (corresponding to the choice of the temporal gauge). Undoing this choice, one then finds a partition function where the plaquettes connecting different timeslices have a Boltzmann weight equal to

$$\sum_{m \in \mathbb{Z}} e^{-i \frac{\alpha}{2\pi} (d\varphi)_p} \exp \left(-\frac{1}{2e^2} ((d\varphi)_p - 2\pi m)^2 \right) e^{i\alpha m}, \quad (3.26)$$

where we set $\epsilon = 1$ since we're interested in the isotropic limit where the lattice spacing is equal in the time and space directions. On the other, the weight of plaquettes lying entirely in the space directions is given simply by $e^{-\epsilon B^2 ((d\varphi)_p)}$, since B^2 is diagonal. It is clear that choosing either the Villain or Wilson form will lead to a Boltzmann weight for the spacelike plaquettes that is *different* from the Boltzmann weight of timelike plaquettes eq. (3.26). The resulting theory breaks the Euclidean cubic symmetry and is non-relativistic. In particular, it should be clear that no choice of B^2 operator will ever lead to a Boltzmann weight matching the one for timelike plaquettes. In fact the Boltzmann weight eq. (3.26) is complex-valued, and it therefore cannot take the form $e^{-\epsilon B^2 ((d\varphi)_p)}$ with Hermitean B^2 . Since we are interested in constructing a Lorentz invariant theory, we therefore simply choose the Boltzmann weights for all plaquettes to match those of timelike plaquettes. This results in the partition function for the new gauge theory in eq. (3.1), i.e.

$$Z = \left(\prod_l \int_0^{2\pi} d\varphi_l \right) \prod_p \left[\sum_{m \in \mathbb{Z}} e^{-i \frac{\alpha}{2\pi} (d\varphi)_p} \exp \left(-\frac{1}{2e^2} ((d\varphi)_p - 2\pi m)^2 \right) e^{i\alpha m} \right]. \quad (3.27)$$

In particular, as we have seen, this partition function does not match any choice of magnetic Hamiltonian. In fact it does not admit a single-timeslice transfer matrix but only a two-timeslice transfer matrix; this is most evident in the dual formulation due to the staggering of the height variables, and in fact also in similar cases (such as staggered fermions) it is only possible to construct a two-timeslice transfer matrix.

3.3 Analytical treatment

As we have seen in Chapter 2, the standard U(1) gauge theory in three dimensions is confining for all values of the coupling [81]. We have reviewed the crucial ingredient of the proof of confinement, which involves the derivation of an “effective theory” valid near the continuum. While reviewing that case, we introduced the possibility of an extra “magnetic field” with an eye towards the case that we will discuss now. Starting from the partition function of the staggered theory,

$$Z = \left(\prod_{x \text{ odd}} \sum_{h_x \in \mathbb{Z} + \frac{1}{2}} \right) \left(\prod_{y \text{ even}} \sum_{h_y \in \mathbb{Z}} \right) \exp \left[-\frac{e^2}{2} \sum_{\langle xy \rangle} (h_x - h_y)^2 \right], \quad (3.28)$$

we proceed much like in Chapter 2 by replacing the discrete variables h with continuous variables σ . On the even sites, where the height variables are integer-valued the situation is the same as for the ordinary U(1). On the other hand, on the odd sites, we set $h_x = m_x + \frac{1}{2}$ so that

$$\sum_{h_x \in \mathbb{Z} + \frac{1}{2}} \delta(\sigma_x - 2\pi h_x) = \sum_{m_x \in \mathbb{Z}} \delta(\sigma_x - \pi - 2\pi m_x) = \sum_{q_x \in \mathbb{Z}} e^{iq_x(\sigma_x - \pi)} \quad (3.29)$$

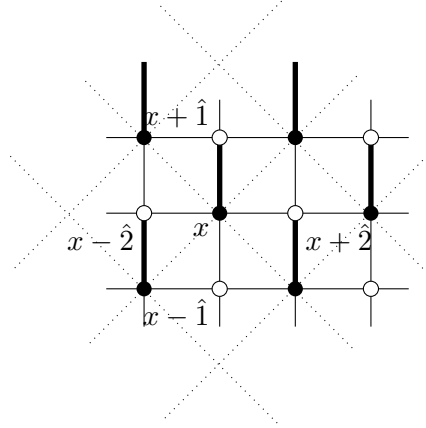


Figure 3.2: A two dimensional slice of the cubic lattice with even (*black*) and odd (*white*) points highlighted. The variables connected by a thick link are joined together into sum and difference variables (here $\mu = 1$). The superimposed dotted lattice is a slice of the tetrahedral-octahedral lattice formed by the even lattice points of the cubic lattice.

Therefore the partition function becomes

$$Z = \left(\prod_x \int_{-\infty}^{+\infty} d\sigma_x \right) \left(\prod_x \sum_{q_x \in \mathbb{Z}} \right) \exp \left[-\frac{e^2}{8\pi^2} \sum_{\langle xy \rangle} (\sigma_x - \sigma_y)^2 + i \sum_x q_x \sigma_x - i \sum_x q_x B_x \right], \quad (3.30)$$

which is the same as for the ordinary theory with the exception of the “magnetic field” B_x , which is given by

$$B_x = \begin{cases} 0 & x \text{ even} \\ \pi & x \text{ odd} \end{cases}. \quad (3.31)$$

We had already anticipated this possibility in the calculation in Chapter 2. Substituting this form of B_x in the final expression that we had obtained for the effective theory, we find that the staggered theory with $\alpha = \pi$ is described for small e^2 (near the continuum) by the theory of a real compact scalar field ϕ_x in a *staggered* potential,

$$S[\phi] = \frac{1}{2} \sum_{\langle xy \rangle} (\phi_x - \phi_y)^2 - 2\lambda \sum_x (-1)^x \cos \left(\frac{2\pi\phi_x}{\sqrt{e^2}} \right). \quad (3.32)$$

where $\lambda \equiv 2e^{-2\pi^2 v_0/e^2}$. For ease of calculation, in what follows we replace $\frac{2\pi\phi_x}{\sqrt{e^2}} \rightarrow \phi_x$, leading to the equivalent action

$$S[\phi] = \frac{e^2}{8\pi^2} \sum_{\langle xy \rangle} (\phi_x - \phi_y)^2 - 2\lambda \sum_x (-1)^x \cos \phi_x. \quad (3.33)$$

Much like in the standard case, the scalar field is in some sense compact because in the original model we are required to identify height configurations which differ by an overall integer; therefore we should identify $\phi_x \sim \phi_x + 2\pi$ where 2π is an overall shift at all sites.

A non-relativistic version of eq. (3.32) provides an effective descriptions of quantum antiferromagnets [188]. Due to the staggering of the cosine model, which is a discontinuous, “high-energy” feature, it is not clear how to take the continuum limit of the staggered scalar theory. To do this, we first need to appropriately modify the field variables. Following [188], we define the sum and difference variables on neighbouring sites,

$$\chi_x = \frac{\phi_x + \phi_{x+\hat{\mu}}}{2}, \quad \xi_x = \frac{\phi_x - \phi_{x+\hat{\mu}}}{2}, \quad (3.34)$$

defined to live only on the *even* lattice sites. Note that this mapping is one-to-one and has unit Jacobian. The resulting theory will then live on the lattice formed by the even sites of the original hypercubic lattice. Note that the definition of these variables requires an arbitrary choice of direction μ which disappears in the final result. The construction of the sum and difference variables is illustrated in Fig. 3.2 on a two-dimensional slice of the lattice. To make use of these variables, we note that

$$\begin{aligned} \sum_x (-1)^x \cos \phi_x &= \sum_{x \text{ even}} \cos \phi_x - \sum_{x \text{ odd}} \cos \phi_x = \\ &= \sum_{x \text{ even}} [\cos \phi_x - \cos \phi_{x+\hat{\mu}}] = \\ &= -2 \sum_{x \text{ even}} \sin \left(\frac{\phi_x + \phi_{x+\hat{\mu}}}{2} \right) \sin \left(\frac{\phi_x - \phi_{x+\hat{\mu}}}{2} \right) = \\ &= -2 \sum_{x \text{ even}} \sin \chi_x \sin \xi_x. \end{aligned} \quad (3.35)$$

Now we need to deal with the kinetic term. This calculation is much more complicated and we skip most of the details. The key point is that, as we will see in a moment, the field ξ_x actually has a mass of the order of the lattice spacings. Therefore we may ignore its fluctuations over its mean-field value [188]. In particular, we ignore its gradients. This is a reasonable approximation, even though not fully justified.

The lattice formed by considering only the even sites of a cubic lattice is known as the *tetrahedral-octahedral honeycomb*. The unit cells alternate between tetrahedrons and octahedrons. Calling three directions in the original lattice $\hat{1}, \hat{2}, \hat{3}$, the nearest neighbour directions for each even site are $\hat{\alpha} = \hat{1} + \hat{2}$, $\hat{\beta} = \hat{1} - \hat{2}$, $\hat{\gamma} = \hat{1} + \hat{3}$ and $\hat{\alpha} + \hat{\beta} - \hat{\gamma} = \hat{1} - \hat{3}$. Thus we may write

$$\begin{aligned} \sum_{\langle xy \rangle} (\phi_x - \phi_y)^2 &= \sum_{x \text{ even}} \sum_{\nu} [(\phi_x - \phi_{x+\nu})^2 + (\phi_x - \phi_{x-\nu})^2] = \\ &= \sum_{x \text{ even}} \sum_{\nu} [(\chi_x + \xi_x - \chi_{x+\nu-\mu} + \xi_{x+\nu-\mu})^2 + (\chi_x + \xi_x - \chi_{x-\nu-\mu} + \xi_{x-\nu-\mu})^2]. \end{aligned} \quad (3.36)$$

From this expression we can already see that ξ acquires a mass term of the form $24\xi_x^2$, which, as anticipated, is therefore of the order of the lattice spacing once units are restored. Then proceeding as discussed above, we ignore all gradients in ξ and, moreover, we also ignore next-to-nearest neighbour terms, resulting in

$$\sum_{\langle xy \rangle} (\phi_x - \phi_y)^2 \approx \sum_{x \text{ even}} \left[24\xi_x^2 + (\Delta_{\alpha}^{-} \chi_x)^2 + (\Delta_{\beta}^{-} \chi_x)^2 + (\Delta_{\gamma}^{-} \chi_x)^2 + (\Delta_{\alpha+\beta-\gamma}^{-} \chi_x)^2 \right], \quad (3.37)$$

where the lattice backwards derivative in a direction $\hat{\rho}$ is defined as

$$\Delta_{\rho}^{-} \chi_x = \chi_x - \chi_{x-\hat{\rho}}. \quad (3.38)$$

Note that in eq. (3.37) we get one extra derivative because the chosen basis is not orthonormal, but the resulting kinetic term is isotropic. Thus we expect to recover a standard Lorentz-invariant kinetic term for χ in the continuum. Putting everything together, we find

$$S = \sum_x \left[\frac{e^2}{8\pi^2} \left((\vec{\nabla}\chi_x)^2 + 24\xi_x^2 \right) + 4\lambda \sin \chi_x \sin \xi_x \right], \quad (3.39)$$

where $(\vec{\nabla}\chi_x)^2$ summarizes the four derivative terms in eq. (3.37). The mass of the field ξ can be inspected by canonically normalizing the kinetic term, in which case we find that the mass squared of ξ is 24 in lattice units. Restoring units, ξ therefore has a mass of the order of the lattice cutoff. It is therefore reasonable to expect that ξ is fixed on its mean-field value (i.e. its minimum) which is given by

$$\xi_x \approx -\frac{2\pi^2}{3} \frac{\lambda}{e^2} \sin \chi_x, \quad (3.40)$$

which we substitute back into the action to find

$$S[\chi] = \sum_x \left[\frac{e^2}{8\pi^2} (\vec{\nabla}\chi_x)^2 + \frac{2\pi^2}{3} \frac{\lambda^2}{e^2} \cos(2\chi_x) \right]. \quad (3.41)$$

Now this model admits a continuum limit as a scalar field theory. In particular the main difference between the effective action for the staggered theory eq. (3.41) compared to that of the ordinary U(1) theory eq. (2.51) is the presence of a double cosine instead of an ordinary cosine, and the prefactor which is roughly $\sim \lambda^2$ rather than $\sim \lambda$.

The harmless-looking factor of 2 is actually responsible for significant differences in the physics of the two models. In particular, as is clear from tracing the effect of the global \mathbb{Z} invariance through eqs. (3.32) and (3.39), configurations of the χ field differing by an overall integer multiple of 2π should be identified. This is true for both the $\alpha = 0$ and $\alpha = \pi$. But while in the ordinary case the cosine potential is of the form $\cos(\chi)$, so that its minima are all identified, in the staggered case the potential $\cos(2\chi)$ admits two inequivalent minima located at $\chi = \pm\pi/2$. Note that ξ could acquire a mass term only because it is invariant under global \mathbb{Z} transformations.

On top of the global redundancy, the effective theory in eq. (3.41) has a $\mathbb{Z}_2 \times \mathbb{Z}_2$ global symmetry structure given by the transformations

$$C : \chi_x \rightarrow -\chi_x + \pi \quad S : \chi_x \rightarrow \chi_x + \pi. \quad (3.42)$$

One has $C^2 = S^2 = 1$ and $CS = SC : \chi_x \rightarrow -\chi_x$. The labels for this symmetry are not chosen arbitrarily. In fact, we have seen several times that complicated transformations of the partition function (such as dualities or the manipulations to reach the effective theory) do not allow a direct tracing of symmetries across the transformations. Nonetheless, we have seen that the microscopic theory also has a $\mathbb{Z}_2 \times \mathbb{Z}_2$ symmetry structure generated by charge conjugation C and the single-site shift symmetry S . By choosing the labels to match, and therefore identifying these symmetries, in both cases we find that C is unbroken, while S is spontaneously broken. This is most obvious from the effective theory point of view, since the double cosine potential has minima at $\chi = \pm\pi/2$ which are preserved by C and interchanged by S . From the point of view of the microscopic theory, numerical simulations show that this is the case, as we will see in Section 3.4.

Finally, we can discuss explicit continuum limits for the staggered theory. Much like we've seen in Chapter 2 for the ordinary theory, in this case one can define a mass (restoring the lattice spacing a)

$$a^2 m^2 = \frac{32\pi^4}{3} \frac{1}{e^4} \exp(-4\pi^2 v_0/e^2), \quad (3.43)$$

where e^2 is the dimensionless coupling. Then taking the continuum limit $a \rightarrow 0$ while holding the mass fixed again requires $e^2 \rightarrow 0$ as expected. Then again the height of the potential separating the two physical minima becomes infinite and one therefore finds that in the continuum limit the theory consists of a single scalar field of mass m , which describes the fluctuations around one of the broken symmetry vacua.

For the string tension σ , similarly to the ordinary theory, a semiclassical approximation [156] leads to a scaling of the form $\sigma \sim m e^2$ (the same as for the ordinary theory). In this picture, the string tension corresponds to the interface tension between different minima of the potential. Unlike the ordinary theory, the staggered theory has physically inequivalent minima. Then a continuum limit where the string tension is held fixed corresponds to a non-trivial theory where tunneling between the \mathbb{Z}_2 minima is allowed, as well as domain walls separating different spontaneously broken vacua. As we will soon see, this picture of the string tension as the interface tension between broken symmetry vacua is also quite clear from the pictures produced during the numerical simulation, see in particular Fig. 3.8.

3.4 Numerical simulation

In order to further investigate the new gauge theory, as well as connect the microscopic description of the theory to the effective theory derived in Section 3.3, we performed numerical simulations of the staggered height model of eq. (3.5). In particular, we construct and investigate appropriate order parameters for the investigation of the possible breaking of charge conjugation C and single-site shift S . We also study other properties of the theory such as its mass and its string tension, as well as qualitative features of the confining string.

The numerical simulations were mostly performed with cluster Monte Carlo algorithms [109, 208, 209]. When Polyakov loops are inserted, we used either standard Metropolis or the snake algorithm discussed in Chapter 2. We always chose isotropic lattices of size L^3 where L ranges from 32 to 256. We investigated values of the coupling in the range [0.3, 2.0]. On general grounds, as well as following the effective theory prediction, we expect the continuum limit to be approached as $e^2 \rightarrow 0$, similarly to the ordinary U(1) theory.

3.4.1 Order parameters

To investigate the possible breaking of the C and S symmetries, we constructed appropriate order parameters. These need not only to appropriately transform under the symmetry, but they also need to satisfy general principles of quantum field theory such as locality. Similar order parameters were previously constructed in other settings [192–195, 198, 199].

For the C symmetry, we consider the order parameter

$$O_{CS} = \sum_x (-1)^x h_x = \sum_{x \text{ even}} h_x - \sum_{x \text{ odd}} h_x , \quad (3.44)$$

which is sensitive to both C and S , and in particular it changes sign under either. Note that O_{CS} is a sum of local operators, and it is also invariant under the global \mathbb{Z} symmetry.

The other order parameter is sensitive to S only, and it is given by a sum over all lattice cubes,

$$O_S = \sum_{c \in \text{cubes}} \sum_{x \in c} (-1)^x (h_x - \bar{h}_c)^2 , \quad (3.45)$$

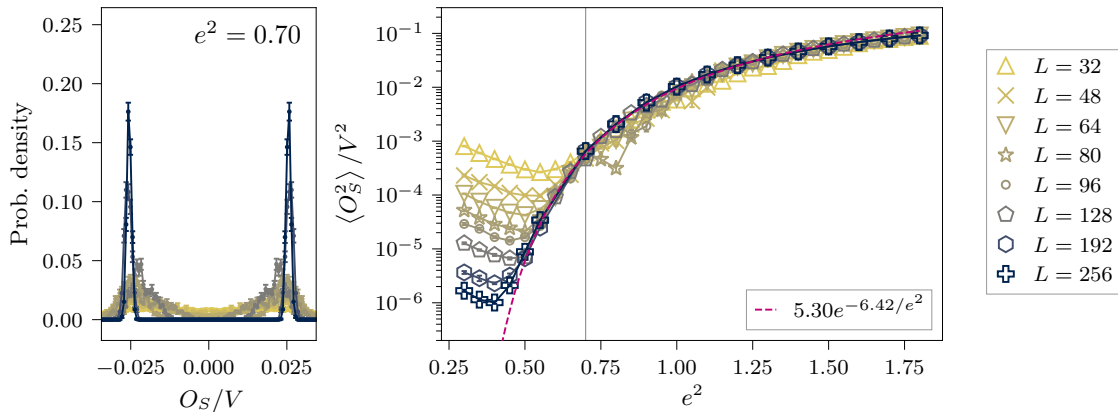


Figure 3.3: Left: Histogram of the operator O_S normalized by the volume V at $e^2 = 0.70$. Right: Susceptibility of O_S normalized by V^2 as a function of e^2 for several volumes, with a fit of the large-volume data to the form $A \exp(-B/e^2)$. The vertical line is located at the coupling $e^2 = 0.70$ where the histogram is shown. The double-peaked structure at large volume (left) and scaling as V^2 (right) indicates spontaneous breaking of the S symmetry. Reprinted from [191].

where the average height variable within the cube is defined as

$$\bar{h}_c = \frac{1}{8} \sum_{x \in c} h_x . \quad (3.46)$$

This somewhat cumbersome construction is necessary in order to ensure that O_S is local, as well as invariant under the global \mathbb{Z} symmetry.

The results of the numerical simulations for the two order parameters are shown in Figs.(3.3) and (3.4). We can look first at the data for the O_S observable, shown in Fig. (3.3). In particular, we have plotted on the right side the normalized susceptibility O_S^2/V^2 where $V = L^3$ is the lattice volume. We see that for a wide range of couplings O_S^2/V^2 is roughly independent of the volume, showing that the operator O_S acquires a vacuum expectation value. This is also confirmed by the histogram of O_S/V on the left taken at $e^2 = 0.8$, which shows two well-defined peaks which become sharper at increasing volume. For small couplings, closer to the transition, the susceptibility O_S^2/V^2 develops volume dependence. However, this effect occurs at smaller and smaller couplings as the volume is increased. Thus it is likely a finite-volume effect, where the simulations were performed on lattices too small to display spontaneous symmetry breaking. Moreover, a fit of the susceptibility to a function of the form $f(e^2) = A \exp(-B/e^2)$ (inspired by the scaling of quantities in the ordinary U(1) theory) for the largest volume in the range $e^2 \in [0.50, 0.80]$ is also shown on the right side of Fig. 3.3. The function provides an excellent fit to the data and would predict that the O_S operator acquires a vacuum expectation value for all values of the coupling. One can also test a functional form $f(e^2) = A \exp(-B/(e^2 - e_c^2))$ with a small offset, to test whether the data is consistent with the symmetry being restored at some non-zero coupling. The fit gives $e_c^2 = 0.04(11)$, consistent with zero.

Overall, we interpret the data as evidence that the S symmetry is broken for all values of the coupling. Note that even though single-site shifts are spontaneously broken, translations by an even number of lattice spacings remain unbroken.

On the other hand, the data for the O_{CS} observable is shown in Fig. 3.4, with a similar presentation as in the previous case. The normalized susceptibility O_{CS}^2/V^2 shows a consistent decrease with the volume V for all values of the coupling. This means that O_{CS} does not acquire

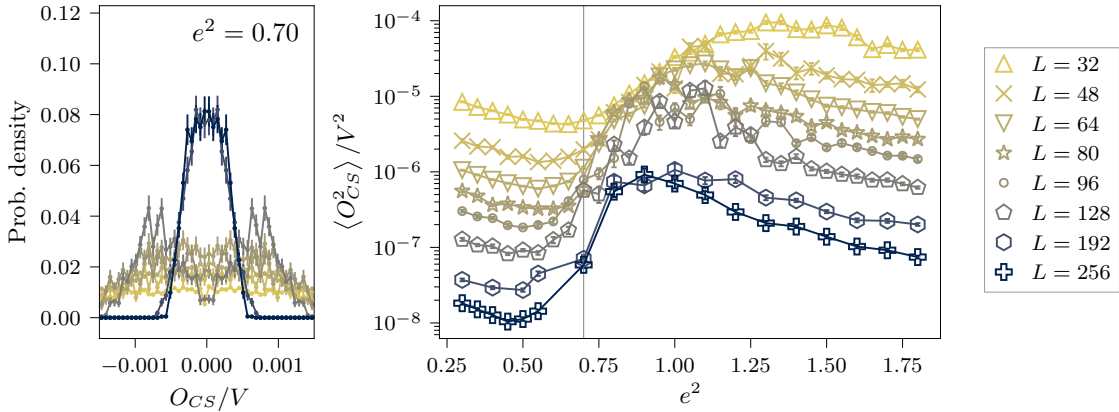


Figure 3.4: Left: Histogram of the operator O_{CS} normalized by the volume at $e^2 = 0.70$. Right: Susceptibility of O_{CS} normalized by V^2 as a function of e^2 for several volumes. The vertical line is located at the coupling $e^2 = 0.70$ where the histogram is shown. A single histogram peak at large volumes (left) and scaling smaller than V^2 (right) indicates that either the C or S symmetries are unbroken. Reprinted from [191].

a vacuum expectation value. In the region $e^2 \in [0.7, 0.8]$, the decrease is not as clear, but the histogram on the left (taken at $e^2 = 0.8$) shows that while two peaks may appear to form for small volumes, they join together in the center for large volumes. Therefore the observable O_{CS} does not acquire a vacuum expectation value at any value of the coupling, which means that at least one of C or S remains unbroken. Since data for the O_S observable implies that S is broken, this means that charge conjugation C remains unbroken for all values of the coupling.

3.4.2 Mass and string tension

Other quantities of interest are the mass and string tension, especially in light of the analytical predictions derived in Section 3.3. The mass may be measured from the exponential decay of the correlation function $(h_x - h_y)^2$ after appropriate momentum projection and subtractions [151, 208]. This choice of observable may be understood as a globally \mathbb{Z} -invariant version of the standard two-point function $h_x h_y$.

The results of the numerical simulations for the mass are shown in Fig. 3.5 for a range of couplings and various volumes. As we know from the discussion of the O_S observable, for small couplings finite-volume effects restore the S symmetry; it is important that all measurements are taken in the correct phase. We see that the mass suffers from finite volume effects for the smaller volumes, but at least in the range $e^2 \in [1.1, 2.0]$ the larger volumes agree. In this range, we have therefore tested various hypothesis for the mass scaling. All of them take the form

$$f(e^2) = Ag(e^2) \exp(-B/e^2), \quad (3.47)$$

where we chose various options for the prefactor g . In particular, we considered $g(e^2) = 1$ (simple exponential decay), $g(e^2) = 1/e^2$ (effective theory prediction, eq. (3.43)), and $g(e^2) = 1/\sqrt{e^2}$ (behaviour of the standard theory, eq. (2.53)). All three choices provide acceptable fits to the data, with $\chi^2/\text{d.o.f} \approx 0.80, 0.95, 0.78$, and exponent $B = 4.85(7), 6.33(7), 5.59(7)$ respectively. The analytical prediction for the fit form is slightly preferred, but our data is insufficient to exclude the other options. For the ordinary $U(1)$ theory, the exponent is predicted to be $\pi^2 v_0 \approx 2.49$ as in eq. (2.53). For the $\alpha = \pi$ theory, our analytical prediction is instead $B = 2\pi^2 v_0 \approx 4.99$

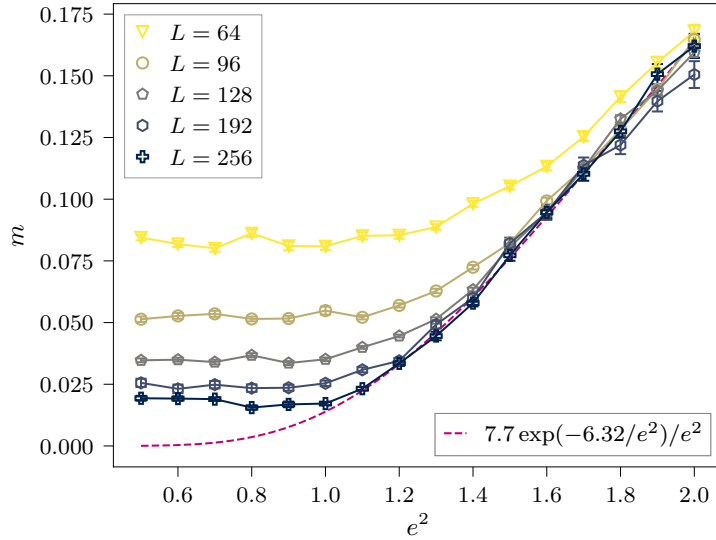


Figure 3.5: Mass m of the $\alpha = \pi$ theory for various values of the coupling e^2 , given in lattice units. Finite volume effects can be seen from the measurements at smaller volumes diverging from larger volumes as e^2 is taken small. The fit is performed with data in the range $e^2 \in [1.1, 2.0]$, with the fit form motivated by our effective theory for $\alpha = \pi$ (eq. (3.43)). Reprinted from [191].

(eq. (3.43)). This is reasonably close to the value obtained with a simple exponential fit, but relatively far from the value obtained with the full analytical prediction. All three fits are in reasonable qualitative agreement with the fact that the $\alpha = \pi$ theory should have a faster decay to zero as the continuum is approached, compared to the standard theory. Again, testing for whether the transition occurs at finite e^2 leads to a value consistent with zero.

The string tension, on the other hand, can be measured in multiple ways. One of the techniques is a variation on the snake algorithm which we presented in Chapter 2. The other technique we adopt is based on the direct measurement of the system’s energy with the static charges inserted, which also allows to “picture” the confining string [192, 210, 211]. With this method, the goal is to derive an expression for the expectation value of the Hamiltonian $\langle H \rangle$ which may be evaluated directly in the dual theory. As explained in Chapter 2, static charges can be inserted into the partition function as a Polyakov loop correlator. Let $Z[s]$ be the partition function of the system with the static charges inserted. Then in terms of the Hamiltonian H , we have

$$Z[s] = \text{tr} (e^{-\epsilon N_T H}) . \quad (3.48)$$

The expectation value of the Hamiltonian can then be extracted as

$$\langle H \rangle = \frac{1}{Z[s]} \text{tr} (H e^{-\epsilon N_T H}) = -\frac{1}{Z[s] N_T} \frac{\partial}{\partial \epsilon} Z[s] . \quad (3.49)$$

The partition function $Z[s]$ can be expressed in terms of the height variables, where it takes the form

$$Z = \left(\prod_{x \in \text{sites}} \sum_{h_x} \right) \exp \left[-\frac{e^2}{2} \sum_{\langle xy \rangle} (h_x - h_y + s_{\langle xy \rangle})^2 \right] . \quad (3.50)$$

To properly take the derivative in terms of the timestep ϵ we also restore the lattice spacing a in the space directions. At the end we will take again the isotropic limit $\epsilon = a$. To correctly restore

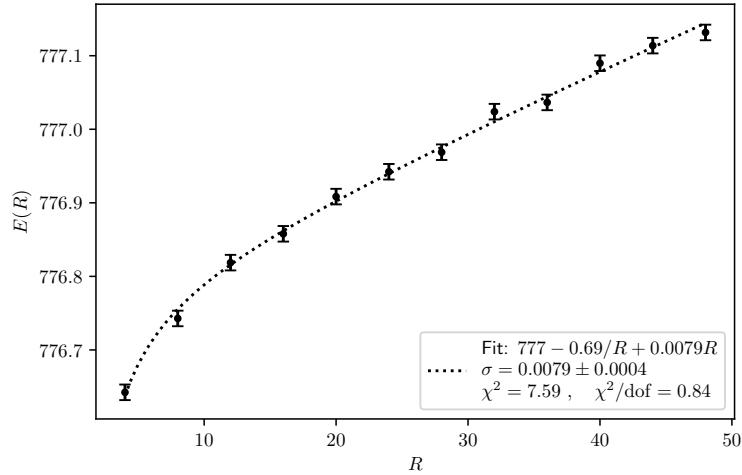


Figure 3.6: Energy $E(R)$ vs charge separation R obtained via the direct measurement method, together with a fit to eq. (3.53), on a 64^3 lattice at $e^2 = 1.2$.

units, we note that the sum over links discretizes a spacetime volume integral which comes with units of ϵa^2 . On the other hand $h_x - h_y$ discretizes a derivative and therefore comes with a factor of $1/a$ for links in the space directions and $1/\epsilon$ for links in the time direction. Overall therefore the action can be written as

$$S = \frac{a^2 e^2}{2\epsilon} \sum_{\langle xy \rangle_{\text{time}}} (h_x - h_y + s_{\langle xy \rangle})^2 + \frac{\epsilon e^2}{2} \sum_{\langle xy \rangle_{\text{space}}} (h_x - h_y + s_{\langle xy \rangle})^2, \quad (3.51)$$

where $\langle xy \rangle_{\text{time}}$ and $\langle xy \rangle_{\text{space}}$ denote links in the time and space directions respectively. The derivative can now be taken explicitly, and restoring $\epsilon = a = 1$ one finds

$$\langle H \rangle = \frac{e^2}{2T} \left\langle - \sum_{\langle xy \rangle_{\text{time}}} (h_x - h_y + s_{\langle xy \rangle})^2 + \sum_{\langle xy \rangle_{\text{space}}} (h_x - h_y + s_{\langle xy \rangle})^2 \right\rangle. \quad (3.52)$$

This expression can be computed via Monte Carlo simulation directly in the dual theory. Note that this expression is only valid up to Trotterization errors; since we set $\epsilon = a$, we then see that this expression is valid only in the continuum limit $a \rightarrow 0$. Moreover, from this expression it is clear that one can associate an energy locally to each link. One may then plot the contribution to the energy of each link individually, thus obtaining a “picture” of the confining string.

From the energy $E(R)$ of static quarks separated by a distance R , one can extract the string tension σ by fitting to a potential inspired by the theoretical prediction of effective string theory [135, 146, 212–214]

$$E(R) = A + \sigma R - \frac{B}{R} + \mathcal{O}(1/R^2). \quad (3.53)$$

As we have seen in Chapter 2, effective string theory predicts a specific value for the coefficient B , but in this case we chose to keep it as a free fit parameter. As shown in Fig. 3.6, this form of the energy provides an excellent fit to the data obtained via the direct measurement method. This confirms that the $\alpha = \pi$ theory is confining. However, we observed a statistically significant dependence of the resulting string tension on the interval chosen for the fit. In general, for unclear reasons, measuring the string tension in this theory is challenging. Alternatively, from the snake algorithm one extracts directly the energy differences

$$E(R+1) - E(R) = \sigma + \mathcal{O}(1/R^2), \quad (3.54)$$

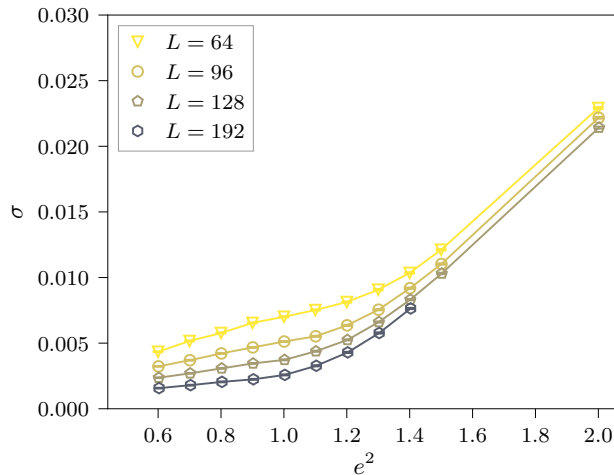


Figure 3.7: String tension σ of the $\alpha = \pi$ theory for various values of the coupling e^2 , given in lattice units. Statistically significant finite-volume effects can be observed over the entire range of couplings, potentially reflecting the more diffuse structure of the double-stranded confining string in this theory. Reprinted from [191].

from which σ can be extracted directly. The results of the snake algorithm simulation for the string tension are shown in Fig. 3.7. These results agree with the direct measurement method on the couplings closest to the transition, as expected. Nonetheless, as is clear from the figure, significant finite volume effects are present for the whole range of couplings studied.

With the direct measurement method, one can also measure the local energy of the string in each direction, which is defined as

$$\begin{aligned} u_0(x) &= \langle -(h_x - h_{x+\hat{0}} + s_0(x))^2 \rangle, \\ u_i(x) &= \langle (h_x - h_{x+\hat{i}} + s_i(x))^2 \rangle, \end{aligned} \quad (3.55)$$

which together define the Hamiltonian energy eq. (3.52),

$$\langle H \rangle = \sum_x [u_0(x) + u_1(x) + u_2(x)]. \quad (3.56)$$

A local version of the electric field is given by

$$\vec{E}(x) = (h_x - h_{x+\hat{2}} + s_2(x), -h_x + h_{x+\hat{1}} - s_1(x)). \quad (3.57)$$

The results of the local measurements are shown in Fig. 3.8 at the largest coupling $e^2 = 2.0$. The same qualitative structure is visible for all couplings studied, but $e^2 = 2.0$ gives the clearest pictures. The energy densities are most interesting. In particular, they depict a string which is qualitatively different from the standard confining string. In particular, it is *fractionalized* into two different strands. One should compare this picture with the equivalent one for the standard theory Fig. 2.1 which we discussed in Chapter 2; in that case, the confining string has a single strand as expected. Similar fractionalization of the confining string was observed in quantum link models [192–195], but as far as we’re aware this is the first time that it has been observed in a gauge theory with an infinite dimensional Hilbert space.

It is also interesting to study the interplay between the confining string and the phases of the theory. In particular, we define local versions of the O_S and O_{CS} in the presence of static

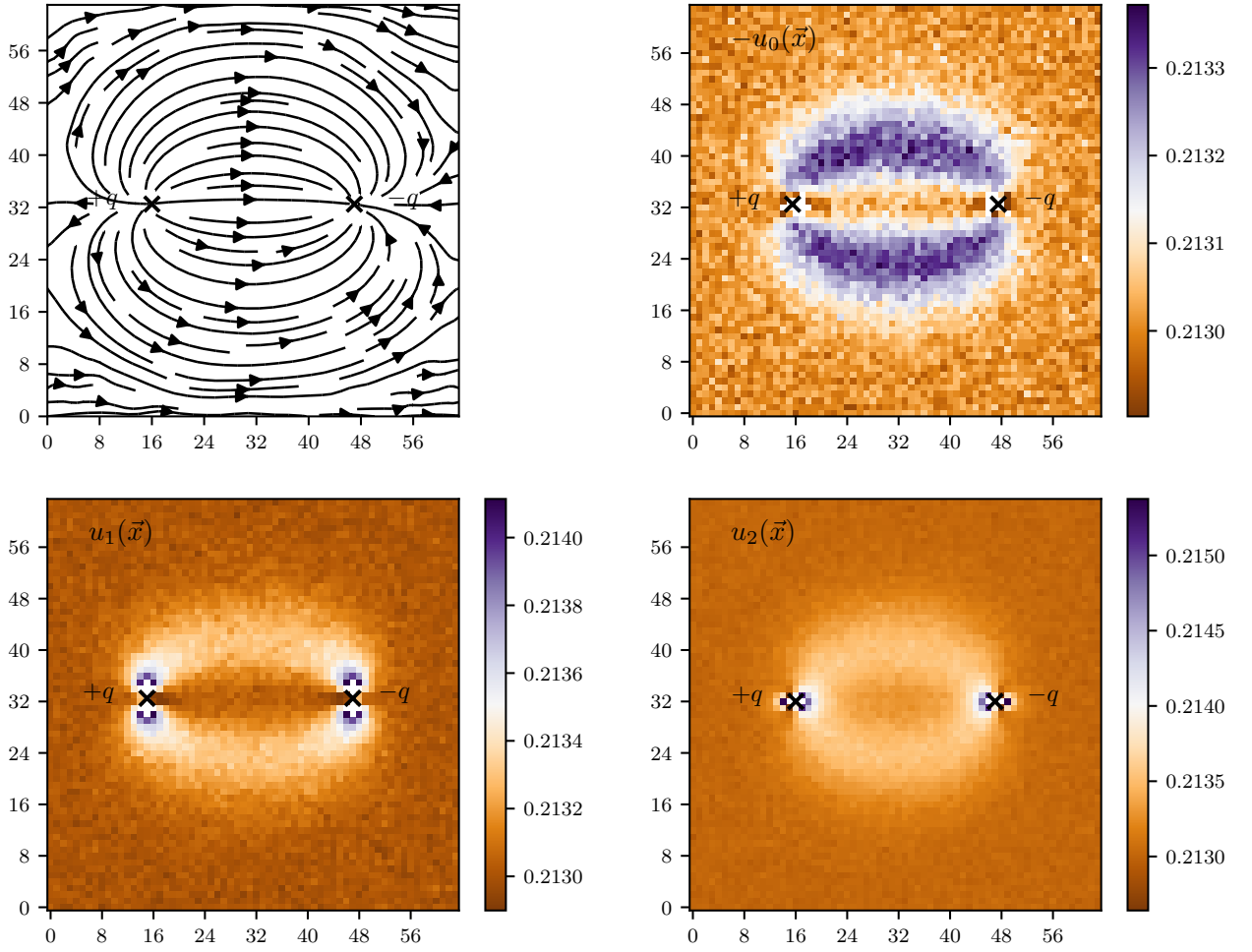


Figure 3.8: Time-averaged local energies and electric field on a spatial $L \times L$ lattice with $L = 64$ measured in the presence of two static charges at coupling $e^2 = 2.0$. The first figure (top left) shows the field lines of the electric field \vec{E} defined in eq. (3.57). The last three figures (top right through bottom right) show the local energy defined in eq. (3.55) in the three spacetime directions. In all three figures, the brightest pixels corresponding to contact energy terms are masked. The energy distributions clearly depict fractionalization of the flux string into two strands. Reprinted from [191].

charges. In particular,

$$O_{CS}(x) = \frac{(-1)^x}{12} \sum_{\hat{\mu} \in \{\pm\hat{0}, \pm\hat{1}, \pm\hat{2}\}} (h_x - h_{x+\hat{\mu}} + s_{\mu}(x)). \quad (3.58)$$

For $O_S(x)$ a similar, but more complicated expression may also be written down. The basic idea is to rewrite it in terms of link variables of the form $h_x - h_{x+\mu}$ and then replacing $h_x - h_{x+\mu} \rightarrow h_x - h_{x+\mu} + s_{\mu}(x)$. It is important to include the Polyakov loop variable s so that the resulting observables are invariant under deformations of the surface bounding the Polyakov loops. In the case $s = 0$ one recovers the usual order parameters by summing over the lattice,

$$O_{CS} = \sum_x O_{CS}(x), \quad O_S = \sum_x O_S(x). \quad (3.59)$$

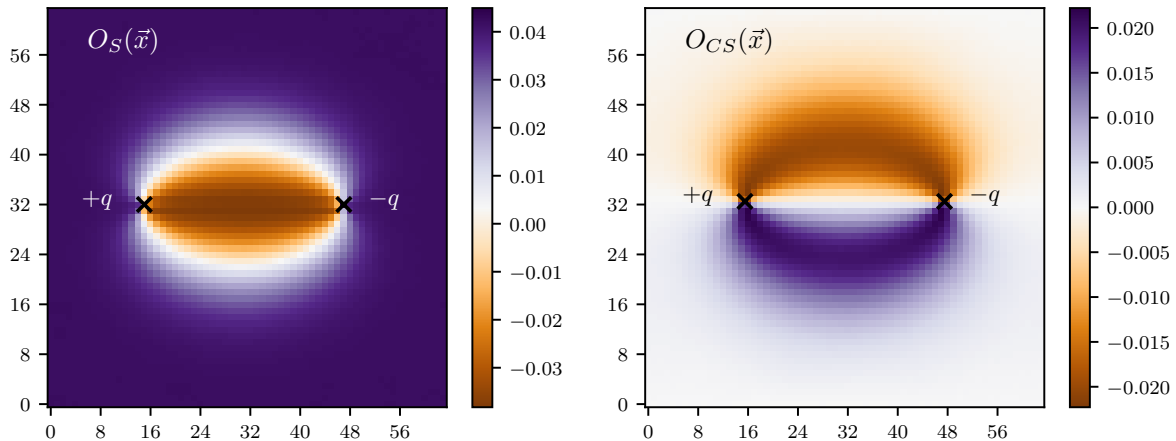


Figure 3.9: Local O_S (left) and O_{CS} (right) observables measured in the presence of two static charges on the ensemble with coupling $e^2 = 2.0$ and lattice size $L = 64$. Shown are the Euclidean-time-averaged measurements over the spatial $L \times L$ lattice. The O_S observable shows that the two string strands separate regions that correspond to the two ground states of the broken \mathbb{Z}_2 symmetry, while the O_{CS} observable shows that the two strands themselves break charge conjugation. Reprinted from [191].

The results of the measurements of the local order parameters are shown in Fig. 3.9. Again, the two strands of the confining string are readily identified. In terms of the phase structure, the confining string separates two different ground states of the broken \mathbb{Z}_2 symmetry S . As anticipated from the analytical description, the string plays the role of a domain wall between different broken symmetry vacua, and the string tension is the interface tension. On the other hand, the O_{CS} observable shows that, as expected, no vacuum expectation value is acquired in the bulk; on the other hand, O_{CS} takes different non-zero values on the two strands, indicating the two strands themselves break charge conjugation C . Note that tunneling events between different vacua may occur during the simulation, which would wash out the pictures. It is important to ensure that one takes measurements in one phase only.

The analytical treatments of both the ordinary $U(1)$ theory and the $\alpha = \pi$ theory predict that the string tension should scale as $\sigma \sim me^2$ in lattice units. Unfortunately, strong finite volume effects, especially in the measurement of the string tension, prevent us from obtaining reliable data on this prediction. It is not immediately clear why measuring the string tension in this theory is difficult. It cannot be simply attributed to the fractionalized nature of the confining string, since the same occurs also in quantum link models, where however the string tension can be accurately determined.

3.5 Conclusions

In this chapter, we have discussed a novel action with $U(1)$ gauge symmetry in three dimensions parametrized by an angle α . We have studied in detail the case $\alpha = \pi$ and used both analytical and numerical techniques to show that it has a continuum limit with a broken \mathbb{Z}_2 symmetry absent in the ordinary theory. We therefore conclude that this action describes different physics compared to the standard Wilson or Villain actions.

We have further studied other properties of the theory, such as the mass and string tension. The confining string in this model shows a qualitatively different behaviour compared to the

standard theory, in that it is fractionalized into two strands. The strands separate different vacua of the spontaneously broken \mathbb{Z}_2 symmetry.

After publishing the paper, we became aware that supersymmetric theories can also exhibit fractionalized flux strings [215–217]. Remarkably, the effective theory for the long-distance physics of SU(2) Super-Yang-Mills theory on $R^3 \times S^1$ is *the same* as the effective theory that we derived for our staggered height model [217]. This is further confirmation that our model describes very different continuum physics compared to ordinary U(1) theory.

These results can be extended in many directions. For example, one could study the U(1) theory with an α angle in four dimensions; or extend the construction to non-Abelian gauge theories. Studying values of α different from π may also be interesting.

Bibliography

- ¹A. Mariani, “Vortex condensate and critical exponents in the (2+1)-dimensional O(2) model”, *Phys. Rev. B* **108**, 134520 (2023), [arXiv:2305.13156](#).
- ²A. J. Leggett, *Quantum liquids* (Oxford University Press, 2022).
- ³V. L. Ginzburg and A. A. Sobyenin, “On the theory of superfluidity of helium II near the λ point”, *J. Low Temp. Phys.* **49**, 507–543 (1982).
- ⁴J. A. Lipa, D. R. Swanson, J. A. Nissen, T. C. P. Chui, and U. E. Israelsson, “Heat Capacity and Thermal Relaxation of Bulk Helium very near the Lambda Point”, *Phys. Rev. Lett.* **76**, 944–947 (1996).
- ⁵J. A. Lipa, J. A. Nissen, D. A. Stricker, D. R. Swanson, and T. C. P. Chui, “Specific heat of liquid helium in zero gravity very near the lambda point”, *Phys. Rev. B* **68**, 174518 (2003).
- ⁶M. Campostrini, A. Pelissetto, P. Rossi, and E. Vicari, “Critical equation of state of three-dimensional XY systems”, *Phys. Rev. B* **62**, 5843–5854 (2000).
- ⁷M. P. A. Fisher, P. B. Weichman, G. Grinstein, and D. S. Fisher, “Boson localization and the superfluid-insulator transition”, *Phys. Rev. B* **40**, 546–570 (1989).
- ⁸S. D. Huber, B. Theiler, E. Altman, and G. Blatter, “Amplitude mode in the quantum phase model”, *Phys. Rev. Lett.* **100**, 050404 (2008).
- ⁹S. Sachdev, *Quantum phase transitions*, 2nd ed. (Cambridge University Press, 2011).
- ¹⁰M. Hornung, J. C. P. Barros, and U.-J. Wiese, *Mass and Charge of the Quantum Vortex in the (2 + 1)-d O(2) Scalar Field Theory*, 2021, [arXiv:2106.16191](#).
- ¹¹M. Hornung, “The Vortex in the (2 + 1)-dimensional O(2) Model and Effective Low-Energy Theory for Spin Chains in a Strong Magnetic Field”, PhD thesis (University of Bern, 2021), <https://boristheses.unibe.ch/id/eprint/3199>.
- ¹²L. Polley and U.-J. Wiese, “Monopole condensate and monopole mass in U(1) lattice gauge theory”, *Nucl. Phys. B* **356**, 629–654 (1991).
- ¹³J. Jersák, T. Neuhaus, and H. Pfeiffer, “Scaling analysis of the magnetic monopole mass and condensate in the pure U(1) lattice gauge theory”, *Phys. Rev. D* **60**, 054502 (1999).
- ¹⁴N. Manton and P. Sutcliffe, *Topological solitons* (Cambridge University Press, 2004).
- ¹⁵M. Nakahara, *Geometry, topology and physics* (CRC Press, 2018).
- ¹⁶N. D. Mermin, “The topological theory of defects in ordered media”, *Rev. Mod. Phys.* **51**, 591–648 (1979).
- ¹⁷G. H. Derrick, “Comments on Nonlinear Wave Equations as Models for Elementary Particles”, *J. Math. Phys.* **5**, 1252–1254 (1964), eprint: https://pubs.aip.org/aip/jmp/article-pdf/5/9/1252/19309416/1252_1_online.pdf.
- ¹⁸S. I. Pohožaev, “On the eigenfunctions of the equation $\Delta u + \lambda f(u) = 0$ ”, *Dokl. Akad. Nauk SSSR* **165**, 36–39 (1965).
- ¹⁹R. Jackiw, “Quantum meaning of classical field theory”, *Rev. Mod. Phys.* **49**, 681–706 (1977).
- ²⁰R. Rajaraman, *Solitons and instantons: volume 15* (North-Holland, 1987).

- ²¹D. Tong, *Statistical Field Theory*, 2017, <http://www.damtp.cam.ac.uk/user/tong/sft.html>.
- ²²K. G. Wilson and J. Kogut, “The renormalization group and the ϵ expansion”, *Phys. Rep.* **12**, 75–199 (1974).
- ²³K. G. Wilson and M. E. Fisher, “Critical exponents in 3.99 dimensions”, *Phys. Rev. Lett.* **28**, 240–243 (1972).
- ²⁴M. Hasenbusch, “A Monte Carlo study of the three-dimensional XY universality class: universal amplitude ratios”, *J. Stat. Mech.: Theory Exp.* **2008**, P12006 (2008).
- ²⁵D. Skinner and D. Chua, *Part III — Advanced Quantum Field Theory*, 2013, <https://dec41.user.srcf.net/notes/>.
- ²⁶R. A. Bertlmann, *Anomalies in Quantum Field Theory* (Oxford University Press, 2000).
- ²⁷M. Lüscher, “Volume dependence of the energy spectrum in massive quantum field theories: ii. scattering states”, *Commun. Math. Phys.* **105**, 153–188 (1986).
- ²⁸K. Osterwalder and R. Schrader, “Axioms for Euclidean Green’s Functions”, *Commun. Math. Phys.* **31**, 83–112 (1973).
- ²⁹K. Osterwalder and R. Schrader, “Axioms for Euclidean Green’s Functions. 2.”, *Commun. Math. Phys.* **42**, 281 (1975).
- ³⁰J. Glimm, A. Jaffe, and T. Spencer, “The Wightman Axioms and Particle Structure in the $\mathcal{P}(\phi)_2$ Quantum Field Model”, *Ann. Math.* **100**, 585 (1974).
- ³¹F. Guerra, L. Rosen, and B. Simon, “The $\mathcal{P}(\phi)_2$ Euclidean Quantum Field Theory as Classical Statistical Mechanics”, *Ann. Math.* **101**, 111 (1975).
- ³²J. Glimm and A. Jaffe, “A $\lambda\phi^4$ Quantum Field Theory without Cutoffs. I”, *Phys. Rev.* **176**, 1945–1951 (1968).
- ³³J. Glimm and A. Jaffe, “The $\lambda(\varphi^4)_2$ Quantum Field Theory Without Cutoffs: II. The Field Operators and the Approximate Vacuum”, *Ann. Math.* **91**, 362 (1970).
- ³⁴J. Glimm and A. Jaffe, “The $\lambda(\varphi^4)_2$ quantum field theory without cutoffs: III. The physical vacuum”, *Acta Math.* **125**, 203–267 (1970).
- ³⁵J. Glimm and A. M. Jaffe, “The $\lambda\phi^4_2$ Quantum Field Theory Without Cutoffs. IV. Perturbations of the Hamiltonian”, *J. Math. Phys.* **13**, 1568–1584 (1972).
- ³⁶J. S. Feldman and K. Osterwalder, “The Wightman Axioms and the Mass Gap for Weakly Coupled (ϕ^4) in Three-Dimensions Quantum Field Theories”, *Ann. Phys.* **97**, 80–135 (1976).
- ³⁷J. Glimm and A. M. Jaffe, “Positivity of the ϕ^4_3 Hamiltonian”, *Fortsch. Phys.* **21**, 327–376 (1973).
- ³⁸J. Glimm, “Boson fields with the $:\Phi^4:$ interaction in three dimensions”, *Commun. Math. Phys.* **10**, 1–47 (1968).
- ³⁹M. Aizenman and H. Duminil-Copin, “Marginal trivality of the scaling limits of critical 4D Ising and $\lambda\phi^4_4$ models”, *Ann. Math.* **194**, 10.4007/annals.2021.194.1.3 (2021).
- ⁴⁰M. Aizenman, “Geometric Analysis of ϕ^4 Fields and Ising Models (Parts 1 & 2)”, *Commun. Math. Phys.* **86**, 1 (1982).
- ⁴¹J. Fröhlich, “On the trivality of $(\lambda\phi^4_d)$ theories and the approach to the critical point in $d_{(-)} > 4$ dimensions”, *Nucl. Phys. B* **200**, 281–296 (1982).
- ⁴²E. Seiler, “Schwinger functions for the Yukawa model in two dimensions with space-time cutoff”, *Commun. Math. Phys.* **42**, 163–182 (1975).
- ⁴³D. Brydges, J. Fröhlich, and E. Seiler, “On the Construction of Quantized Gauge Fields. I. General Results”, *Ann. Phys.* **121**, 227–284 (1979).
- ⁴⁴D. C. Brydges, J. Fröhlich, and E. Seiler, “Construction of Quantized Gauge Fields. II. Convergence of the Lattice Approximation”, *Commun. Math. Phys.* **71**, 159–205 (1980).

- ⁴⁵D. C. Brydges, J. Fröhlich, and E. Seiler, “On the Construction of Quantized Gauge Fields. III: The Two-dimensional Abelian Higgs Model Without Cutoffs”, *Commun. Math. Phys.* **79**, 353 (1981).
- ⁴⁶A. Jaffe and E. Witten, *Quantum Yang-Mills Theory*, <https://www.claymath.org/millennium/yang-mills-the-maths-gap/>.
- ⁴⁷S. A. Albeverio, R. J. Høegh-Krohn, and S. Mazzucchi, *Mathematical Theory of Feynman Path Integrals* (Springer Berlin Heidelberg, 2008).
- ⁴⁸G. W. Johnson and M. L. Lapidus, *The Feynman integral and Feynman’s operational calculus* (Clarendon Press, 2002).
- ⁴⁹M. Hairer, “A theory of regularity structures”, *Invent. Math.* **198**, 269–504 (2014).
- ⁵⁰A. Jaffe, “Quantum Fields, Stochastic PDE, and Reflection Positivity”, (2014), [arXiv:1411.2964](https://arxiv.org/abs/1411.2964).
- ⁵¹A. Kupiainen, “Renormalization Group and Stochastic PDEs”, *Ann. Henri Poincaré* **17**, 497–535 (2015).
- ⁵²J.-C. Mourrat and H. Weber, “The Dynamic Φ_3^4 Model Comes Down from Infinity”, *Commun. Math. Phys.* **356**, 673–753 (2017).
- ⁵³M. Gubinelli and M. Hofmanová, “A PDE Construction of the Euclidean Φ_3^4 Quantum Field Theory”, *Commun. Math. Phys.* **384**, 1–75 (2021).
- ⁵⁴A. Chandra, I. Chevyrev, M. Hairer, and H. Shen, “Stochastic quantisation of Yang-Mills-Higgs in 3D”, (2022), [arXiv:2201.03487 \[math.PR\]](https://arxiv.org/abs/2201.03487).
- ⁵⁵S. Cao and S. Chatterjee, “A State Space for 3D Euclidean Yang–Mills Theories”, *Commun. Math. Phys.* **405**, 3 (2024), [arXiv:2111.12813 \[math.PR\]](https://arxiv.org/abs/2111.12813).
- ⁵⁶B. C. Hall, *Quantum theory for mathematicians* (Springer New York, 2013).
- ⁵⁷L. H. Karsten and J. Smit, “Lattice fermions: species doubling, chiral invariance and the triangle anomaly”, *Nucl. Phys. B* **183**, 103–140 (1981).
- ⁵⁸H. B. Nielsen and M. Ninomiya, “Absence of Neutrinos on a Lattice. 1. Proof by Homotopy Theory”, *Nucl. Phys. B* **185**, [Erratum: *Nucl.Phys.B* 195, 541 (1982)], 20 (1981).
- ⁵⁹M. Lüscher, “Chiral gauge theories revisited”, in *Theory and experiment heading for new physics* (2002).
- ⁶⁰M. Lüscher, “Abelian chiral gauge theories on the lattice with exact gauge invariance”, *Nucl. Phys. B* **549**, 295–334 (1999).
- ⁶¹M. Lüscher, “Weyl fermions on the lattice and the non-Abelian gauge anomaly”, *Nucl. Phys. B* **568**, 162–179 (2000), [arXiv:hep-lat/9904009](https://arxiv.org/abs/hep-lat/9904009).
- ⁶²D. Kadoh and Y. Kikukawa, “A construction of the glashow-weinberg-salam model on the lattice with exact gauge invariance”, *JHEP* **2008**, 095–095 (2008).
- ⁶³T. Neuhaus, A. Rajantie, and K. Rummukainen, “Numerical study of duality and universality in a frozen superconductor”, *Phys. Rev. B* **67**, 014525 (2003).
- ⁶⁴H. Grosse and H. Kühnelt, “Phase Structure of Lattice Gauge Theories for Nonabelian Subgroups of $SU(3)$ ”, *Phys. Lett. B* **101**, 77–81 (1981).
- ⁶⁵J. Fröhlich and T. Spencer, “Massless phases and symmetry restoration in abelian gauge theories and spin systems”, *Commun. Math. Phys.* **83**, 411–454 (1982).
- ⁶⁶M. Lüscher, “Topology and the axial anomaly in abelian lattice gauge theories”, *Nucl. Phys. B* **538**, 515–529 (1999).
- ⁶⁷E. Cobanera, G. Ortiz, and Z. Nussinov, “The bond-algebraic approach to dualities”, *Adv. Phys.* **60**, 679–798 (2011).
- ⁶⁸L. Lootens, C. Delcamp, G. Ortiz, and F. Verstraete, “Dualities in One-Dimensional Quantum Lattice Models: Symmetric Hamiltonians and Matrix Product Operator Intertwiners”, *PRX Quantum* **4**, 020357 (2023).

- ⁶⁹L. Lootens, C. Delcamp, and F. Verstraete, “Dualities in One-Dimensional Quantum Lattice Models: Topological Sectors”, [PRX Quantum](#) **5**, 010338 (2024).
- ⁷⁰R. Savit, “Duality in field theory and statistical systems”, [Rev. Mod. Phys.](#) **52**, 453–487 (1980).
- ⁷¹K. Drühl and H. Wagner, “Algebraic formulation of duality transformations for abelian lattice models”, [Ann. Phys.](#) **141**, 225–253 (1982).
- ⁷²A. W. Knap, *Lie groups beyond an introduction* (Birkhäuser Boston, 1996).
- ⁷³T. Tannaka, “Über den Dualitätssatz der nichtkommutativen topologischen Gruppen”, [Tôhoku Math. J.](#) **45**, 1–12 (1939).
- ⁷⁴M. Krein, “A principle of duality for a bicomact group and square block algebra”, [Dokl. Akad. Nauk. SSSR](#) **69**, 725–728 (1949).
- ⁷⁵D. Harlow and H. Ooguri, “Symmetries in Quantum Field Theory and Quantum Gravity”, [Commun. Math. Phys.](#) **383**, 1669–1804 (2021).
- ⁷⁶M. Caselle and M. Hasenbusch, “Deconfinement transition and dimensional cross-over in the 3D gauge Ising model”, [Nucl. Phys. B](#) **470**, 435–453 (1996).
- ⁷⁷D. Kadoh, Y. Kikukawa, and Y. Nakayama, “Solving the local cohomology problem in U(1) chiral gauge theories within a finite lattice”, [JHEP](#) **2004**, 006–006 (2004).
- ⁷⁸J. Fröhlich and P. A. Marchetti, “Soliton quantization in lattice field theories”, [Commun. Math. Phys.](#) **112**, 343–383 (1987).
- ⁷⁹C. Borgs and F. Nill, “The phase diagram of the Abelian lattice Higgs model. A review of rigorous results”, [J. Stat. Phys.](#) **47**, 877–904 (1987).
- ⁸⁰A. Polyakov, “Quark confinement and topology of gauge theories”, [Nucl. Phys. B](#) **120**, 429–458 (1977).
- ⁸¹M. Göpfert and G. Mack, “Proof of confinement of static quarks in 3-dimensional U(1) lattice gauge theory for all values of the coupling constant”, [Commun. Math. Phys.](#) **82**, 545–606 (1982).
- ⁸²T. A. DeGrand and D. Toussaint, “Topological excitations and Monte Carlo simulation of Abelian gauge theory”, [Phys. Rev. D](#) **22**, 2478–2489 (1980).
- ⁸³O. Aharony, N. Seiberg, and Y. Tachikawa, “Reading between the lines of four-dimensional gauge theories”, [JHEP](#) **2013**, 10.1007/jhep08(2013)115 (2013).
- ⁸⁴B. Schroer, “Infra-particles in the quantum field theory”, [Fortsch. Phys.](#) **11** (1963).
- ⁸⁵D. Buchholz, “The physical state space of quantum electrodynamics”, [Commun. Math. Phys.](#) **85**, 49–71 (1982).
- ⁸⁶J. Fröhlich, G. Morchio, and F. Strocchi, “Infrared problem and spontaneous breaking of the Lorentz group in QED”, [Phys. Lett. B](#) **89**, 61–64 (1979).
- ⁸⁷T. Kennedy and C. King, “Symmetry Breaking in the Lattice Abelian Higgs Model”, [Phys. Rev. Lett.](#) **55**, 776–778 (1985).
- ⁸⁸T. Kennedy and C. King, “Spontaneous symmetry breakdown in the abelian Higgs model”, [Commun. Math. Phys.](#) **104**, 327–347 (1986).
- ⁸⁹J. Fröhlich, G. Morchio, and F. Strocchi, “Higgs Phenomenon without Symmetry Breaking Order Parameter”, [Nucl. Phys. B](#) **190**, 553–582 (1981).
- ⁹⁰E. Fradkin and S. H. Shenker, “Phase diagrams of lattice gauge theories with Higgs fields”, [Phys. Rev. D](#) **19**, 3682–3697 (1979).
- ⁹¹R. Verresen, U. Borla, A. Vishwanath, S. Moroz, and R. Thorngren, “Higgs Condensates are Symmetry-Protected Topological Phases: I. Discrete Symmetries”, (2022), [arXiv:2211.01376](#).
- ⁹²R. Thorngren, T. Rakovszky, R. Verresen, and A. Vishwanath, “Higgs Condensates are Symmetry-Protected Topological Phases: II. U(1) Gauge Theory and Superconductors”, (2023), [arXiv:2303.08136](#).

- ⁹³T. Banks, R. Myerson, and J. B. Kogut, “Phase Transitions in Abelian Lattice Gauge Theories”, *Nucl. Phys. B* **129**, 493–510 (1977).
- ⁹⁴T. Sulejmanpasic and C. Gattringer, “Abelian gauge theories on the lattice: θ -Terms and compact gauge theory with(out) monopoles”, *Nucl. Phys. B* **943**, 114616 (2019), [arXiv:1901.02637 \[hep-lat\]](https://arxiv.org/abs/1901.02637).
- ⁹⁵P. Gorantla, H. T. Lam, N. Seiberg, and S.-H. Shao, “A modified Villain formulation of fractons and other exotic theories”, *J. Math. Phys.* **62**, 102301 (2021), [arXiv:2103.01257 \[cond-mat.str-el\]](https://arxiv.org/abs/2103.01257).
- ⁹⁶E. Fradkin, “Disorder operators and their descendants”, *J. Stat. Phys.* **167**, 427–461 (2017).
- ⁹⁷D. Tong, *Gauge theory*, 2018, <http://www.damtp.cam.ac.uk/user/tong/gaugetheory.html>.
- ⁹⁸M. E. Peskin, “Mandelstam-’t Hooft duality in abelian lattice models”, *Ann. Phys.* **113**, 122–152 (1978).
- ⁹⁹C. Dasgupta and B. I. Halperin, “Phase transition in a lattice model of superconductivity”, *Phys. Rev. Lett.* **47**, 1556–1560 (1981).
- ¹⁰⁰K. Kajantie, M. Laine, T. Neuhaus, A. Rajantie, and K. Rummukainen, “Duality and scaling in 3-dimensional scalar electrodynamics”, *Nucl. Phys. B* **699**, 632–656 (2004).
- ¹⁰¹N. Seiberg, T. Senthil, C. Wang, and E. Witten, “A duality web in $2 + 1$ dimensions and condensed matter physics”, *Ann. Phys.* **374**, 395–433 (2016).
- ¹⁰²A. Kronfeld and U.-J. Wiese, “SU(N) gauge theories with C-periodic boundary conditions (I). Topological structure”, *Nucl. Phys. B* **357**, 521–533 (1991).
- ¹⁰³U.-J. Wiese, “C- and G-periodic QCD at finite temperature”, *Nucl. Phys. B* **375**, 45–66 (1992).
- ¹⁰⁴C. Bonati, A. Pelissetto, and E. Vicari, “Lattice Abelian-Higgs model with noncompact gauge fields”, *Phys. Rev. B* **103**, 085104 (2021).
- ¹⁰⁵Z. Davoudi, J. Harrison, A. Jüttner, A. Portelli, and M. J. Savage, “Theoretical aspects of quantum electrodynamics in a finite volume with periodic boundary conditions”, *Phys. Rev. D* **99**, 10.1103/physrevd.99.034510 (2019).
- ¹⁰⁶K. Jansen, J. Jersák, I. Montvay, G. Münster, T. Trappenberg, and U. Wolff, “Vacuum tunneling in the four-dimensional Ising model”, *Phys. Lett. B* **213**, 203–209 (1988).
- ¹⁰⁷K. Jansen, I. Montvay, G. Münster, T. Trappenberg, and U. Wolff, “Broken phase of the 4-dimensional Ising model in a finite volume”, *Nucl. Phys. B* **322**, 698–720 (1989).
- ¹⁰⁸B. Widom, “Equation of state in the neighborhood of the critical point”, *J. Chem. Phys.* **43**, 3898–3905 (1965).
- ¹⁰⁹U. Wolff, “Collective Monte Carlo Updating for Spin Systems”, *Phys. Rev. Lett.* **62**, 361–364 (1989).
- ¹¹⁰M. Hasenbusch, “Monte Carlo study of an improved clock model in three dimensions”, *Phys. Rev. B* **100**, 224517 (2019).
- ¹¹¹J.-L. Gervais and D. Zwanziger, “Derivation From First Principles of the Infrared Structure of Quantum Electrodynamics”, *Phys. Lett. B* **94**, 389–393 (1980).
- ¹¹²D. Buchholz, “Gauss’ Law and the Infraparticle Problem”, *Phys. Lett. B* **174**, 331–334 (1986).
- ¹¹³M. Karliner and G. Mack, “Mass gap and string tension in QED3: Comparison of theory with Monte Carlo simulation”, *Nucl. Phys. B* **225**, 371–376 (1983).
- ¹¹⁴M. Loan, M. Brunner, C. Sloggett, and C. Hamer, “Path integral Monte Carlo approach to the U(1) lattice gauge theory in (2+1)-dimensions”, *Phys. Rev. D* **68**, 034504 (2003), [arXiv:hep-lat/0209159](https://arxiv.org/abs/hep-lat/0209159).
- ¹¹⁵A. Athenodorou and M. Teper, “On the spectrum and string tension of U(1) lattice gauge theory in $2 + 1$ dimensions”, *JHEP* **01**, 063 (2019), [arXiv:1811.06280](https://arxiv.org/abs/1811.06280).
- ¹¹⁶M. Caselle, M. Panero, R. Pellegrini, and D. Vadicchino, “A different kind of string”, *JHEP* **01**, 105 (2015), [arXiv:1406.5127](https://arxiv.org/abs/1406.5127).
- ¹¹⁷P. D. Coddington, A. J. G. Hey, A. A. Middleton, and J. S. Townsend, “The Deconfining Transition for Finite Temperature U(1) Lattice Gauge Theory in (2+1)-dimensions”, *Phys. Lett. B* **175**, 64–68 (1986).

- ¹¹⁸M. N. Chernodub, E.-M. Ilgenfritz, and A. Schiller, “Lattice study of 3D compact QED at finite temperature”, *Phys. Rev. D* **64**, 054507 (2001).
- ¹¹⁹O. Borisenko, M. Gravina, and A. Papa, “Critical behavior of the compact 3d U(1) theory in the limit of zero spatial coupling”, *J. Stat. Mech.* **0808**, P08009 (2008), [arXiv:0806.2081](#).
- ¹²⁰O. Borisenko, R. Fiore, M. Gravina, and A. Papa, “Critical behavior of the compact 3d U(1) gauge theory on isotropic lattices”, *J. Stat. Mech.* **1004**, P04015 (2010), [arXiv:1001.4979](#).
- ¹²¹O. Borisenko, V. Chelnokov, M. Gravina, and A. Papa, “Deconfinement and universality in the 3D U(1) lattice gauge theory at finite temperature: study in the dual formulation”, *JHEP* **09**, 062 (2015), [arXiv:1507.00833](#).
- ¹²²M. Caselle, A. Nada, M. Panero, and D. Vadicchino, “Conformal field theory and the hot phase of three-dimensional U(1) gauge theory”, *JHEP* **05**, 068 (2019), [arXiv:1903.00491](#).
- ¹²³J. Villain, “Theory of one-dimensional and two-dimensional magnets with an easy magnetization plane. 2. The Planar, classical, two-dimensional magnet”, *J. Phys. (France)* **36**, 581–590 (1975).
- ¹²⁴M. Creutz, L. Jacobs, and C. Rebbi, “Monte Carlo Computations in Lattice Gauge Theories”, *Phys. Rept.* **95**, 201–282 (1983).
- ¹²⁵J. Kogut and L. Susskind, “Hamiltonian formulation of Wilson’s lattice gauge theories”, *Phys. Rev. D* **11**, 395–408 (1975).
- ¹²⁶G. ’t Hooft, in High Energy Physics, Proceedings of the EPS International Conference (1975).
- ¹²⁷S. Mandelstam, “Vortices and quark confinement in non-Abelian gauge theories”, *Phys. Rep.* **23**, 245–249 (1976).
- ¹²⁸M. Lüscher and P. Weisz, “Quark confinement and the bosonic string”, *JHEP* **2002**, 049–049 (2002).
- ¹²⁹P. de Forcrand, M. D’Elia, and M. Pepe, “A Study of the ’t Hooft loop in SU(2) Yang-Mills theory”, *Phys. Rev. Lett.* **86**, 1438 (2001), [arXiv:hep-lat/0007034](#).
- ¹³⁰P. de Forcrand, B. Lucini, and M. Vettorazzo, “Measuring interface tensions in 4d SU(N) lattice gauge theories”, *Nucl. Phys. B Proc. Suppl.* **140**, 647–649 (2005), [arXiv:hep-lat/0409148](#).
- ¹³¹M. Caselle, M. Hasenbusch, and M. Panero, “String effects in the 3d gauge Ising model”, *JHEP* **2003**, 057–057 (2003).
- ¹³²J. Polchinski, *String theory. Vol. 1: An introduction to the bosonic string* (Cambridge University Press, 2007).
- ¹³³S. Dubovsky, R. Flauger, and V. Gorbenko, “Effective string theory revisited”, *JHEP* **2012**, 10.1007/jhep09(2012)044 (2012).
- ¹³⁴M. Lüscher, “Symmetry Breaking Aspects of the Roughening Transition in Gauge Theories”, *Nucl. Phys. B* **180**, 317–329 (1981).
- ¹³⁵M. Lüscher, K. Symanzik, and P. Weisz, “Anomalies of the free loop wave equation in the WKB approximation”, *Nucl. Phys. B* **173**, 365–396 (1980).
- ¹³⁶T. D. Cohen, “Center symmetry and area laws”, *Phys. Rev. D* **90**, 047703 (2014), [arXiv:1407.4128](#).
- ¹³⁷M. Nguyen, Y. Tanizaki, and M. Ünsal, “Semi-Abelian gauge theories, non-invertible symmetries, and string tensions beyond N -ality”, *JHEP* **03**, 238 (2021), [arXiv:2101.02227](#).
- ¹³⁸M. Nguyen, Y. Tanizaki, and M. Ünsal, “Noninvertible 1-form symmetry and Casimir scaling in 2D Yang-Mills theory”, *Phys. Rev. D* **104**, 065003 (2021), [arXiv:2104.01824](#).
- ¹³⁹H. B. Meyer, “Poincaré invariance in effective string theories”, *JHEP* **2006**, 066 (2006).
- ¹⁴⁰O. Aharony and E. Karzbrun, “On the effective action of confining strings”, *JHEP* **2009**, 012–012 (2009).
- ¹⁴¹O. Aharony and M. Dodelson, “Effective string theory and nonlinear Lorentz invariance”, *JHEP* **2012**, 10.1007/jhep02(2012)008 (2012).

- ¹⁴²M. Billó, M. Caselle, F. Gliozzi, M. Meineri, and R. Pellegrini, “The Lorentz-invariant boundary action of the confining string and its universal contribution to the inter-quark potential”, *JHEP* **2012**, [10.1007/jhep05\(2012\)130](https://arxiv.org/abs/10.1007/jhep05(2012)130) (2012).
- ¹⁴³O. Aharony and Z. Komargodski, “The effective theory of long strings”, *JHEP* **2013**, [10.1007/jhep05\(2013\)118](https://arxiv.org/abs/10.1007/jhep05(2013)118) (2013).
- ¹⁴⁴B. B. Brandt and M. Meineri, “Effective string description of confining flux tubes”, *Int. J. Mod. Phys. A* **31**, 1643001 (2016), [arXiv:1603.06969](https://arxiv.org/abs/1603.06969).
- ¹⁴⁵M. Caselle, L. Castagnini, A. Feo, F. Gliozzi, U. Gürsoy, M. Panero, and A. Schäfer, “Thermodynamics of SU(N) Yang-Mills theories in 2+1 dimensions II — The deconfined phase”, *JHEP* **2012**, [10.1007/jhep05\(2012\)135](https://arxiv.org/abs/10.1007/jhep05(2012)135) (2012).
- ¹⁴⁶J. Arvis, “The exact $q\bar{q}$ potential in Nambu string theory”, *Phys. Lett. B* **127**, 106–108 (1983).
- ¹⁴⁷A. Baffigo and M. Caselle, “Ising string beyond the Nambu-Goto action”, *Phys. Rev. D* **109**, 034520 (2024), [arXiv:2306.06966](https://arxiv.org/abs/2306.06966).
- ¹⁴⁸A. M. Polyakov, “Confining strings”, *Nucl. Phys. B* **486**, 23–33 (1997), [arXiv:hep-th/9607049](https://arxiv.org/abs/hep-th/9607049).
- ¹⁴⁹D. Vadicchino, M. Caselle, M. Panero, and R. Pellegrini, “Effective string description of the interquark potential in the 3D $U(1)$ lattice gauge theory”, *PoS LATTICE2014*, 349 (2014), [arXiv:1410.7436 \[hep-lat\]](https://arxiv.org/abs/1410.7436).
- ¹⁵⁰M. Caselle, “Effective string description of the confining flux tube at finite temperature”, *Universe* **7**, 170 (2021).
- ¹⁵¹J. Bricmont, A. E. Mellouki, and J. Fröhlich, “Random surfaces in statistical mechanics: Roughening, rounding, wetting, ...”, *J. Stat. Phys.* **42**, 743–798 (1986).
- ¹⁵²G. N. Watson, “Three Triple Integrals”, *Q. J. Math. os-10*, 266–276 (1939), eprint: <https://academic.oup.com/qjmath/article-pdf/os-10/1/266/4363160/os-10-1-266.pdf>.
- ¹⁵³G. Mack, T. Kalkreuter, G. Palma, and M. Speh, “Effective field theories”, *Lect. Notes Phys.* **409**, 205–249 (1992), [arXiv:hep-lat/9205013](https://arxiv.org/abs/hep-lat/9205013).
- ¹⁵⁴G. S. Joyce and I. J. Zucker, “Evaluation of the Watson integral and associated logarithmic integral for the d -dimensional hypercubic lattice”, *J. Phys. A: Math. Gen.* **34**, 7349–7354 (2001).
- ¹⁵⁵E. W. Montroll and G. H. Weiss, “Random Walks on Lattices. II”, *J. Math. Phys.* **6**, 167–181 (1965).
- ¹⁵⁶V. F. Müller and W. Rühl, “Discrete field variables, the Coulomb gas, and low temperature behaviour”, *Z. Phys. C* **9**, 261 (1981).
- ¹⁵⁷R. J. Wensley and J. D. Stack, “Monopoles and confinement in three dimensions”, *Phys. Rev. Lett.* **63**, 1764–1767 (1989).
- ¹⁵⁸M. Loan, T. Byrnes, and C. Hamer, “Hamiltonian study of improved $U(1)$ lattice gauge theory in three dimensions”, *Phys. Rev. D* **70**, 014504 (2004), [arXiv:hep-lat/0307029](https://arxiv.org/abs/hep-lat/0307029).
- ¹⁵⁹A. Athenodorou and M. Teper, “SU(N) gauge theories in 2+1 dimensions: glueball spectra and k-string tensions”, *JHEP* **02**, 015 (2017), [arXiv:1609.03873](https://arxiv.org/abs/1609.03873).
- ¹⁶⁰A. Athenodorou and M. Teper, “SU(N) gauge theories in 3+1 dimensions: glueball spectrum, string tensions and topology”, *JHEP* **12**, 082 (2021), [arXiv:2106.00364](https://arxiv.org/abs/2106.00364).
- ¹⁶¹L. Gross, “Convergence of $U(1)_3$ lattice gauge theory to its continuum limit”, *Commun. Math. Phys.* **92**, 137–162 (1983).
- ¹⁶²G. E. Andrews, “A simple proof of Jacobi’s triple product identity”, *Proc. Am. Math. Soc.* **16**, 333–334 (1965).
- ¹⁶³J. Ambjørn, A. J. G. Hey, and S. Otto, “String Tensions for Lattice Gauge Theories in (2+1)-dimensions”, *Nucl. Phys. B* **210**, 347–368 (1982).
- ¹⁶⁴K. R. Ito, “Upper and Lower Bound for the String Tension in the Three-dimensional Lattice Quantum Electrodynamics”, *Nucl. Phys. B* **205**, [Erratum: *Nucl.Phys.B* 215, 136 (1983)], 440 (1982).

- ¹⁶⁵E. Seiler, “Upper bound on the color-confining potential”, *Phys. Rev. D* **18**, 482–483 (1978).
- ¹⁶⁶B. Svetitsky and L. G. Yaffe, “Critical behavior at finite-temperature confinement transitions”, *Nucl. Phys. B* **210**, 423–447 (1982).
- ¹⁶⁷K. Holland, P. Minkowski, M. Pepe, and U.-J. Wiese, “Exceptional confinement in G(2) gauge theory”, *Nucl. Phys. B* **668**, 207–236 (2003), [arXiv:hep-lat/0302023](https://arxiv.org/abs/hep-lat/0302023).
- ¹⁶⁸M. Pepe and U.-J. Wiese, “Exceptional Deconfinement in G(2) Gauge Theory”, *Nucl. Phys. B* **768**, 21–37 (2007), [arXiv:hep-lat/0610076](https://arxiv.org/abs/hep-lat/0610076).
- ¹⁶⁹K. Holland, M. Pepe, and U.-J. Wiese, “The deconfinement phase transition in Yang-Mills theory with general Lie group G”, *Nucl. Phys. B Proc. Suppl.* **129**, 712–714 (2004), [arXiv:hep-lat/0309062](https://arxiv.org/abs/hep-lat/0309062).
- ¹⁷⁰N. Parga, “Finite Temperature Behavior of Topological Excitations in Lattice Compact QED”, *Phys. Lett. B* **107**, 442–445 (1981).
- ¹⁷¹J. Engels, J. Fingberg, F. Karsch, D. Miller, and M. Weber, “Non-perturbative thermodynamics of SU(N) gauge theories”, *Phys. Lett. B* **252**, 625–630 (1990).
- ¹⁷²D. Tong, *Lectures on statistical physics*, 2012, <http://www.damtp.cam.ac.uk/user/tong/statphys.html>.
- ¹⁷³M. Caselle, L. Castagnini, A. Feo, F. Gliozzi, and M. Panero, “Thermodynamics of SU(N) Yang-Mills theories in 2+1 dimensions I — The confining phase”, *JHEP* **2011**, 10.1007/jhep06(2011)142 (2011).
- ¹⁷⁴R. Hagedorn, “Statistical thermodynamics of strong interactions at high-energies”, *Nuovo Cim. Suppl.* **3**, 147–186 (1965).
- ¹⁷⁵R. Hagedorn, “Hadronic matter near the boiling point”, *Nuovo Cim.*, 1027–57 (1968).
- ¹⁷⁶T. D. Cohen, “QCD and the Hagedorn spectrum”, *JHEP* **2010**, 10.1007/jhep06(2010)098 (2010).
- ¹⁷⁷T. D. Cohen and V. Krejcirik, “The Hagedorn spectrum and large N_c QCD in 2+1 and 3+1 dimensions”, *JHEP* **08**, 138 (2011), [arXiv:1104.4783](https://arxiv.org/abs/1104.4783).
- ¹⁷⁸N. Isgur and J. E. Paton, “A Flux Tube Model for Hadrons in QCD”, *Phys. Rev. D* **31**, 2910 (1985).
- ¹⁷⁹R. W. Johnson and M. J. Teper, “String models of glueballs and the spectrum of SU(N) gauge theories in (2+1)-dimensions”, *Phys. Rev. D* **66**, 036006 (2002), [arXiv:hep-ph/0012287](https://arxiv.org/abs/hep-ph/0012287).
- ¹⁸⁰H. B. Meyer, “High-precision thermodynamics and Hagedorn density of states”, *Phys. Rev. D* **80**, 051502 (2009).
- ¹⁸¹S. Borsányi, G. Endrődi, Z. Fodor, S. D. Katz, and K. K. Szabó, “Precision SU(3) lattice thermodynamics for a large temperature range”, *JHEP* **2012**, 10.1007/jhep07(2012)056 (2012).
- ¹⁸²M. Caselle, A. Nada, and M. Panero, “Hagedorn spectrum and thermodynamics of SU(2) and SU(3) Yang-Mills theories”, *JHEP* **07**, [Erratum: *JHEP* 11, 016 (2017)], 143 (2015), [arXiv:1505.01106](https://arxiv.org/abs/1505.01106).
- ¹⁸³M. Caselle, L. Castagnini, A. Feo, F. Gliozzi, and M. Panero, “Thermodynamics of SU(N) gauge theories in 2+1 dimensions in the $T < T_c$ regime”, *PoS LATTICE2010*, edited by G. Rossi, 184 (2010), [arXiv:1011.4883](https://arxiv.org/abs/1011.4883).
- ¹⁸⁴L. Giusti and M. Pepe, “Equation of state of the SU(3) Yang-Mills theory: A precise determination from a moving frame”, *Phys. Lett. B* **769**, 385–390 (2017), [arXiv:1612.00265](https://arxiv.org/abs/1612.00265).
- ¹⁸⁵G. Baskaran and P. W. Anderson, “Gauge theory of high temperature superconductors and strongly correlated Fermi systems”, *Phys. Rev. B* **37**, 580–583 (1988).
- ¹⁸⁶E. Fradkin, *Field Theories of Condensed Matter Physics* (Cambridge University Press, 2013).
- ¹⁸⁷R. Moessner and J. E. Moore, *Topological phases of matter* (Cambridge University Press, 2021).
- ¹⁸⁸N. Read and S. Sachdev, “Spin-Peierls, valence-bond solid, and Néel ground states of low-dimensional quantum antiferromagnets”, *Phys. Rev. B* **42**, 4568–4589 (1990).
- ¹⁸⁹S. Takashima, I. Ichinose, and T. Matsui, “Deconfinement of spinons on critical points: Multiflavor $CP^1 + U(1)$ lattice gauge theory in three dimensions”, *Phys. Rev. B* **73**, 075119 (2006).

- ¹⁹⁰M. Hermele, M. P. A. Fisher, and L. Balents, “Pyrochlore photons: the $U(1)$ spin liquid in a $S = \frac{1}{2}$ three-dimensional frustrated magnet”, *Phys. Rev. B* **69**, 064404 (2004).
- ¹⁹¹A. Banerjee, D. Banerjee, G. Kanwar, A. Mariani, T. Rindlisbacher, and U.-J. Wiese, “Broken symmetry and fractionalized flux strings in a staggered $U(1)$ pure gauge theory”, *Phys. Rev. D* **109**, 014506 (2024), [arXiv:2309.17109](#).
- ¹⁹²D. Banerjee, F.-J. Jiang, P. Widmer, and U.-J. Wiese, “The $(2 + 1)$ -d $U(1)$ quantum link model masquerading as deconfined criticality”, *J. Stat. Mech.* **2013**, P12010 (2013), [arXiv:1303.6858](#).
- ¹⁹³D. Banerjee, F.-J. Jiang, T. Z. Olesen, P. Orland, and U.-J. Wiese, “From the $SU(2)$ quantum link model on the honeycomb lattice to the quantum dimer model on the kagomé lattice: Phase transition and fractionalized flux strings”, *Phys. Rev. B* **97**, 205108 (2018), [arXiv:1712.08300](#).
- ¹⁹⁴D. Banerjee, M. Bögli, C. P. Hofmann, F.-J. Jiang, P. Widmer, and U.-J. Wiese, “Finite-Volume Energy Spectrum, Fractionalized Strings, and Low-Energy Effective Field Theory for the Quantum Dimer Model on the Square Lattice”, *Phys. Rev. B* **94**, 115120 (2016), [arXiv:1511.00881](#).
- ¹⁹⁵D. Banerjee, S. Caspar, F.-J. Jiang, J.-H. Peng, and U.-J. Wiese, “Nematic confined phases in the $U(1)$ quantum link model on a triangular lattice: Near-term quantum computations of string dynamics on a chip”, *Phys. Rev. Res.* **4**, 023176 (2022), [arXiv:2107.01283](#).
- ¹⁹⁶M. F. Golterman and J. Smit, “Self-energy and flavor interpretation of staggered fermions”, *Nucl. Phys. B* **245**, 61–88 (1984).
- ¹⁹⁷A. Cheng, A. Hasenfratz, and D. Schaich, “Novel phase in $SU(3)$ lattice gauge theory with 12 light fermions”, *Phys. Rev. D* **85**, 094509 (2012), [arXiv:1111.2317](#).
- ¹⁹⁸B. B. Beard, M. Pepe, S. Riederer, and U.-J. Wiese, “Study of $CP(N - 1)$ theta-vacua by cluster-simulation of $SU(N)$ quantum spin ladders”, *Phys. Rev. Lett.* **94**, 010603 (2005), [arXiv:hep-lat/0406040](#).
- ¹⁹⁹W. Evans, U. Gerber, M. Hornung, and U.-J. Wiese, “ $SU(3)$ quantum spin ladders as a regularization of the $CP(2)$ model at non-zero density: From classical to quantum simulation”, *Ann. Phys.* **398**, 94–122 (2018), [arXiv:1803.04767](#).
- ²⁰⁰M. Creutz, “Gauge Fixing, the Transfer Matrix, and Confinement on a Lattice”, *Phys. Rev. D* **15**, 1128 (1977).
- ²⁰¹M. Lüscher, “Construction of a Selfadjoint, Strictly Positive Transfer Matrix for Euclidean Lattice Gauge Theories”, *Commun. Math. Phys.* **54**, 283 (1977).
- ²⁰²M. Cheng and N. Seiberg, “Lieb-Schultz-Mattis, Luttinger, and ’t Hooft - anomaly matching in lattice systems”, *SciPost Phys.* **15**, 051 (2023), [arXiv:2211.12543](#).
- ²⁰³A. G. Abanov, *Topology, geometry and quantum interference in condensed matter physics*, 2017, [arXiv:1708.07192](#).
- ²⁰⁴M. Reed and B. Simon, *II: Fourier Analysis, Self-Adjointness: Volume 2* (Academic Press, 1975).
- ²⁰⁵F. Gieres, “Mathematical surprises and Dirac’s formalism in quantum mechanics”, *Rept. Prog. Phys.* **63**, 1893 (2000), [arXiv:quant-ph/9907069](#).
- ²⁰⁶M. H. Al-Hashimi and U.-J. Wiese, “Alternative momentum concept for a quantum mechanical particle in a box”, *Phys. Rev. Res.* **3**, L042008 (2021).
- ²⁰⁷I. Albrecht, J. Herrmann, A. Mariani, U.-J. Wiese, and V. Wyss, “Bouncing wave packets, Ehrenfest theorem, and uncertainty relation based upon a new concept for the momentum of a particle in a box”, *Ann. Phys.* **452**, 169289 (2023).
- ²⁰⁸H. G. Evertz, M. Hasenbusch, M. Marcu, K. Pinn, and S. Solomon, “Cluster algorithms for surfaces”, *Int. J. Mod. Phys. C* **3**, 235 (1992).
- ²⁰⁹J.-S. Wang and R. H. Swendsen, “Cluster Monte Carlo algorithms”, *Physica A* **167**, 565–579 (1990).
- ²¹⁰T. Sterling and J. Greensite, “Portraits of the flux tube in QED3: A Monte Carlo simulation with external sources”, *Nucl. Phys. B* **220**, 327–350 (1983).

- ²¹¹D. G. Caldi and T. Sterling, “Graphic evidence for non-abelian flux tubes”, *Phys. Rev. Lett.* **60**, 2454–2457 (1988).
- ²¹²M. Lüscher and P. Weisz, “String excitation energies in SU(N) gauge theories beyond the free-string approximation”, *JHEP* **07**, 014 (2004), [arXiv:hep-th/0406205](#).
- ²¹³M. Lüscher, “Symmetry-breaking aspects of the roughening transition in gauge theories”, *Nucl. Phys. B* **180**, 317–329 (1981).
- ²¹⁴J. D. Stack and M. Stone, “Elementary derivation of the universal attractive Coulomb term in the interquark potential”, *Phys. Lett. B* **100**, 476–480 (1981).
- ²¹⁵M. M. Anber, E. Poppitz, and T. Sulejmanpasic, “Strings from domain walls in supersymmetric Yang-Mills theory and adjoint QCD”, *Phys. Rev. D* **92**, 021701 (2015), [arXiv:1501.06773](#).
- ²¹⁶A. A. Cox, E. Poppitz, and S. S. Y. Wong, “Domain walls and deconfinement: a semiclassical picture of discrete anomaly inflow”, *JHEP* **12**, 011 (2019), [arXiv:1909.10979](#).
- ²¹⁷M. W. Bub, E. Poppitz, and S. S. Y. Wong, “Confinement on $\mathbb{R}^3 \times \mathbb{S}^1$ and double-string collapse”, *JHEP* **01**, 044 (2021), [arXiv:2010.04330](#).

Acknowledgements

First of all, I would like to thank my advisor, Uwe-Jens Wiese. I've learned a lot from him - perhaps most importantly, that there's a lot to gain in doing things "the right way", and that even very hard things are possible.

I also want to thank the many people who accompanied me in this scientific journey - in particular João Pinto Barros, Manes Hornung and Debasish Banerjee. I feel especially grateful towards Tej Kanwar, who taught me many things through both words and example.

I also want to thank all the students and postdocs in Bern for the lively discussions, the endless coffee breaks and for surviving together the plagues of the GS building.

Finally, I want to thank my wife Jeinny for being an amazing partner, for her constant support and for making me feel like the luckiest person in the world.

Selbstständigkeitserklärung

gemäss Art. 18 PromR Phil.-nat. 2019

Name/Vorname: Mariani Alessandro

Matrikelnummer: 20-131-595

Studiengang: Theoretische Physik, Doktorat
Bachelor Master Dissertation

Titel der Arbeit: Abelian lattice gauge theories in three dimensions

Leiter der Arbeit: Prof. Dr. Uwe-Jens Wiese

Ich erkläre hiermit, dass ich diese Arbeit selbständig verfasst und keine anderen als die angegebenen Quellen benutzt habe. Alle Stellen, die wörtlich oder sinngemäss aus Quellen entnommen wurden, habe ich als solche gekennzeichnet. Mir ist bekannt, dass andernfalls der Senat gemäss Artikel 36 Absatz 1 Buchstabe r des Gesetzes über die Universität vom 5. September 1996 und Artikel 69 des Universitätsstatuts vom 7. Juni 2011 zum Entzug des Dokortitels berechtigt ist. Für die Zwecke der Begutachtung und der Überprüfung der Einhaltung der Selbstständigkeitserklärung bzw. der Reglemente betreffend Plagiate erteile ich der Universität Bern das Recht, die dazu erforderlichen Personendaten zu bearbeiten und Nutzungshandlungen vorzunehmen, insbesondere die Doktorarbeit zu vervielfältigen und dauerhaft in einer Datenbank zu speichern sowie diese zur Überprüfung von Arbeiten Dritter zu verwenden oder hierzu zur Verfügung zu stellen.

Datum/Ort: 11.06.2024
3012 Bern

Unterschrift:

Alessandro Mariani